UNIVERSITY CARLOS III OF MADRID
ELECTRICAL ENGINEERING DEPARTMENT

DOCTORAL THESIS:

MOISTURE DYNAMICS IN TRANSFORMERS INSULATED WITH NATURAL ESTERS

A thesis submitted by Rafael David Villarroel Rodríguez
for the degree of PhD in the
University Carlos III of Madrid

Thesis supervisors:

PhD. Belén García de Burgos
PhD. Diego F. García Gómez

Leganés (Madrid), June 2015

DOCTORAL THESIS

MOISTURE DYNAMICS IN TRANSFORMERS INSULATED WITH NATURAL ESTERS

Author:

Rafael David Villarroel Rodríguez

Supervisors:

PhD. Belén García de Burgos

PhD. Diego F. García Gómez

The evaluation panel for this PhD Thesis will be formed for the following professionals:

President: PhD. Alfredo Ortiz Fernández

Secretary: PhD. Carlos Gonzalez-García

Vocal: PhD. Iliana Portugues

This panel has granted qualification:

Leganés (Madrid), June 2015

Dedicated to:

My Parents
and
My Wife

«El éxito depende del esfuerzo.»

Sófocles

Agradecimientos

Este trabajo hubiese sido imposible de realizar sin la ayuda de las instituciones y de las muchas personas que de una manera u otra me apoyaron y ayudaron en este difícil, pero gratificante periplo que ha durado 3 años. Me siento muy agradecido y afortunado de haber contado con todos ustedes, es por eso que quisiera mencionarlos a continuación:

Gracias a toda mi familia, muy especialmente a mis padres Argelia y Jesús porque aún en la distancia han sabido escuchar y aconsejar sobre las decisiones que he tomado. Madre, sé que siempre confiaste en mí y apostaste todo por mis éxitos, mis logros son tus logros.

A mi esposa, Hegla tu apoyo incondicional ha sido pilar fundamental en este proyecto, dejaste atrás muchas cosas importantes por estar a mi lado y así seguiremos siempre. Eres la mejor esposa que se pueda tener.

Me siento muy agradecido y complacido de mis directores Belén y Diego, han sido apoyo y referencia para mí en todo momento, con una altísima calidad profesional pero sobre toda humana. Sin ustedes, otro sería el resultado.

Gracias especiales a Juan Carlos Burgos, nuestro lider de grupo y guía indisctuble en nuestro trabajo.

A mis compañeros del departamento de ingeniería eléctrica: Sandra, Ricardo, Javier, Jorge, Ignacio, Gloria, Manuel, Angel, Jaime, Miriam, Quino, Mónica, Miguel M. y Miguel S. También quiero agradecer a todos los profesores del departamento y por su puesto a Eva. Perdonen si olvido a alguien.

Quiero agradecer a todas las personas que laboran en el Grupo de Investigación de Alta Tensión (GRALTA) de la Universidad del Valle en Colombia, por recibirme muy amablemente en dos ocasiones y permitirme trabajar en sus instalaciones, espe-

cialmente al Profesor Guillermo Aponte, a mi director Diego García, al Ing. Héctor Gongora y familia. Son un grupo excelente de trabajo y mejores personas.

También quiero agradecer a todos los integrantes del grupo de investigación en transformadores de la Universidad de Manchester en el Reino Unido por la oportunidad de trabjar en conjunto durante seis meses y brindarme sus instalaciones para continuar con mi investigación, muy especialmente a la Profesora Zhongdong Wang y al Dr. Qiang Liu, no quisiera olvidar a mis compañeros: Shanika, Ram, Tee, Bevan y Zhao.

Agradecimiento especial al Profesor Donald Hepburn de la Universidad Glasgow Caledonian por su valiosa contribución en la revisión y redacción de un informe sobre la tesis en calidad de experto internacional.

Gracias a Pablo Cirujano del grupo Ormazabal, fabricante de transformadores de distribución por la colaboración prestada y por los materiales suministrados, fundamentales para la realización de este proyecto.

Por último pero no menos importante, a la familia Quirós Hecker, por abrirnos las puertas de su casa a nuestra llegada a Manchester y ayudarnos de manera incondicional y desinteresada, son excelentes amigos y familia.

Gracias a todos...

Abstract

Power transformers are one of the most important components in an electrical system. Knowing their condition is essential to meeting the goals of maximizing the return of the investment and reducing the total cost associated with transformer operation.

As is well known, moisture has a strong influence on the performance of cellulose-oil systems in power and distribution transformers. An excessive water content accelerates the paper ageing rates, increases the presence of partial discharges (PDs) and decreases the dielectric strength of the insulation.

Traditionally the insulation system of a power transformer is composed of oil impregnated paper and pressboard as well as mineral oil acting as dielectric fluid and coolant.

In recent years, the use of natural esters as an alternative to mineral oil has increased considerably in distribution transformers and, although less usual, some experiences are starting to be reported on its use in power transformers. Natural esters are synthesized from a vegetable base, as the seeds of soya, sunflower, rapeseed, etc. They have greater affinity for water than mineral oils due to the fact of hydrogen bonds existing on molecules of natural esters.

The behaviour of moisture inside the transformer insulation is a key aspect in loading studies. If the insulation operates drier the ageing of the paper rate is lower, and thus higher operating temperatures would be acceptable for solid insulation. Cellulose and oil have a very different behaviour with regard to moisture; cellulosic materials are hydrophilic while oil is highly hydrophobic. In consequence water in transformers is mainly contained in cellulosic insulation. However, the distribution of moisture between paper and oil is not static, but depends on the transformer operation condition, and specially on the temperature reached by the different materials.

Moisture migration inside cellulosic insulation is a complex process involving heat and mass transfer phenomena. However, as the thermal time constant is much smaller than the diffusion time constant, moisture migration can be modeled as a diffusion process, using Fick's second law. The diffusion coefficient of cellulosic materials depends on moisture concentration, and thus Fick's equation becomes non-linear and the application of a numerical method is required to solve it.

In this work, the moisture dynamics inside transformers insulated with natural esters have been studied. Different experiments have been developed to obtain solubility curves of natural esters and drying curves of cellulosic materials.

In addition, theoretical models based in finite elements, and an optimization process were used to obtain the moisture diffusion coefficients for different materials.

As a final result of the thesis, a multi-physical model is proposed that allows studing the dynamic behavior of moisture inside a transformer, insulated with mineral oil or with natural esters, under real operation.

Resumen

Los transformadores de potencia son los componentes más importantes de un sistema eléctrico. Conocer su condición de funcionamiento es fundamental para maximizar el retorno de la inversión y reducir el coste total asociado a la operación y el mantenimiento del transformador.

Como es bien sabido, la humedad tiene una fuerte influencia en el rendimiento del sistema celulosa-aceite en los transformadores de distribución y potencia, el contenido excesivo de agua acelera el envejecimiento del papel, aumenta la presencia de descargas parciales (PDs) y disminuye la resistencia dieléctrica del aislamiento.

Tradicionalmente el sistema de aislamiento de un transformador de potencia se construye a partir de papel y cartón prensado impregnado en aceite mineral, que actúa como fluido dieléctrico y refrigerante.

En los últimos años, el uso de ésteres naturales como una alternativa al aceite mineral ha aumentado considerablemente en transformadores de distribución y aunque menos habitual, se está comenzando a implementar su uso en transformadores de potencia. Los aceites o ésteres naturales se sintetizan a partir de una base vegetal, como es semillas de soja, girasol, colza, etc. Estos fluidos tienen mayor afinidad por el agua que los aceites minerales aislantes debido al hecho de presentar enlaces de hidrógeno en sus moléculas

El comportamiento de la humedad en el interior del aislamiento del transformador es un aspecto clave en los estudios de capacidad de carga. Si el aislamiento opera seco la tasa de envejecimiento del papel es menor y por lo tanto aceptaría una mayor temperatura de funcionamiento. La celulosa y el aceite tienen un comportamiento muy diferente con respecto a la humedad; los materiales celulósicos son hidrófilos mientras que el aceite es altamente hidrofóbo. En consecuencia la mayor

humedad en un transformador está contenido en su aislamiento celulósico, sin embargo la distribución de la humedad entre el papel y el aceite no es estática, sino que depende de la condición de funcionamiento del transformador y principalmente de la temperatura alcanzada por los diferentes materiales.

La migración de humedad en el interior del aislamiento celulósico es un proceso complejo que implica la transferencia de calor y de difusión. Sin embargo, como la constante de tiempo de transferencia de calor es mucho menor que la constante de tiempo de difusión, la migración de humedad puede ser modelada como un proceso de difusión, utilizando la segunda ley de Fick. El coeficiente de difusión de materiales celulósicos depende de la concentración de humedad y por lo tanto la ecuación se convierte en no lineal y se necesita implementar un método numérico para resolverlo.

En este trabajo, se ha estudiado la dinámica de humedad dentro de transformadores aislados con ésteres naturales. Diferentes experimentos han sido desarrollados para obtener las curvas de solubilidad de los ésteres naturales y curvas de secado de materiales celulósicos.

Adicionalmente, se utilizaron modelos teóricos basados en elementos finitos y un proceso de optimización para calcular los diferentes coeficientes de difusión de humedad para diferentes materiales.

Como resultado final de la tesis se propone un modelo multifísico que permite estudiar el comportamiento dinámico de la humedad en el interior del transformador, aislado con aceite mineral o con ester natural, en condiciones de funcionamiento reales.

Contents

List of Figures

List of Tables

Chapter 1

Introduction

Transformer is one of the most important and expensive equipment in the electrical power system. Most power and distribution transformers rely on dielectric liquids as an insulating medium and for heat transferring purposes. The dielectric liquid more commonly used is the mineral oil, which is produced from the middle range of petroleum-derived distillates. In the last years the interest in the application of natural and synthetic ester to electric equipments as a substitute of mineral oil has grown significantly [9]. At present, these fluids are mainly being used in the range of small to medium distribution transformers [3], but some experiences in big power transformers are reported as well [10].

Ester fluids are biodegradable liquids and present some other good properties, as their high fire temperatures that make them a valuable alternative to mineral oils. On the other hand, they present some disadvantages like their high cost, high viscosity and oxidation rates [2].

One of the differential properties of natural ester is that they are able to absorb a much greater amount of water than mineral oils [11]. This fact would affect the moisture distribution in the oil-paper insulation and the moisture dynamics processes inside the transformer.

This thesis provides a study about the moisture dynamics in transformers insulated with natural esters. The work involves an experimental study in which the moisture migration processes in transformers insulating materials were studied under static and dynamic conditions. New diffusion coefficients are proposed to characterize the moisture dynamics in ester-impregnated pressboard insulation. An optimization method based on particle swarm (PSO) was used for determining the moisture diffusion coefficients and the results were compared with the coefficients obtained using the optimization process based on a genetic algorithm (GAs). Finally, a multi-physical model is proposed that links the thermal and mass transfer processes in the transformer. The model allows the simulation of the global behaviour of the moisture within the transformer insulation under different operating conditions.

1.1 Moisture in transformer insulation

Moisture is one of the variables that deserves more attention in transformers. Excessive water level in the insulation increases the presence of partial discharges (PDs), reduces the dielectric strength of the insulation, accelerates the paper ageing rates and increases the risk of failure of the equipment. Being able to predict the behaviour of moisture within the transformer insulation is important to optimize the transformer operation, the maintenance programs, and the life remaining of the transformer could be estimated.

1.1.1 Moisture in cellulosic insulation of transformer

Cellulose is the most commonly used solid insulation in power and distribution transformers. It is an inhomogeneous material consisting of a maze of fibers, interfiber and intrafiber spaces, as shown in figure 1.1 [1, 12]. One of the disadvantage of cellulosic material for electrical use is that it is highly hygroscopic and needs to be processed

after the transformer manufacturing to reach moisture levels lower than 0.5-1%.

During the transformer life, the water content of its insulation always increases, because of the degradation of the molecular chain by thermal stresses and oxidative processes [13], and also because of water ingress by the conservator or through leaks in the tank. Therefore, it is common to find moisture levels in the solid insulation between 4 - 6% in weight in older transformers. However, it is not unusual to find high humidity levels in newer transformers as well, for example, in those that have been subjected to on-site repairs.

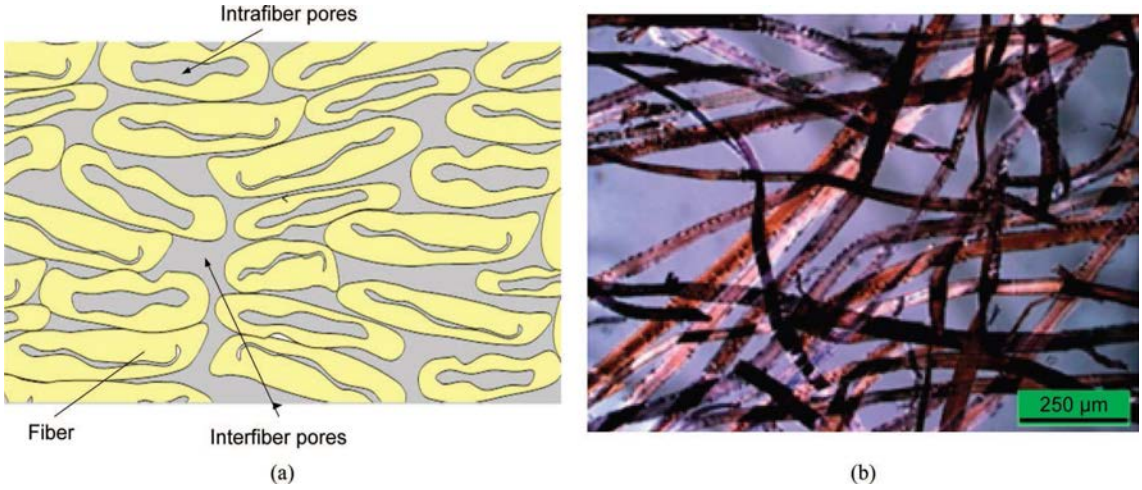

Figure 1.1: Schematic (a) and microscopic view (b) of cellulosic transformer insulation. Taken from [1].

The cellulosic insulation structure consists of the HV and LV insulation, support structures, winding tubes, spacer blocks, and formed items for end closing. Figure 1.2 shows a close-up view of a Kraft paper tape-wrapped HV transformer coil (core type) (a) and pieces formed from pressboard for structure of power transformer (b).

Because of the hydrophobic nature of oil and the hydrophilic character of cellulose, water is absorbed in the paper in a proportion of 1% in oil versus 99% in cellulose and a greater amount of water is usually concentrated in the thick cellulosic insulation [13]. In some cases free water can be found spread on the bottom of the transformer tank, on the core, in the radiators, etc. This can result from suction of rainwater through

poor sealing or from condensation of excessive moisture in the oil during a cooling cycle. Free water will very slowly move to the cellulosic insulation as it dissolves into the oil.

(a) Power transformer coil structure. (b) Formed pieces from pressboard.

Figure 1.2: Differents uses for cellulose insulation. Taken from [1].

The life expectancy of the transformer is extremely related with life expectancy of cellulosic insulation and this largely relies on the amount of moisture inside of the solid insulation. According to the IEEE standard C57.91-2011 [8], a transformer with moisture content in its insulation of greater than 4% is too wet to be operated safely. When high water contents are found in units with a significant remaining service life, it is common to schedule drying treatments that are usually performed in the field.

According to [13], there are three sources of excessive water in transformer insulation:

- Residual moisture in the thick structural components not removed during the factory dryout or moistening of the insulation surface during assembly, generally reduced by evacuation of the tank.
- Ingress from the atmosphere (breathing during load cycles, site erection process)
- Ageing (decomposition) of cellulose and oil.

1.1.2 Moisture equilibrium in paper-oil system

In the dynamic operation of a transformer the moisture distribution tends towards equilibrium and the steady state conditions depend on temperature, geometry and moisture content of the insulation. The temperature distribution of a transformer is related to its load and the atmospheric temperature. If atmospheric temperature or load changes, oil-pressboard insulation will work under transient temperature condition. In this case, water will move from oil to cellulose or from cellulose to oil. Hence, moisture diffusion between oil and paper insulation is continuously taking place during transformer operation because of the load changes [14].

With increasing temperature the water solubility in oil increases while the water adsorption capacity of cellulose decreases. Thus the equilibrium process forces water molecules to migrate from cellulose to oil. At decreasing temperatures the cellulose materials again take up water molecules from the oil [13]. There are several moisture equilibrium curves proposed that represent the relationship between moisture in oil and paper insulation system at different temperature levels, the most representative are published in [15, 16, 17, 18]. They will be explained in following chapters.

1.2 Esters fluids for electrotechnical use

As is well known, the insulating fluid is one of the essential components to ensure proper operation of the transformers. They must guarantee a good insulation of various parts of the equipment while ensuring its cooling. Nowadays, there is growing interest in and usage of natural esters for transformer applications, these fluids are currently being used in high voltage technological applications including a range of small distribution class transformers to medium power transformers, circuit breakers and components of pulsed power systems [3].

One of the most important properties of these oils is their biodegradability, they are biodegradable at 95 - 100% and non toxic; they present lower aquatic or earth danger than conventional mineral oils [19]. Figure 1.3 shows the good biodegradability of ester based insulating liquids.

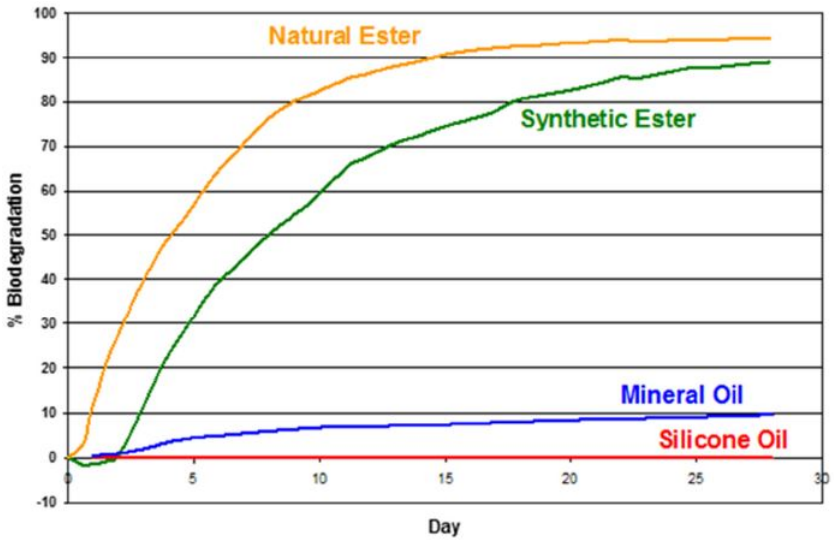

Figure 1.3: Biodegradability of various insulating fluids. Taken from [2].

1.2.1 Fluid type and history

Experimental investigation of vegetable oils as insulating liquid began around the early 1900s, although the use of mineral oils has been justified until now by its wide availability, its good properties and its low cost. However, with environmental issues now becoming extremely important, the use of a product with high biodegradability is becoming extremely attractive, therefore for several years, developments have been in progress in order to permit a replacement of mineral oils by materials based on vegetable oils.

The availability of synthetic ester as well as natural ester fluid, or so-called *'vegetable ester fluid'* can be seen as a solution to solve this problem. The use of vegetable fluids took place mainly in the USA for distribution transformers. In Europe, they have been used for almost 20 years.

The growing interest in the vegetable oil-based dielectric fluids is also motivated by their properties like the electrical strength and viscosity followed by dissipation factor [20]. Otherwise, natural esters are also widely used for their ability to operate at higher temperatures while providing enhanced safety.

Unfortunately, natural esters are not as resistant to oxidation as mineral oils. For this reason, their application in freebreathing transformers and other equipment (e.g., bladderless conservator design) is not recommended and all practical measures should be taken to avoid continuous, long-term exposure (years) to unlimited air exchange, particularly at operating temperatures.

1.2.2 Solubility of water in natural esters

Water may be present in insulating fluids in several forms, water in solution cannot be detected visually and is normally determined by either physical or chemical methods. In figure 1.4, natural esters have significantly higher water saturation values (approximately 15 to 20 times at room temperature) than mineral oil at a given temperature. Figure 1.4 shows the relative moisture saturation of natural esters compared to conventional mineral oil according to [3].

1.2.3 Moisture dynamic in natural ester

To date not many authors have studied the dynamic behaviour of moisture inside ester-insulated transformers. The most important studies have focused in moisture diffusion coefficients and equilibrium curves [18, 21, 22].

In [21], Zhang proposed an expression for the moisture diffusion coefficient of Kraft paper impregnated with a natural ester. Zhang's equation is based on the empirical equation proposed by Guidi in [23] and considers the dependence of the coeffi-

cient with temperature and moisture concentration. As far as the author of this thesis knows, that is the only reference available on the determination of diffusion coefficients in ester-insulated materials.

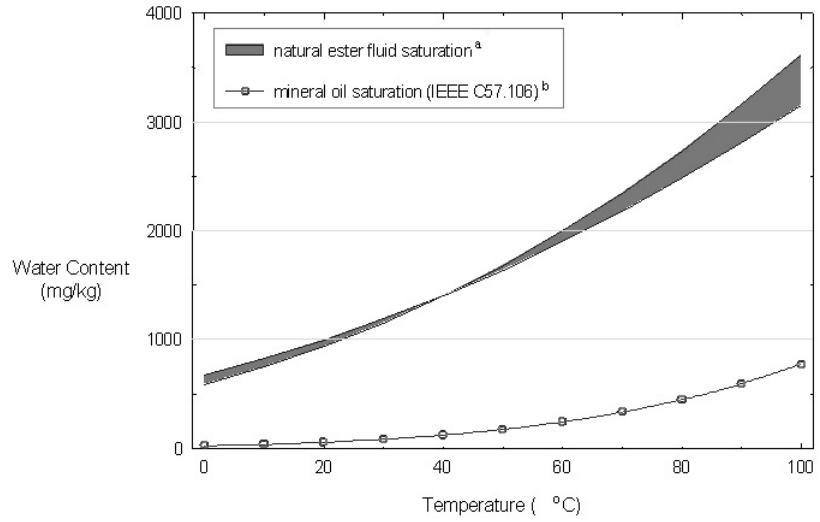

Figure 1.4: Natural ester fluid versus mineral oil saturation curves. Taken from [3]. (a) Modified with permission from Doble Engineering Company. (b) Source: IEEE Std C57.106-2002.

On the other hand, different authors have recently published works regarding the determination of the equilibrium curves in ester-cellulose systems. Jovalekic obtained moisture equilibrium curves using natural esters as insulating liquids and high density (HD) pressboard and Nomex as cellulosic material [17]. Vasovic developed moisture equilibrium curves using natural esters and a combination of Kraft paper and pressboard as cellulosic insulation [18].

1.3 Scope of Thesis

The main objective of the PhD thesis is to study the dynamic behaviour of the moisture in the transformers insulated with natural esters, and to compare this behaviour with that of transformers insulated with mineral oil. To achieve this, some specific objectives have been proposed below:

- To determine experimentally the equilibrium curves of the oil-paper systems in transformers insulated with natural esters.
- To determine the moisture diffusion coefficients in transformer insulation impregnated with natural ester and with mineral oil.
- To develop theoretical models to represent the moisture dynamic inside transformers insulated with natural esters as a function of the load profile.
- To compare the moisture dynamics in transformers insulated with natural esters and with mineral oils.

1.4 Outline of Thesis

This thesis has been written as a series of independent articles with its own structure like introduction, development and conclusions.

In this first chapter a general introduction to the work is presented, the main objectives are exposed and the outline of the thesis is shown too.

In the second chapter a review of the moisture diffusion coefficients proposed by other authors to describe the behaviour of moisture in transformers solid insulation is done.

In the third chapter, the experimental determination of solubility curves and the moisture equilibrium curves in natural and mineral paper-oil system is presented.

In the fourth chapter, the methodology applied to obtain the diffusion coefficients of the different materials is described. An optimization process based in Particle Swarm Optimization is proposed, which is novel with regard to previous works performed in this field [24, 25, 26]. A comparison between Particle Swarm Optimization

(PSO) and Genetic Algorithm (GA) is presented in the chapter.

In the fifth and sixth chapters the moisture diffusion coefficients of transformer pressboard are determined. To this end pressboard impregnated with mineral oil and with two different natural esters was characterized. The results obtained in these chapters allows making a comparative study of the moisture dynamics in pressboard impregnated with the different fluids.

In the seventh chapter a moisture dynamic model for transformers insulated with natural esters is proposed as result of all the work performed during the thesis.The model allows estimation the moisture dynamics inside the transformer insulation under real operation if the load profile and the transformer parameters are known. This kind of model can help to take decisions related with the transformer operation and maintenance, different study cases are presented in the chapter.

Finally a conclusion chapter is included which shows the general conclusions obtained in the thesis, the main contributions, the publications derived from the work and the further works that could be tackled beyond this thesis.

Chapter 2

A review of moisture diffusion coefficients in transformer solid insulation

2.1 Introduction

In order to understand moisture dynamics inside cellulosic insulation, a mathematical model of diffusion may be used. The model is based on Fick's second law [27, 28], and its main parameter is the moisture diffusion coefficient. Although the accuracy of the models depends greatly on the value of the diffusion coefficient, its experimental determination is not easy.

Several researchers have estimated the moisture diffusion coefficient in cellulosic insulation such as Kraft paper or pressboard, employing diverse methodologies. Different values of the diffusion coefficient can be found in the literature, presented as mathematical expressions, tables, or experimental curves showing the dependence of the coefficient on local moisture concentration and temperature. Most of this work was carried out more than 25 years ago.

In 1966 Ast [29] published values for the coefficients in one type of cellulose insu-

lation for several moisture concentration levels and temperatures. In 1974 Guidi and Fullerton [23] proposed a mathematical expression for the diffusion coefficient in cellulosic insulation as a function of local moisture concentration and temperature. This equation has been widely referenced in the literature and several researchers [30, 31, 32] determined parameter values to be substituted in Guidi's equation for various insulation materials.

This chapter presents a review of the moisture diffusion coefficients for transformer solid insulation that have been proposed by various researchers.

2.2 Modelling moisture dynamics within transformer solid insulation

Moisture accumulation inside a transformer may be due to moisture ingress through seals, cellulosic insulation degradation or oil oxidation as explained in the first chapter. Because of the hydrophilic nature of cellulosic insulation and the hydrophobic nature of oil, the moisture accumulates mainly in the cellulosic insulation. However, its distribution between oil and insulation depends on the transformer operating conditions, particularly temperature.

Moisture accumulation in the insulation can lead to hazardous operating conditions and reduces the life expectancy of the transformer. To minimize the amount of water in the insulation, new transformers are subjected to a drying process prior to filling with oil. In service drying may also be necessary during the transformer life.

To optimize the drying processes, it is important to use accurate mathematical models that predict the evolution of the moisture profiles in the solid insulation during drying [27, 28, 33]. Such models are also useful for the analysis of moisture dynamics within operating transformers and for the development of sensors to measure the

moisture content in the insulation [30, 33].

Moisture migration inside cellulosic insulation is a complex process involving heat transfer and mass diffusion. However, as the heat transfer time constant is much smaller than the diffusion time constant, moisture migration can be modeled as a diffusion process, using Fick's second law [30, 32, 33].

Water inside transformer insulation can move as vapor, through the interfiber and intrafiber spaces (see figure 1.1), or as liquid by capillarity, molecular (or Knudsen) flux, or superficial diffusion. In order to model water movement, the diffusion coefficients associated with these mechanisms must be known [12, 34, 35, 36].

An additional term, describing the change of state from liquid to vapor and vice versa inside the solid insulation, is required. Zhang [37] developed a model based on the laws of conservation of mass and considered water diffusion in only one direction, similar to the movement of moisture inside solid insulation [27]. Thus

$$\frac{\partial W}{\partial t} = \frac{\partial}{\partial x}\left(D_W \cdot \frac{\partial W}{\partial x}\right) - I \tag{2.1}$$

$$\frac{\partial V}{\partial t} = \frac{\partial}{\partial x}\left(D_V \cdot \frac{\partial V}{\partial x}\right) + I \tag{2.2}$$

where W is the concentration of liquid water, V is the concentration of water vapor per volume unit (kg/m^3), D_W and D_V are the respective diffusion coefficients (m^2/s), and I is the mass of moisture that changes from one phase to the other per unit time and volume during the diffusion process ($kg/m^3 s$).

Unfortunately, it is not easy to determine the diffusion coefficients for liquid and vapor water separately or the amount of water changing state during the process. However, the model may be simplified by eliminating the term I, combining (2.1) and (2.2), and using the total water concentration, i.e., liquid plus vapor. Then

$$\frac{\partial c}{\partial t} = \frac{\partial}{\partial x}\left(D \cdot \frac{\partial c}{\partial x}\right) \tag{2.3}$$

where D is the effective moisture diffusion coefficient in the solid insulation, c is the local total moisture concentration, t is the time and x is the distance into the material in the direction of moisture movement.

The effective diffusion coefficient in (2.3) may be interpreted as a combination of the coefficient corresponding to vapor water moving mainly through the interfiber pores and the coefficient corresponding to liquid water moving mainly through the intrafiber pores [12, 34, 35, 37]. Combining the two coefficients is equivalent to considering the solid as a homogeneous material in which the diffusion resistance is independent of position when temperature and moisture concentration are constant throughout the material [36]. The effective diffusion coefficient in cellulosic insulation is dependent on moisture concentration and temperature, and has been used by all authors studying moisture dynamics in transformer solid insulation.

2.2.1 Moisture diffusion model adopted in the thesis

During this thesis, a model based in the solution of equation 2.3 with adequate boundary conditions has been adopted, using, to this end, the finite elements method (FEM). The FEM computation tool Comsol Multiphysics has been used in this work.

In order to implement the model, some assumptions should be made [27].

1. Moisture diffusion is a very slow process, since water must travel through solid insulation until attaining the surface where it is absorbed by oil. Mass transport processes are much slower than heat transfer and fluid-dynamic processes taking place in the transformer. In other words, Schmidt and Lewis numbers in the oil are:

$$Sc_{oil} = \frac{\nu_{oil}}{D_{oil}} = \frac{\mu_{oil}}{\rho_{oil} D_{oil}} \gg 1 \tag{2.4}$$

$$Le_{oil} = \frac{\alpha_{oil}}{D_{oil}} = \frac{k_{oil}}{\rho_{oil} C p_{oil} D_{oil}} \gg 1 \tag{2.5}$$

where ν is cinematic viscosity, μ is the dynamic viscosity, ρ is the oil density, α is the thermal diffusivity and C_p is the specific heat of the oil. Also, the equivalent Lewis number considering now pressboard properties [1] is:

$$Le_{presb} = \frac{\alpha_{presb}}{D_{presb}} = \frac{k_{presb}}{\rho_{presb} C p_{presb} D_{presb}} \gg 1 \tag{2.6}$$

Therefore, the temperature in the entire transformer (insulation and oil) and velocity field in the oil can be considered in steady state during the transient moisture diffusion within the insulation.

2. The height of the transformer active part, is typically more than one meter, whereas the thickness of the insulation in a real transformer (even thick insulation) is only a few millimetres thick. From this, concentration gradients in the transverse direction are much higher than those in the longitudinal direction ($\Delta C/e \gg \Delta C/h$) and thus, diffusion in the longitudinal direction can be neglected. Therefore, the problem will be studied by means of one dimensional (1-D) models representing insulation sections. 2-D simulations only increase the computational cost without improving the final results.

Additionally, the way moisture is absorbed by oil from the paper surface must be established. To stablish the boundary condition to solve equation 2.3 it must be considered that water absorption on the surface of the insulation behaves as a convective process. Howe in [39] showed that water interchange on paper-oil contact surface is much faster than moisture diffusion processes within solid insulation. Therefore, the equilibrium concentration is achieved very fast on the surface and this equilibrium concentration can be assumed as the boundary condition to solve the slow transient

[1] Schmidt number and Lewis number represent respectively the ratio between the momentum diffusivity and the mass diffusivity and the ratio between the thermal diffusivity and the mass diffusivity.

diffusion in the interior of the insulation. Equilibrium moisture can be obtained from the moisture equilibrium charts, which will be widely discussed in chapter 3.

This model is used in this chapter to compare and validate the moisture diffusion coefficients proposed by several authors. The same model will be also applied in chapters 4, 5 and 6, to the determination of the new expressions for the diffusion coefficient proposed in this work.

2.3 Moisture diffusion coefficient studies

Coefficients for moisture diffusion in Kraft paper and pressboard, non-impregnated with oil and oil-impregnated, can be found in the technical literature. The experimental procedures followed by the various researchers differ, as do the resulting coefficients.

2.3.1 Coefficients of Ast

The first diffusion coefficient measurements in transformer insulation, specifically in Kraft paper (type A50P281A), were published by Ast in 1966 [29]. The experimental procedure was the so called permeation method, in which one side of a paper sheet was exposed to air at 0% relative humidity (maintained using anhydrous calcium sulfate) and the opposite surface was exposed to air at constant relative humidity (maintained using a saline regulator). The rate of moisture migration from the wet side to the dry side of the paper was determined periodically by measuring the loss of mass of the saline regulator. The measurements were made for three paper thicknesses and various temperatures. The mathematical model used by Ast was based on Fick's first law:

$$F = \frac{dQ}{dt} = -D \cdot \frac{dc}{dx} \tag{2.7}$$

where F is the moisture flux per unit area per unit time, Q is the mass of moisture per unit area, c is the moisture concentration, and D is the effective diffusion coefficient

Ast made two important assumptions. The first was that each surface remains in equilibrium with its own atmosphere, equivalent to assuming that diffusion takes place through an infinitesimal thickness of paper. The second was that the moisture concentration varies linearly across the paper thickness. The latter is not strictly true, because the diffusion coefficient in cellulosic materials depends on the moisture concentration, and consequently the moisture concentration profile is not linear.

2.3.2 Coefficients of Guidi and Fullerton

Guidi and Fullerton [23, 31] used a diffusion model to estimate the drying times of power transformers in the factory, and to determine the moisture adsorption rates for the transformer insulation when exposed to the atmosphere. They proposed the empirical relationships (2.8) and (2.9) for the dependence of the diffusion coefficient of oil through impregnated paper on local moisture concentration and temperature:

$$D_{(c,T)} = D_0 \cdot e^{k \cdot c} \tag{2.8}$$

$$D_0 = D_G \cdot e^{E_a\left(\frac{1}{T_0} - \frac{1}{T}\right)} \tag{2.9}$$

Combining (2.8) and (2.9) yields,

$$D = D_G \cdot e^{\left[k \cdot c + E_a\left(\frac{1}{T_0} - \frac{1}{T}\right)\right]} \tag{2.10}$$

where D is the diffusion coefficient (m^2/s), c is the local moisture concentration (kg of H_2O/kg), T is the temperature (K), T_0 is the reference temperature (298 K), k is a

dimensionless parameter, D_G is a pre-exponential factor (m^2/s), and E_a is the activation energy of the diffusion process (K).

The specimens under test consisted of multiple layers of Kraft paper impregnated with oil. Moisture-adsorption experiments were performed on dry samples using an environmental chamber, and moisture-desorption experiments were carried out on previously moistened samples dried under vacuum.

The moisture concentrations at various depths were determined using the Karl Fischer method, at various stages during wetting or drying, and the values of local concentration of moisture as a function of depth $[c(x)]$ were fitted to a high-order polynomial.

Figure 2.1 shows the measured moisture concentrations and the fitted concentration profiles at 50% relative humidity and 22 °C used in their experiments.

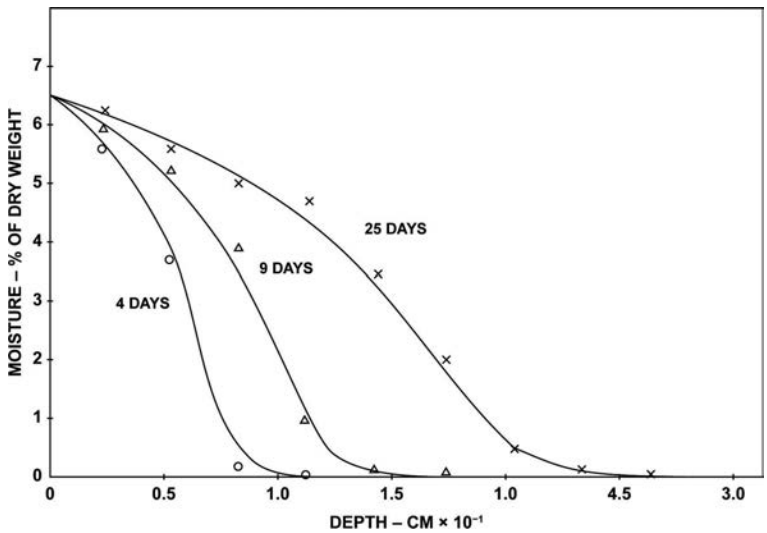

Figure 2.1: Experimental and calculated moisture profiles from adsorption experiments at 22 °C and 50% relative humidity. Taken from [4].

Guidi and Fullerton determined the diffusion coefficient using the equations for the concentration profiles and (2.11), given by Crank [38], which they later related to the moisture concentration and the temperature using (2.8) and (2.9). They obtained

k = 0.5, $D_G = 6.44 \cdot 10^{-14}\ m^2/s$ and E_a = 7,700 (K) in (2.10) (for oil-impregnated Kraft paper).

$$D_{(c)} = -\frac{1}{2t} \cdot \frac{dx}{dc} \Bigg| \cdot \int_{c_0}^{c} x \cdot dc \tag{2.11}$$

2.3.3 Coefficients of Howe and Asem

Howe determined the moisture diffusion coefficient for manila paper and the longitudinal diffusion coefficient for pressboard [39]. In both cases the samples were not oil-impregnated. The pressboard samples, 70 mm long, 50 mm wide, and 15 mm thick, were compressed between a pair of steel plates under a pressure of 500 $kN \cdot m^{-2}$, approximating the forces to which pressboard components in transformer insulation are typically subjected (figure 2.2). In this configuration water migration was assumed to occur only in the longitudinal direction.

The manila paper samples consisted of 50 layer strips, 12 mm wide and 0.045 mm thick, wound over a copper tube that was 21.5 mm in diameter and 178 mm long. The total thickness of the insulation was thus 4.5 mm (figure 2.2).

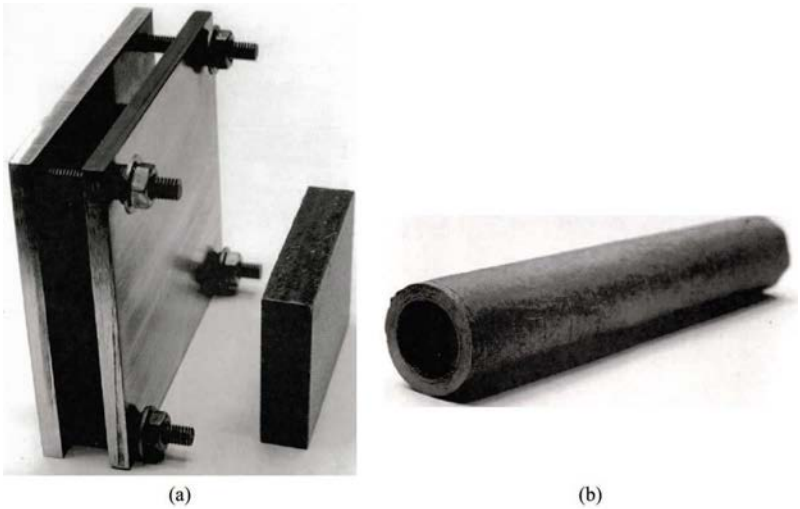

Figure 2.2: Samples used by Howe: (a) pressboard, (b) manila paper. Taken from [4].

Both types of sample were dried under vacuum at 113 °C for four days in an oven fitted with a liquid nitrogen cold trap, so that nearly complete drying of the insulation could be assumed. Subsequently the samples were subjected to a wetting process in a environmental chamber at 64 °C and 44% relative humidity. During the wetting process the average moisture concentration was determined by weight measurements and the moisture concentration profile at various stages of the wetting process obtained.

Using the finite difference technique and curve fitting, the diffusion equation was solved, yielding the diffusion coefficient values shown in table 2.1 for moisture concentrations between 1 and 4% of total weight in paper and between 1 and 3% in pressboard.

Table 2.1: Diffusion coefficient values determined by Howe for moisture concentrations c between 1 and 4% of total weight.

	D (m^2/s)	
c (%)	**Pressboard**	**Manila paper**
1	$(4.5 \pm 2.0) \cdot 10^{-10}$	$(0.6 \pm 0.15) \cdot 10^{-11}$
2	$(1.8 \pm 0.9) \cdot 10^{-10}$	$(0.9 \pm 0.2) \cdot 10^{-11}$
3	$(0.9 \pm 0.5) \cdot 10^{-10}$	$(1.3 \pm 0.4) \cdot 10^{-11}$
4	—	$(2.5 \pm 0.8) \cdot 10^{-11}$

Following the same methodology, Asem [32] determined diffusion coefficients for oil-impregnated paper and for non-impregnated paper and pressboard. The samples were pre-moistened in a environmental chamber at 60 °C and 44% relative humidity and dried in an oven at 80 °C. The oven was fitted with a cold trap, which created a pressure gradient of water vapor around the samples and thus accelerated moisture desorption from the insulation.

The measurements were repeated at atmospheric pressure and in a vacuum oven at a pressure of 1.3 $N \cdot m^{-2}$ ($1.3 \cdot 10^{-5}$ bar). In the case of oil-impregnated paper the moisture concentration was determined by the Karl Fischer method. The diffusion coefficients obtained by Asem [32] from wetting and drying experiments are presented in tables 2.2 and 2.3, respectively. It is important to point out that Howe and Asem did not determine the dependence of the coefficients on temperature because all tests were

done at 80 °C.

Table 2.2: Diffusion coefficient values determined by Asem in paper and pressboard obtained from wetting experiments for moisture concentrations c between 1 to 4% of total weight.

	D (m^2/s)		
c (%)	**Compressed pressboard**	**Non-impregnated paper**	**Impregnated paper**
1	$(11.0 \pm 5.75) \cdot 10^{-10}$	$(0.74 \pm 0.36) \cdot 10^{-11}$	$(0.54 \pm 0.34) \cdot 10^{-11}$
2	$(5.3 \pm 2.5) \cdot 10^{-10}$	$(1.18 \pm 0.58) \cdot 10^{-11}$	$(0.82 \pm 0.48) \cdot 10^{-11}$
3	$(3.6 \pm 1.7) \cdot 10^{-10}$	$(1.64 \pm 0.78) \cdot 10^{-11}$	$(1.22 \pm 0.58) \cdot 10^{-11}$
4	$(2.7 \pm 1.3) \cdot 10^{-10}$	$(2.16 \pm 0.92) \cdot 10^{-11}$	$(1.94 \pm 0.74) \cdot 10^{-11}$

Table 2.3: Diffusion coefficient values determined by Asem in paper and pressboard obtained from drying experiments for moisture concentrations c between 1 to 3% of total weight.

	D (m^2/s)		
c (%)	**Non-impregnated paper (atm pressure)**	**Non-impregnated paper (vacuum)**	**Impregnated paper (vacuum)**
1	$2.4 \cdot 10^{-10}$	$4.2 \cdot 10^{-10}$	$2.2 \cdot 10^{-10}$
2	$3.8 \cdot 10^{-10}$	$6.9 \cdot 10^{-10}$	$4.2 \cdot 10^{-10}$
3	$5.6 \cdot 10^{-10}$	$10.7 \cdot 10^{-10}$	$6.8 \cdot 10^{-10}$

2.3.4 Coefficients of Foss

Foss determined a set of parameters for the empirical equation (2.10), using the experimental data obtained by other workers for impregnated and non-impregnated Kraft paper. Most of the procedure is described in internal company reports, and therefore some details are not available. However a general description of the work may be obtained from [31]. Table 2.4 summarizes the parameters reported by Foss.

Table 2.4: Values of the diffusion coefficient parameters determined by Foss.

	k	D_G (m^2/s)	E_a (K)
Oil-impregnated Kraft paper	0.5	$1.34 \cdot 10^{-13}$	8,074
Non-impregnated Kraft paper	0.5	$2.62 \cdot 10^{-11}$	8,140

2.3.5 Coefficients of Du

Du [30, 40] determined the moisture diffusion coefficient for non-impregnated pressboard as a function of temperature and moisture concentration. She used an interdigital dielectrometric sensor that determined the moisture concentration profiles in samples subjected to a moisture adsorption process. Figure 2.3 (a) shows the experimental setup schematically.

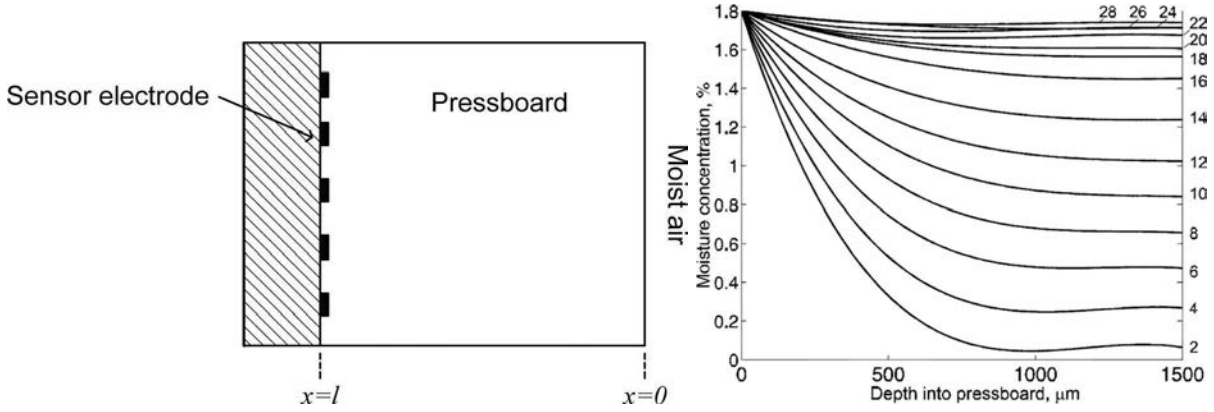

(a) Experimental setup.

(b) Moisture concentration profiles calculated from dielectrometric measurements on nonimpregnated pressboard samples.

Figure 2.3: Experimental setup used by Du and moisture concentration profiles. Taken from [4].

A pressboard sample, initially free of moisture, was exposed on one side to an air flow with controlled humidity and temperature. To ensure unidirectional diffusion, the other exposed faces were sealed with silicone glue. Using the sensor the moisture concentration profile was determined every two hours over a 28 hour period. Figure 2.3 (b) shows concentration profiles after various adsorption times.

To determine the dependency of the diffusion coefficient on temperature and moisture concentration, the experiment was repeated for 1.8 and 3% initial equilibrium moisture concentrations and over the range 30 to 70 °C in 10 °C increments.

To analyse the experimental data, Du used Fick's second law, this equation was

solved by applying the finite difference method. Finally, Du obtained k = 0.45, D_G = $6.70 \cdot 10^{-13}$ m^2/s and E_a = 7,646 (K) for non-impregnated pressboard. She also fitted Ast's data to (2.10) and obtained $D_G = 2.25 \cdot 10^{-11}$ m^2/s, k = 0.1955 and E_a = 8,834 (K) for non-impregnated Kraft paper.

2.3.6 Coefficients of García

García [41, 25, 42] proposed moisture diffusion coefficients for mineral-oil-impregnated and non-impregnated Kraft paper as a function of temperature, moisture concentration and insulation thickness. He was the first author who considered the effect of the insulation thickness in the moisture migration inside the cellulosic insulation. He used thermogravimetric analysis on non-impregnated Kraft paper samples, and a hot circulation drying process on mineral-oil impregnated Kraft paper.

The conditions applied to mineral oil-impregnated and non-impregnated Kraft paper samples used by García during his drying experiments are summarized in table 2.5.

Table 2.5: Mineral oil impregnated and non-impregnated Kraft paper samples used by García.

	Kraft paper (Non-Impregnated)	**Kraft paper (Impregnated)**
Thickness (mm)	1, 2, 3 and 4	1, 3 and 5
Temperature (ºC)	40, 50, 60, 70 and 80	60, 70, 80 and 85

To find the parameters k and D_0 of the moisture diffusion coefficient, García used an optimization process based in genetic algorithms. The moisture diffusion coefficients proposed for these materials are shown below:

$$D_{(Non-impregnated-Kraftpaper)} = 3.1786 \cdot l^{-3.665} \cdot e^{\left(0.32458 \cdot c - \frac{8{,}241.76 \cdot l^{-0.254}}{T}\right)} \tag{2.12}$$

$$D_{(Impregnated-Kraftpaper)} = 0.5 \cdot e^{\left(0.5 \cdot c - \frac{10{,}193 - 264.7 \cdot l}{T}\right)} \tag{2.13}$$

In these equations, the insulation thickness (l) is expressed in millimetres, c is the concentration of moisture in paper, and T is the temperature in K.

Moisture diffusion dependence of cellulose insulation on geometric properties like thickness has not been reported in literature until García's works as it is shown in 2.12 and 2.13. He was the first author who includes the effect of the thickness in a mathematical model to study the water mobility inside cellulosic insulation. This can be explained because in the general diffusion theory, the moisture diffusion coefficient is considered an intrinsic property of the material and therefore it is only affected by local conditions like temperature and moisture concentration [43].

The work made by García has been used as a reference to establish the experimental procedures and the theoretical models proposed in this thesis.

2.3.7 Diffusion coefficient for natural-ester-impregnated insulation

In [21], Zhang proposed an expression for the moisture diffusion coefficient of Kraft paper impregnated with a natural ester. That is the only reference available about diffusion coefficients of cellulose impregnated with ester fluids. Zhang solved Fick's second law by applying the finite difference method. He obtained the following parameters for Guidi's equation using the results of his experiments on ester-impregnated Kraft paper: $k = 0.497$, $D_G = 7.34 \cdot 10^{-14}\ m^2/s$ and $E_a = 6{,}940$ (K). The validation of the moisture diffusion coefficient proposed by Zhang is described in chapter 6.

2.4 Comparison of the proposed coefficients

The values of D_G, k and E_a obtained by the workers mentioned above are summarized in table 2.6, Asem's and Howe's coefficients are not included in the table since they did

not propose a mathematical expression but a series of values.

Table 2.6: Comparison of the moisture diffusion coefficients proposed by various authors for Kraft paper and pressboard.

Authors	**Insulation type**	k	D_G (m^2/s)	E_a (K)
Guidi	Oil-impregnated Kraft paper	0.5	$6.44 \cdot 10^{-14}$	7,700
Foss	Oil-impregnated Kraft paper	0.5	$1.34 \cdot 10^{-13}$	8,074
Foss	Non-impregnated Kraft paper	0.5	$2.62 \cdot 10^{-11}$	8,140
Du	Non-impregnated pressboard	0.45	$6.70 \cdot 10^{-13}$	7,646
Ast(*)	Non-impregnated Kraft paper	0.195	$2.25 \cdot 10^{-11}$	8,834
García	Non-impregnated Kraft paper	0.32458	$3.1786 \cdot l^{-3.665}$(**)	—
García	Oil-Impregnated Kraft paper	0.5	0.5(**)	—
Zhang	Oil-impregnated Kraft paper (***)	0.497	$7.34 \cdot 10^{-14}$	6,940
(*) Calculated by Du from Ast's experimental data.				
(**) Only paremeters k and D_G have been determined.				
(***) Using natural ester.				

In order to compare the different coefficients, the drying process of a 5 mm coil of Kraft paper non impregnated, and impregnated with mineral oil was simulated by means of the model described in section 2.2.1. The simulation process involved the resolution of Fick's second law using Comsol Multiphysics, considering the following assumptions:

- A homogeneous initial moisture concentration of 3%.
- An equilibrium moisture concentration of 0.5% at the boundary between the paper and the surrounding medium.
- A constant temperature of 62 °C throughout the paper. This temperature was used by Howe and Asem in their experiments.

The results for non-impregnated paper are shown in figure 2.4, using the coefficients tabulated in table 2.6. Figure 2.4 (a) shows the moisture concentration profiles after 5 hours of drying, and figure 2.4 (b) shows average moisture concentrations as functions of drying time.

It can be seen (figure 2.4 (a)) that Howe's coefficients yield slower moisture desorption, and after 100 hours, equilibrium has still not been reached (figure 2.4 (b)). It can also be seen that the drying curves estimated using Foss's and Ast's coefficients are similar; in both cases the time required to reach moisture concentration equilibrium was close to 15 hours. This result is perhaps not surprising because both sets of coefficients were derived from the same experimental data. The drying time predicted from the Asem coefficients is approximately 40 hours.

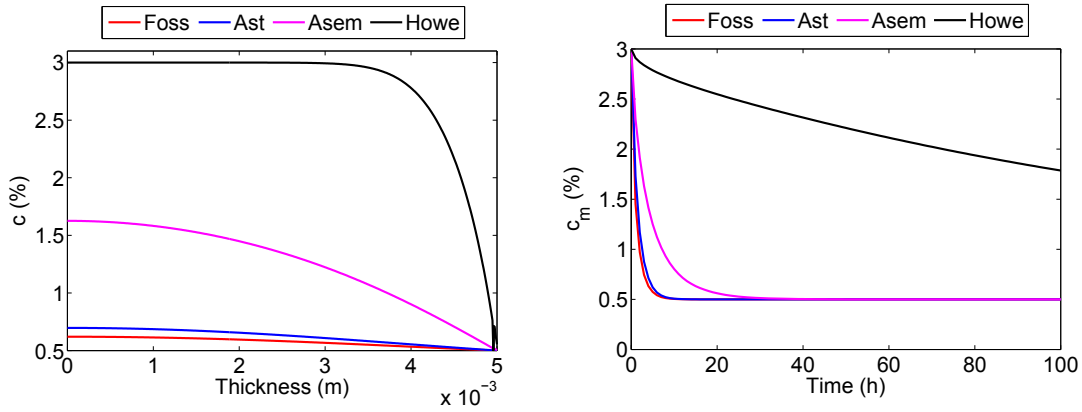

(a) Moisture concentration profiles after drying for 5 hours.

(b) Average moisture concentrations as functions of drying time.

Figure 2.4: Simulation of the drying of a 5 mm thick section of non-impregnated Kraft paper, using different coefficients.

Figure 2.5 shows the results of the simulations for mineral oil-impregnated paper. The moisture concentration profiles shown in (a) are those estimated after 20 hours of drying. Figure 2.5 (b) shows the average moisture concentrations as a function of the drying time. Asem's coefficient for oil-impregnated paper in table 2.3 leads to moisture equilibrium after 50 hours of drying whereas the other three coefficients do not predict moisture equilibrium even after 300 hours of drying.

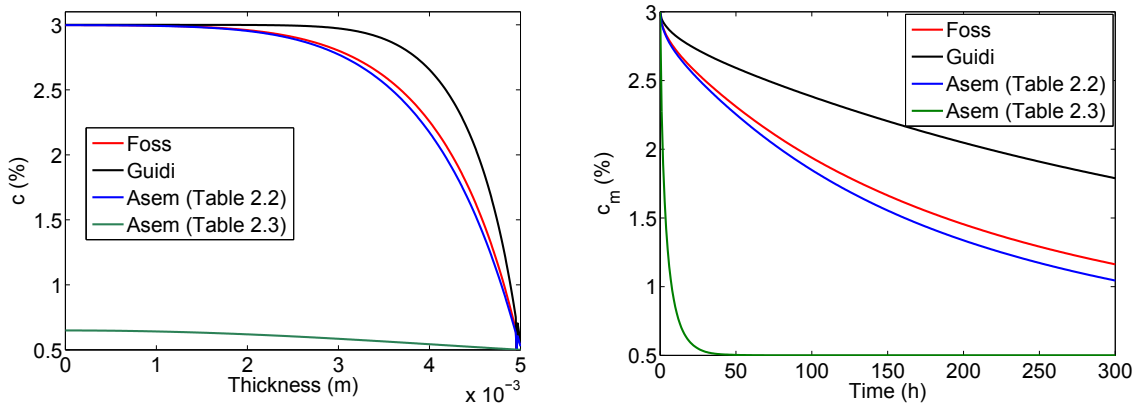

(a) Moisture concentration profiles after 20 hours of drying.

(b) Average moisture concentrations as functions of drying time.

Figure 2.5: Simulation of the drying of a 5 mm thick section of oil-impregnated Kraft paper, using different coefficients.

2.5 Experimental validation of the coefficients

As was shown in the previous section, the estimations of the coefficients proposed by the different authors differ significantly. In order to determine the precision of the available coefficients, García, Villarroel et al. performed an experimental study on different materials. The full study is reported in [7], however, the main aspects of it are summarized in this section.

Drying experiments were carried out on oil-impregnated and non-impregnated Kraft paper and pressboard samples at various temperatures and for several insulation thicknesses. The verification of the diffusion coefficients was performed by using the data obtained from two sets of drying experiments:

- For non-impregnated insulation, thermo-gravimetric experiments were performed determining the weight of a sample while being dried.
- For impregnated Kraft paper, drying experiments were carried out in hot oil in which samples were periodically extracted and analyzed by Karl Fischer method.

2.5.1 Experiments on non-impregnated insulation

To validate the moisture diffusion coefficients for non-impregnated Kraft paper and pressboard proposed by the various researchers, drying tests were carried out using a thermo-gravimetric analyzer (*TGA*). This method has been used by several researchers [44, 45] in analyzing the drying processes in various materials, for example, food and construction materials.

A *TGA* continuously monitors the weight of a sample subjected to a temperature profile selected by the user. In the case of non-impregnated insulation samples, the weight loss is related to the loss of water, and thus with the rate of drying of the sample.

Thermo-gravimetric experiments were carried out using a thermo-gravimetric analyzer TA model Q500 on several thicknesses of Kraft paper and pressboard subjected to various drying temperatures.

Before starting the *TGA* experiments, the samples were prepared with an specific initial moisture content by placing them in a environmental chamber under controlled temperature of 35 °C and relative humidity of 70% for pressboard and 30 °C and relative humidity of 67.5% for Kraft paper. The wetting conditions were established according to Jeffries's curves (figure 2.6) [5].

The moisture content of non-impregnated Kraft paper and presspoard samples before the drying process was calculated as percentage mass of absorbed water per mass of dry sample using following equation (2.14):

$$W_{H_2O} = \frac{m_h - m_d}{m_d} \cdot 100 \tag{2.14}$$

where W_{H_2O} is absorbed water (%), m_h is mass of conditioned sample (g) and m_d is mass of dried non-impregnated sample (g).

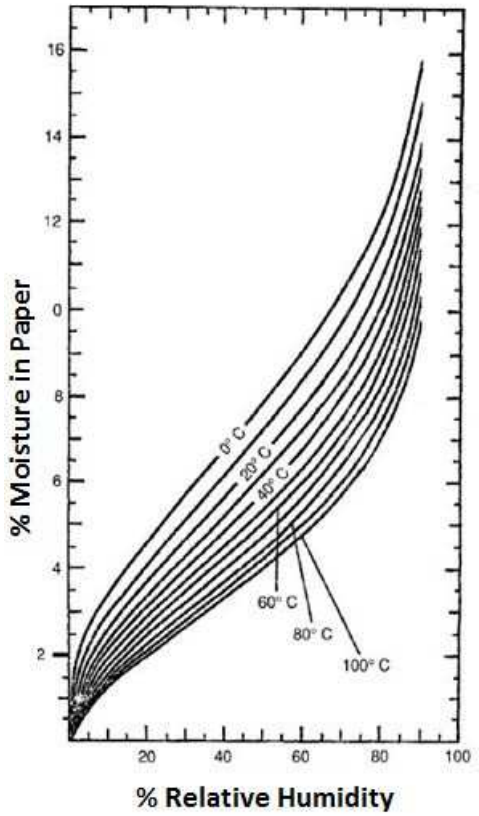

Figure 2.6: Moisture in paper as a function of relative humidity of the ambient by Jeffries. Taken from [5].

To determine the drying rate of the different materials, multiple layers of Kraft paper and single layers of pressboard were stacked into a pan with a single opening at the top to ensure unidirectional diffusion during the *TGA* experiments.

The conditions applied to the Kraft paper and pressboard samples during the drying experiments are summarized in table 2.7.

Table 2.7: Kraft paper and pressboard samples for *TGA* experiments.

	Kraft paper	**Pressboard**
Thickness (mm)	1, 2, 3 and 4	1, 2 and 3
Temperature (^{o}C)	40, 50, 60, 70 and 80	40, 50, 60, 70, 80, 90, 100 and 120

The pans, filled with the insulation were introduced into the *TGA* oven (figure 2.7), where they were dried under controlled temperature until full moisture desorption. During the tests, dry nitrogen was circulated through the oven to prevent oxida-

tion of the materials and to ensure a moisture-free atmosphere.The loss of mass of the samples was continuously monitored during the drying experiments.

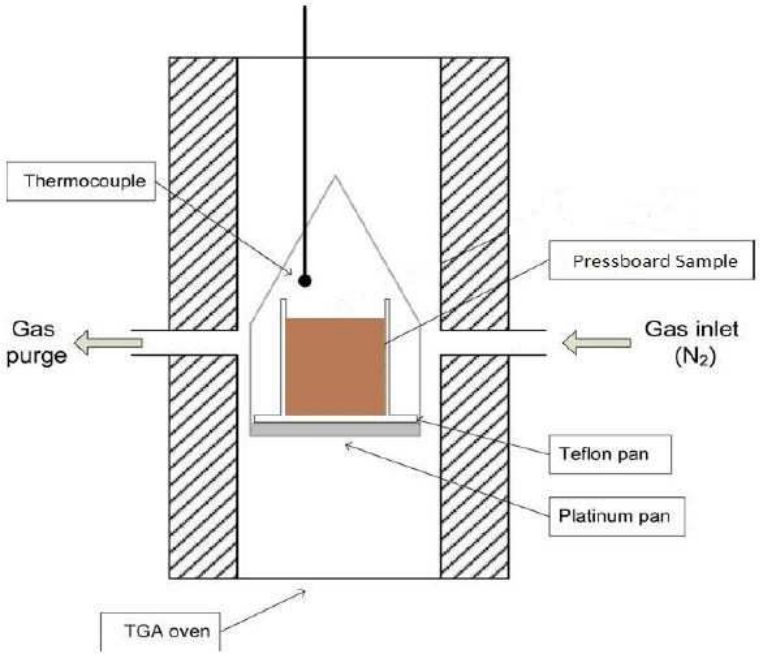

Figure 2.7: Illustration of pan filled with insulation in *TGA* oven. Taken from [6].

2.5.2 Experiments on oil-impregnated insulation

To carry out drying experiments on oil-impregnated samples, a drying plant was constructed to achieve moisture desorption by circulating hot and dry oil. General scheme and operation of this drying plant will be explaining in detail in following chapters

For the validation of the coefficients of oil-impregnated paper experiments were performed on insulation specimens of 1, 3, and 5 mm thicknesses obtained by paper sheets of 0.1 mm thickness wound on an aluminium core (figure 2.8). The core is fitted with stoppers at the top and bottom limiting moisture desorption in longitudinal direction.

The specimens were submerged in oil at room temperature and at atmospheric pressure for a minimum of one week. Finally, the oil-impregnated test specimens were

reintroduced into the environmental chamber to re-wet the insulation prior to the drying experiments.

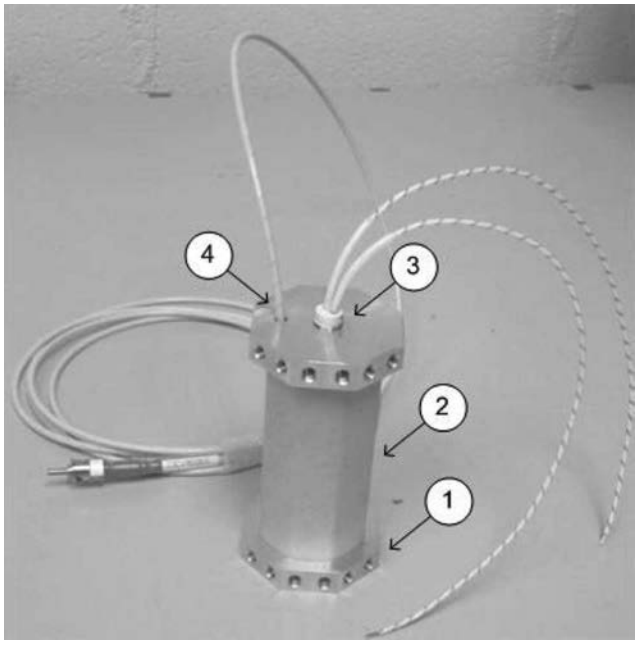

Figure 2.8: Insulation test sample details: aluminium core (1), paper insulation (2), heating element lead (3) and internal insulation temperature sensor (4). Taken from [7].

The drying experiments consisted of subjecting the specimens previously wetted and impregnated with mineral oil, to a constant flow of hot dry oil. The moisture content before and after the drying process of oil-impregnated Kraft paper was determined by using Karl Fischer titration method according to the international standard IEC 60814 [46], which determines the average moisture throughout the thickness of the samples.

During the whole drying process, samples were periodically extracted from the specimens to determine the moisture evolution. To validate the diffusion coefficients for oil-impregnated paper, specimens of three thicknesses (1, 3, and 5 mm) were dried by oil circulation at four temperatures (60, 70, 80, and 85 °C).

2.5.3 Validation process

The experiments described in previous sections were simulated using finite element described in section 2.2.1, and with the different diffusion coefficients included in table 2.6.

The difference between the simulated and the experimental curves was quantified by the root mean square deviation (*RMSD*) (2.15) applied to the complete drying time:

$$RMSD = \sqrt{\frac{1}{n}\sum_{i=1}^{n}\left[c_{m-est(t_i)} - c_{m-exp(t_i)}\right]^2} \tag{2.15}$$

where n is the number of experimental measurements, c_{m-exp} is the measured average moisture concentration, c_{m-est} is the estimated average moisture concentration and t_i is the instant of the drying experiment when the i-th measurement was performed.

Validation of the coefficients for non-impregnated pressboard

As described in previous sections, drying experiments were performed using *TGA* to validate Du's coefficient. These experiments were simulated by finite element analysis applying Du's coefficient to (2.10), and the difference between the measured and simulated drying curves was calculated using (2.15).

It can be seen that the *RMSDs* are very different (figure 2.9) and as large as two orders of magnitude, depending on temperature and sample thickness. It is observed that lower *RMSDs* between measured and simulated drying curves are obtained with the experiments performed on 1 mm thick samples. For thicker samples, the results of Du's coefficient were worse.

Figure 2.10 shows two simulations, 2.10 (a) corresponds to a measurement performed on a 1 mm thick sample dried at 60 °C, the *RMSD* obtained is 0.13 and the simulated values show good agreement with the experimental ones. Figure 2.10 (b) shows the same comparison on a 2 mm thick sample dried at 70 °C, the *RMSD* obtained is 0.92, and the simulated values show poor agreement with the experimental ones, with drying times estimated by Du's coefficient being one-third of the actual times, i.e., 500 verses 1,500 minutes.

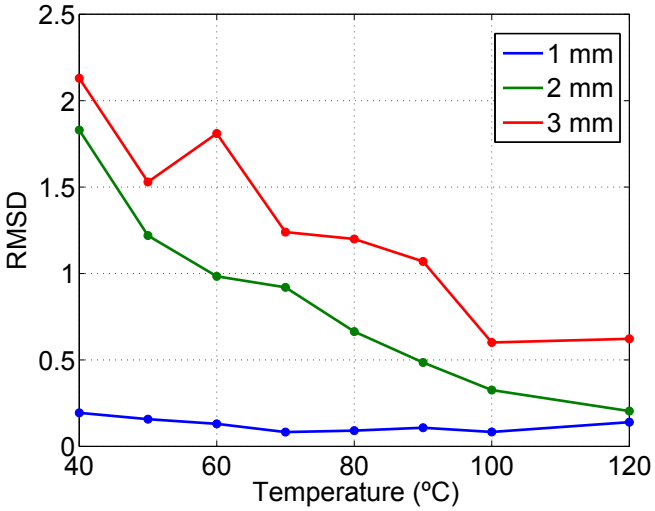

Figure 2.9: *RMSD* of Du's coefficient for non-impregnated pressboard.

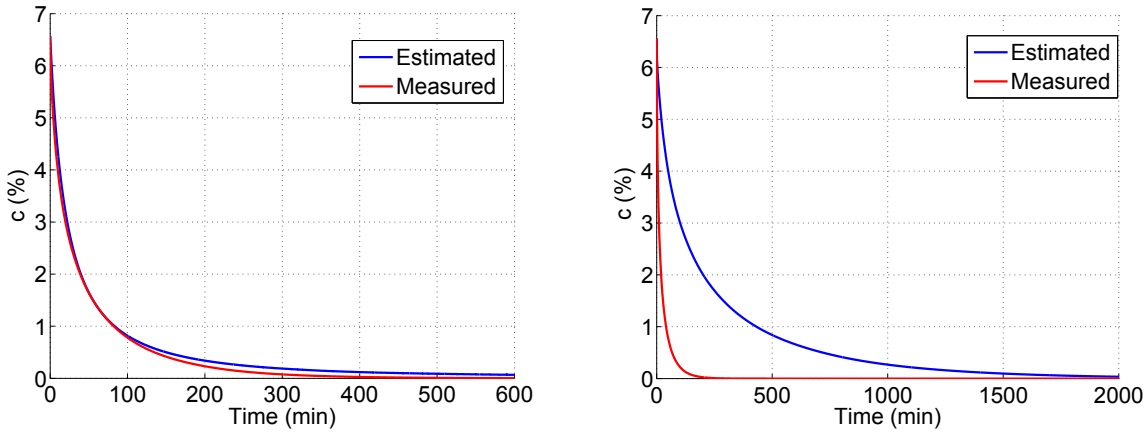

(a) 1 mm thickness at 60 °C.

(b) 2 mm thickness at 70 °C.

Figure 2.10: Simulated and measured drying curves using Du's moisture diffusion coefficient for non-impregnated pressboard.

It is evident that Du's coefficient works well when it is applied to thin samples

while the estimation of the moisture diffusion for thick samples is poor. To understand this result, it must be remarked that all the diffusion experiments performed by Du for the determination of her coefficient were carried out on samples of 1.5 mm thickness, and the obtained results seem to indicate that the coefficient is valid in the thickness range studied, whereas the obtained results are poorer when applied to thicker insulation.

Validation of the coefficients for non-impregnated Kraft paper

In the case of non-impregnated Kraft paper, two different coefficients have been proposed by Foss and Ast (table 2.6), and both are based on Guidi's equation (2.10).

These coefficients are used to simulate the *TGA* drying experiments of Kraft paper samples dried at various temperatures (table 2.7). The *RMSDs* between the simulated and measured values when Foss's or Ast's coefficients are used are shown in figure 2.11.

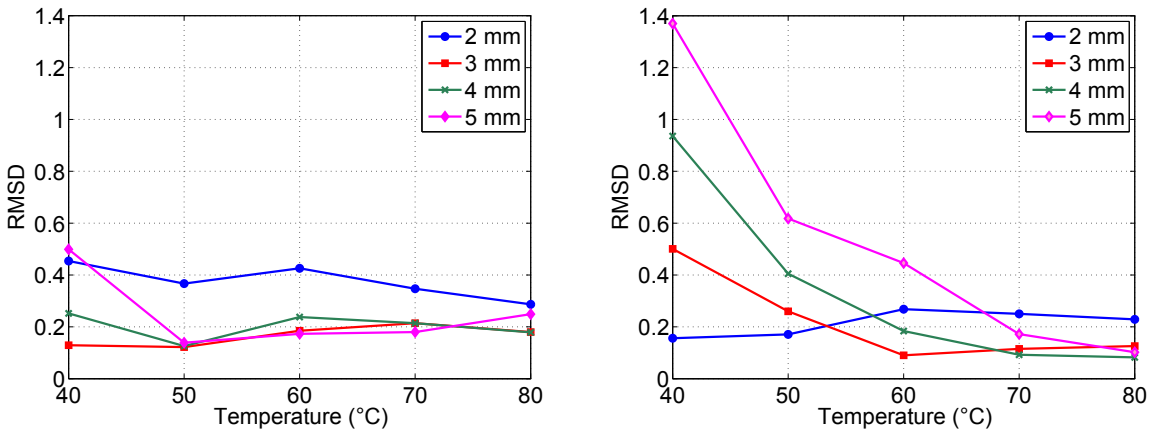

(a) Using Foss's coefficient.

(b) Using Ast's coefficient.

Figure 2.11: *RMSD* of Foss's and Ast's coefficients for non-impregnated Kraft paper.

The experimental and simulated curves for two different cases are plotted in figure 2.12. It can be seen in figure 2.12 that Foss's coefficient is more accurate in most

cases, especially at low temperatures.

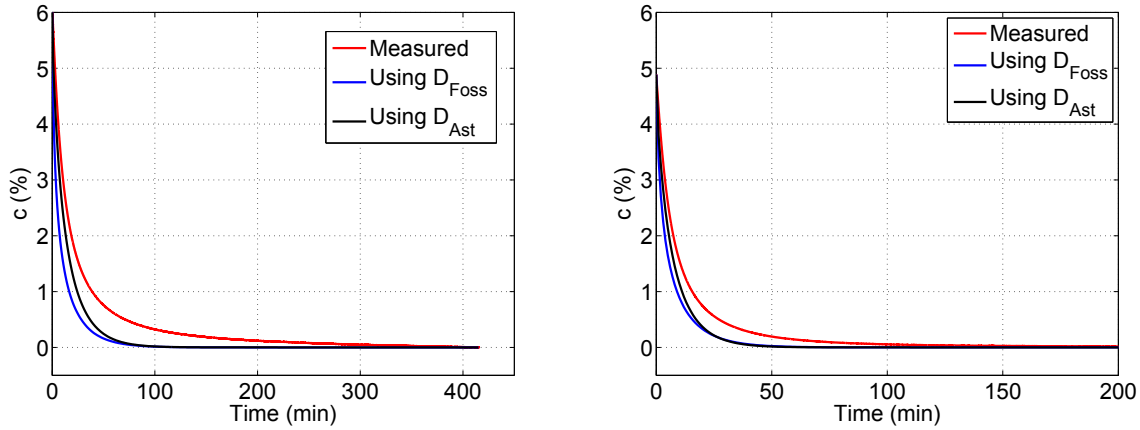

(a) 2 mm thickness at 60 °C.

(b) 3 mm thickness at 80 °C.

Figure 2.12: Simulated and measured drying curves using Foss's and Ast's moisture diffusion coefficient for non-impregnated Kraft paper.

Validation of the coefficients for oil-impregnated Kraft paper

The moisture diffusion coefficients proposed by Foss and Guidi were validated on samples of oil-impregnated Kraft paper of various thicknesses and oil temperatures. The *RMSDs* for the diffusion coefficients are significantly higher than those simulated for non-impregnated insulation. Possible reasons for the increased *RMSD* include the uncertainty in the Karl Fischer measurements and the discrete rather than continuous moisture measurements during the drying experiments.

On the other hand, the determination of the moisture diffusion coefficient in oil-impregnated materials is complex, and the obtained expressions are less precise compared with those on non-impregnated samples. It may also be observed that Guidi's coefficient provides better estimates than does Foss's coefficient. The comparison between the measured and estimated values for two simulations is shown in figure 2.13. The simulations correspond to a 5 mm thick sample dried in oil at 60 °C and a 3 mm thick sample dried at 70 °C.

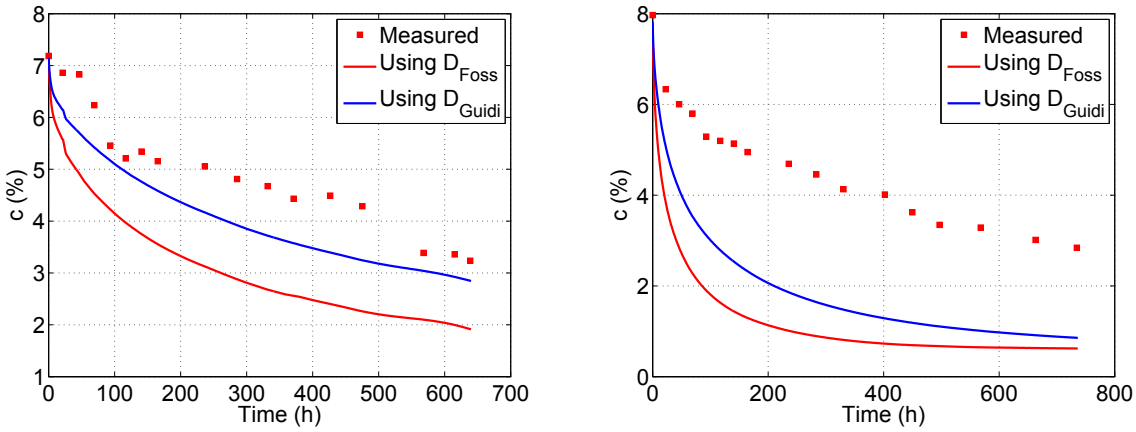

(a) 5 mm thickness at 60 °C.

(b) 3 mm thickness at 70 °C.

Figure 2.13: Simulated and measured drying curves using Foss's and Guidi's moisture diffusion coefficient for oil-impregnated Kraft paper.

From the plots shown in figure 2.13, the moisture level after the drying process was about 3 %, in both cases, and the time to attain this level was nearly 25 days for the 5 mm sample at 60 °C (figure 2.13 (a)) and about 20 days for the 3 mm thick sample dried at 70 °C (figure 2.13 (b)).

In the two simulations, the estimated curves using both moisture diffusion coefficients predicts a moisture level of 3% too fast. This estimation could be considers erroneous because doesn't have good agreement with the experimental ones.

2.6 Conclusions

The diffusion coefficient is an important parameter that allows modelling the moisture dynamics in transformer solid insulation. In order to obtain precise estimations is essential to use accurate, using accurate diffusion coefficients. Various workers have obtained coefficients for Kraft paper and pressboard using diverse methodologies.

One of the more widely accepted expressions for the coefficient is the empirical

equation (2.10) proposed by Guidi. It incorporates the dependence of the coefficient on temperature and moisture concentration. Several workers have determined values of k, D_G and E_a for different materials. The methodologies applied were diverse, and the resulting coefficients sometimes differed substantially for the same material.

In this chapter a revision of all these coefficients has been performed, including a comparison of their predictions. In a previous work, the author of the thesis and his supervisors performed an experimental validation of the coefficients. The main results of that work are summarized in this chapter as well.

As a general conclusion, it appears that the available coefficients to model moisture dynamics in transformer insulation are not as precise as would be desirable in all the studied conditions. It is also important to remark, that, to date, no author have proposed an expression for the diffusion coefficient of mineral-oil impregnated pressboard. Moreover, it has been verified, that the literature on moisture diffusion coefficients in ester-impregnated materials is very scarce.

In the following chapters of the thesis new coefficients are determined for pressboard impregnated with natural esters and with mineral oil.

Chapter 3

Determination of moisture equilibrium curves of paper-ester systems

3.1 Introduction

As was discussed previously, being able to determine the moisture content of the solid insulation of a transformer is highly desirable to optimize the operation and maintenance of the equipment. Unfortunately the direct measurement of this variable is not an easy task, because of the difficulties involved in taking solid insulation samples from in service transformers. Different techniques are used nowadays to estimate moisture content of transformer solid insulation, as the application of dielectric response measurements [47] or the application of on-line monitoring systems [48].

Several authors have developed equilibrium curves that allow calculating the moisture content of paper when the temperature and the moisture in oil are known. The curves are based in the fact that the amount of water accepted by cellulose and by oil depends on the temperature. While cellulose's affinity for water decreases as the temperature increases, the behaviour of the oil is the opposite. In consequence, the moisture will migrate from one material to the other when the temperature changes [13].

It should be noted that moisture-equilibrium curves are only valid under equilibrium conditions. In real operation the temperature of a transformer is related to its load and to the atmospheric temperature and so, equilibrium conditions would not be generally attained.

Most of the equilibrium charts available to date are based on mineral oil-paper insulation. Recently, some curves have been proposed for ester-cellulose systems as well.

The moisture-equilibrium curves for mineral oil-paper insulation system were first reported by Fabre and Pichon in 1960 [49]. The curves were obtained by direct measurement of the moisture content of oil and oil-impregnated pressboard.

Another set of moisture equilibrium curves were proposed by Oommen in 1983 [50], which were obtained by combining the moisture sorption data of non-impregnated paper with the moisture sorption data of oil under different temperatures.

Oommen's indirect method is based on the principle that the equilibrium curves represent the same relative saturation for the oil and for the paper at the same temperature.

Several authors have used the method proposed by Oommen to develop additional curves in mineral-oil-cellulose systems, as Griffin [51], Du [15], and most recently Maik Koch in [52].

As previously discussed, ester fluids are much more hygroscopic than mineral oils, which are hydrophobic . In consequence the moisture equilibrium curves of ester-cellulose systems will be very different from those of mineral oil. Some authors have proposed curves for these materials.

In 2011 Jovalekic et al. [17] obtained moisture equilibrium curves using mineral

oil, natural esters and synthetic esters as insulating liquids.

In 2014 Vasovic et al. [18] developed moisture equilibrium curves using mineral oil and natural esters as insulating liquids, and Kraft paper and pressboard as cellulosic insulation.

In this chapter the equilibrium curves of a mineral oil and two natural esters are determined using the indirect method proposed by Oommen [50]. To obtain the curves, experiments were done focused in studying the water saturation limits of the different insulating liquids.

The proposed curves are later used to determine the diffusion coefficients of mineral-oil impregnated and ester-impregnated pressboard, and as a boundary condition of the dynamic model proposed in chapter 7.

3.2 Methodology applied to obtain the moisture equilibrium curves

The equilibrium curves determined in this thesis were obtained using the method proposed by Oommen in [50, 53].

The method is based on a simple physical law, the relative moisture content W_{rel} in adjacent materials become equals under equilibrium conditions. The surrounding medium could be air or oil, supposed they are at the same temperature and pressure.

$$W_{rel,cel} = W_{rel,oil} = RH \tag{3.1}$$

where $W_{rel,cel}$ is the relative moisture content of the cellulose (%), $W_{rel,oil}$ is the

relative moisture content of the oil (ppm), and RH is the relative humidity of the surrounding air (%).

In consequence, the paper-oil equilibrium curves can be obtained by combining the *moisture in oil* versus *relative humidity* curves in air with *moisture in paper* versus *relative humidity* curves in air, according with the following steps:

1. Plot isotherms showing percent moisture in paper vs. relative humidity.
2. Obtain water saturation levels in oil as a function of relative humidity.
3. Combine the two sets of data obtained in steps 1 and 2 to obtain a new set of isotherms

To achieve point 2 it is necessary to determine the solubility curve of the insulating fluid that is being studied. The water solubility for oil can be expressed in Arrhenius forms as:

$$LogW_S = A - \frac{B}{T} \tag{3.2}$$

where W_s is the saturation solubility of water in oil in ppm and T is the temperature in Kelvin, and A and B are the parameters dependent on the properties of the fluid.

The method described above has been used in this chapter to determine the equilibrium curves of different systems, i.e. paper-mineral oil and paper-natural ester fluids. The solubility equations of the different fluids were obtained experimentally as will be explained next. To define the equilibrium condition in paper, Jeffries curves, shown in figure 2.6, were applied [5].

The relation between the moisture content in oil and the relative humidity of the surrounding air can be expressed as follows:

$$W = W_s \cdot RH \tag{3.3}$$

where W is the moisture content of the oil (ppm), W_s is the water saturation solubility of the oil (ppm) at temperature T, and RH is the relative humidity of oil, which is equal to the relative humidity of the surrounding air (%).

3.3 Experimental procedure

Solubility experiments were carried out on different kinds of fluids at various temperatures and 50% of relative humidity, these experiments are summarized in table 3.1. In all cases new materials were used for the experiments. The experiments were done in an environmental chamber, shown in figure 3.1.

Table 3.1: Summary of the temperatures and relative humidities characterized in the solubility experiments.

Insulating liquids	**Temperatures (°C)**	***RH* (%)**
Mineral oil	30, 40, 50, 60, 70 and 80	50
Biotemp		
Bioelectra		

For this work, eighteen solubility experiments were performed on two kinds of natural esters and on mineral oil. 50 ml of the three analysed fluids were put in glass containers inside the environmental chamber. Humidity and temperature were set to a constant value until the equilibrium was reached between the environment and the fluids.

The moisture content in oil samples was measured every two days until the equilibrium was reached. A sample was considered to be in equilibrium, when its moisture

content remained constant for 6 days. All the moisture measurements were performed using Karl Fischer titration method, according to the international standard IEC 60814 [46].

Figure 3.1: Environmental chamber used in the solubility experiments.

The natural esters used in this work were Bioelectra by Repsol and Biotemp by ABB, whose technical characteristics are shown in table 3.2. Also, the mineral oil Nytro Taurus, by Nynas, was used to determine and compare the solubility curves of mineral oil with those of natural esters. The technical characteristics for this oil are shown in table 3.3. All the oil samples used in this work were new.

Table 3.2: Biotemp and Bioelectra technical characteristics.

	Biotemp	**Bioelectra**
Viscosity at 40 °C	45 cSt	39.2 cSt
Moisture content	150 ppm	150ppm
Flash point min limit	330 °C	330 °C
Pour point max limit	-15 °C	-26 °C
Dielectric Breakdown	65 kV	65 kV
Power Factor	0.2 % 100 °C	0.3 % 100 °C
Source	Sunflower seed	Sunflower seed

Table 3.3: Nytro Taurus technical characteristics.

	Method	**Value**
Viscosity at 40 °C	ISO 3104	10 mm^2/s
Density at 20 °C	ISO 12185	0.870 kg/dm^2
Flash point min limit	ISO 2719	152 °C
Pour point max limit	ISO 3016	-48 °C
Breakdown voltage	− − −	− − −
- Before treatment	IEC 60156	30 kV
- After treatment	IEC 60156	70 kV

3.4 Results

3.4.1 Water saturation limits of insulating liquids

Table 3.4 shows the results obtained from the solubility experiments summarized in table 3.1. As is explained in [17], the water content in oil have a linear increase with the relative humidity in the oil. In order to calculate the water saturation content in all oils, the data obtained in the solubility experiments (table 3.4) were extrapolated according with the equation (3.3).

Table 3.4: Water content of the three fluids at 50% of relative humidity (expressed in ppm) obtained from the solubility experiments.

	Temperature (°C)					
Insulating liquids	**30**	**40**	**50**	**60**	**70**	**80**
Mineral oil	38	58	80	119	171	228
Biotemp	575	699	837	1001	1182	1330
Bioelectra	590	720	860	1030	1210	1405

Figure 3.2 shows the calculated water content in oil for both natural esters, and the mineral oil used in this work for the entire range of relative humidities.

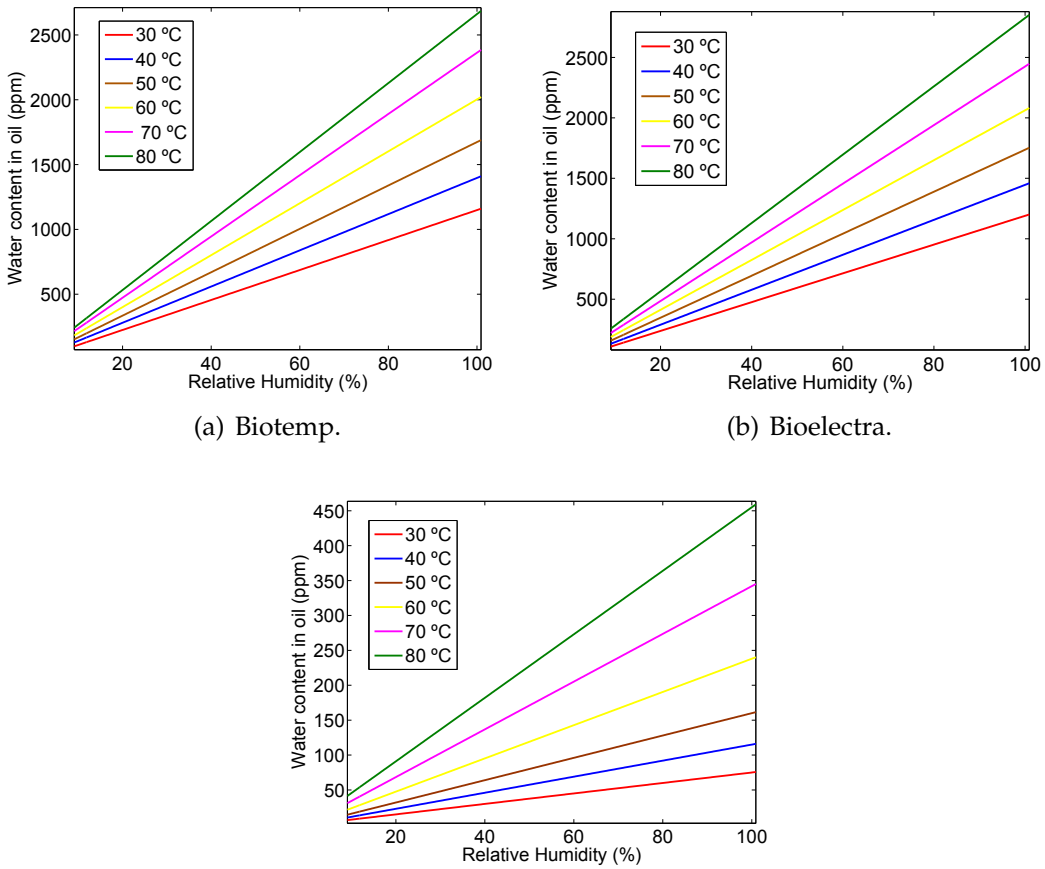

(a) Biotemp.

(b) Bioelectra.

(c) Mineral oil.

Figure 3.2: Calculated moisture content in oil at different temperatures and relative humidities.

As it was mentioned in the previous paragraph, the water saturation limits of the three fluids were calculated from the experimental data obtained in the lab using the equation 3.3, finding the values shown in table 3.5.

As can be seen, both natural esters have similar saturation limits, while the saturation limit for mineral oil is considerably lower than those of natural esters. This is due to the polar composition of mineral oil, their non-polar molecule structure is not able to establish a Van Der Vaals bond with water, as was explained before in this chapter.

Table 3.5: Calculated water saturation content (100% of relative humidity) of the three fluids expressed in ppm.

	Temperature (°C)					
Insulating liquids	**30**	**40**	**50**	**60**	**70**	**80**
Mineral oil	75	115	160	238	342	455
Biotemp	1152	1397	1673	2003	2363	2660
Bioelectra	1180	1440	1720	2060	2420	2810

Figure 3.3 (a) shows the water saturation values of all kinds of oils used in this work, for the mathematical description of the saturation curves, a function can be used as seen in equation (3.2). The Arrhenius equation was used to determine the water saturation parameters A and B for the different fluids used in this work (figure 3.3 (b)). The parameters found in each case are given in table 3.6.

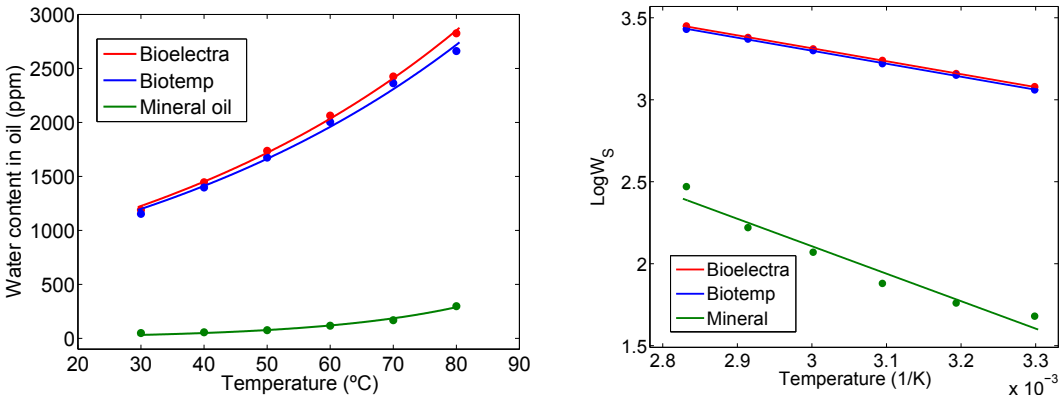

(a) Water solubility.

(b) Linearised values after applied the Arrhenius equation.

Figure 3.3: Water solubility of vegetable and mineral oil as a function of temperature and the linearised values using the Arrhenius equation.

Table 3.6: Parameters A and B of equation 3.2 calculated for both natural esters and mineral oil.

	A	**B**
Biotemp	5.67	791
Bioelectra	5.74	808
Mineral oil	7.44	1,686

3.4.2 Moisture equilibrium curves determination

To establish the moisture equilibrium curves of oil-paper, the moisture in paper vs. relative humidity curves of figure 2.6 and the moisture content in oil vs. relative humidity (figure 3.2) were combined using the equation 3.1, as is explained in section 3.2. The obtained curves are shown in figure 3.4. Figure 3.4 (a) and 3.4 (b) show the curves of a paper-Biotemp and a paper-Bioelectra system, while figure 3.4 (c) shows the obtained curves for a paper-mineral oil system. As can be seen ester fluid are able to adsorb a much greater amount of water under the same conditions of temperature and moisture in paper.

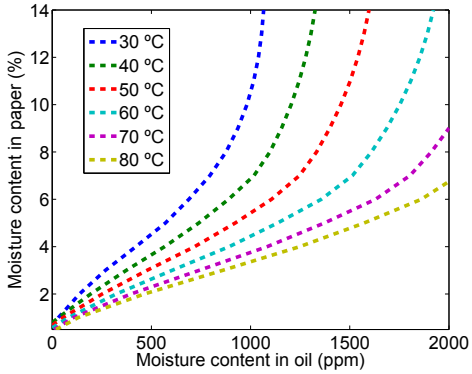

(a) Biotemp.

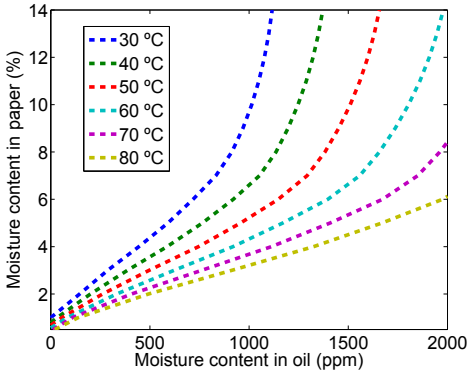

(b) Bioelectra.

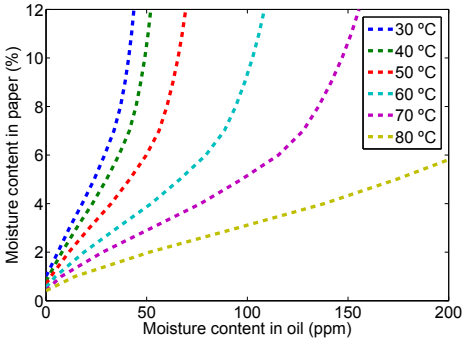

(c) Mineral oil.

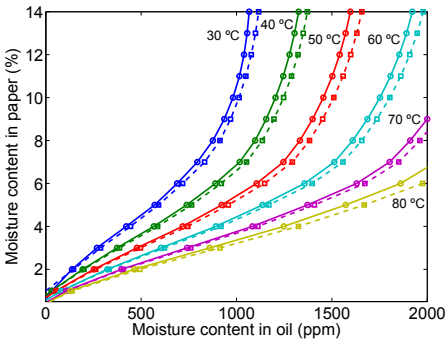

(d) Comparison using natural esters, solid line shows the equilibrium curves for Biotemp and dotted line shows the equilibrium curves for Bioelectra.

Figure 3.4: Moisture equilibrium curves for paper-oil system in natural esters and mineral oil.

Figure 3.4 (d) shows a comparison between both kinds of esters. As can be seen their behaviour are very close and the equilibrium is attained at similar conditions in both of them. However Bioelectra has a slightly bigger water absorption capacity compared to Biotemp.

3.5 Parametrization of the equilibrium curves

In [54], Fessler proposed equation (3.4) to parametrize the equilibrium curves of mineral oil-paper insulation. This equation has been widely accepted and used by several authors, as it eases the inclusion of the moisture equilibrium curves in simulation models.

$$C_{equil} = 2.173 \cdot 10^{-5} \cdot p_v^{0.6685} \cdot e^{\left(\frac{42{,}725.6}{T}\right)} \tag{3.4}$$

where C_{equil} is the equilibrium moisture in pressboard, expressed in %, and T is the temperature in oil-pressboard interface.

An equation similar to (3.4) has been obtained to parametrize the equilibrium curves of natural ester-paper systems. To this aim a fitting process was carried out using the curves in figure 3.4 obtainig equation 3.5. This equation allows the calculation of moisture concentration in paper, knowing the moisture content in oil.

$$\begin{aligned} C_{equil\_vegetal} = {} & 1.18 \cdot 10^{-18} \cdot {p_v}^3 \cdot e^{\left(\frac{16{,}570}{T}\right)} - 5.39 \cdot 10^{-12} \cdot {p_v}^2 \cdot e^{\left(\frac{10{,}960}{T}\right)} \\ & + 9 \cdot 10^{-6} \cdot p_v \cdot e^{\left(\frac{5{,}418}{T}\right)} + \frac{1{,}004}{T} - 3 \end{aligned} \tag{3.5}$$

where $C_{equil\_vegetal}$ is the equilibrium moisture in pressboard impregnated with natural ester, expressed in %, T is the temperature in oil-pressboard interface.

For both equations, p_v is the partial pressure of water vapour, expressed in atmospheres, and can be calculated from oil relative humidity RH as:

$$p_v = RH \cdot p_{v,sat} = \frac{ppm}{ppm_{sat}} \cdot p_{v,sat} \tag{3.6}$$

where ppm is moisture concentration in oil expressed in parts per million (ppm) and ppm_{sat} and $p_{v,sat}$ are moisture concentration and partial pressure (atm) in saturation condition of the oil [23]. The moisture concentration for saturation can be obtained from the equation (3.2), and the partial pressure of the saturated water can be calculated by the correlation proposed by Foss in [55] (equation 3.7).

$$p_{v,sat} = \frac{P_c}{760} \cdot 10^{\left[\left(\frac{T_{ex}-T_c}{T_{ex}}\right)\cdot\left(\frac{a+b\cdot(T_c-T_{ex})+c\cdot(T_c-T_{ex})^3}{1+d\cdot(T_c-T_{ex})}\right)\right]} \tag{3.7}$$

where $p_{v,sat}$ is the partial pressure (atm) in saturation condition, P_c is the critical pressure of the water, $P_c = 1,65807 \cdot 10^5$ (mmHg), T_c is the critical temperature of the water, $T_c = 647,26$ (K), the parameters $a = 3,2437814$, $b = 5,86826 \cdot 10^{-3}$, $c = 1,1702379 \cdot 10^{-8}$, and $d = 2,1878462 \cdot 10^{-3}$ are constants.

3.6 Conclusions

A new set of curves is proposed in this chapter to determine the moisture equilibrium in different systems of insulation. Curves for vegetable oil-paper and mineral oil-paper systems were experimentally obtained.

A comparison is given for the moisture equilibrium curves of vegetable paper-oil insulation and mineral oil-paper insulation. The result shows that the moisture content in vegetable oil is much greater than that in mineral oil when sharing the same moisture content in paper.

The differences between the moisture equilibrium curves in vegetable paper-oil insulation and mineral paper-oil insulation are mainly due to the fact that the ester group in the molecules of vegetable oils has a strong ability to participate in hydrogen bonding.

An equation to parametrize the curves in ester-paper systems is proposed, which can be used to integrate the curves in theoretical models. This equation will be used in the following chapters of the thesis.

Chapter 4

Particle Swarm Optimization and Genetic Algorithm

4.1 Introduction

From a classical approach, the experimental determination of the moisture diffusion coefficient in most solid hygroscopic materials is a difficult task, because it is necessary to know the evolution of the moisture distribution inside the insulation samples during a moisture transient process such as drying or wetting [23, 30, 31, 32, 39].

In previous studies [6, 25, 42, 56], a new methodology to determine the moisture diffusion coefficient in cellulosic insulations (Kraft paper and pressboard) was proposed. Unlike the classical approach, this methodology required measurement of the average moisture evolution in the insulation samples during drying (drying curve), which is easier to carry out from the experimental point of view. However, to find the moisture diffusion coefficient, this methodology needs an optimization process whose objective function includes a diffusion drying model solved by the finite element method (FEM drying model) which was implemented by means of the computational tool Comsol Multiphysics, according to that explained in section 2.2.1.

Due to the presence of the FEM drying model, the objective function is not a differentiable function; therefore, classical optimization methods based on the gradient (e.g. Levenberg-Marquard or Newton-Raphson) cannot be used.

The optimization problem of finding the global minimum or maximum of a function has been an interesting research area for scientists and engineers. Genetic algorithms (GA's), as a branch of evolutionary algorithms, and particle swarm optimization (PSO), as a branch of swarm intelligence, are some useful paradigms in such cases. PSO and GA's are population-based meta-heuristics, which means that both searches are based on social components, but PSO is simpler than the GA in operation because PSO does not realize mutation and crossover [57]. PSO works with real-numbers in its operation, avoiding encoding and decoding binary strings, so making PSO easy to implement with less dimensions to the problem compared with GA's.

PSO is a global optimization algorithm for dealing with problems in which a best solution can be represented as a point or surface in an n-dimensional space; it does not need sort elements, as in the GA, and this also reduces the computational load when the number of agents is large (typical of the GA).

As aforementioned, in the previous methodology, to determine the moisture diffusion coefficient of cellulose insulations, an optimization process based on GA's was used. The convergence of the GA optimization process was determined by comparing a pre-defined fitness value with the objective function output. The objective function can be the Euclidean distance or the root mean square deviation ($RMSD$) between the experimental drying data and those estimated from the FEM drying model.

Because of the way that the GA optimization process works, during the determination of the moisture diffusion coefficient, optimization of each experimental data had to be repeated several times and after this it is necessary to carry-out statistical analysis. For this reason, the determination of the moisture diffusion coefficient using the optimization process based on GA's took a long time. As an alternative to the GA,

a PSO method was considered.

In this chapter, an optimization process for determining the moisture diffusion coefficient of cellulosic insulations, based on the particle swarm method, was implemented and validated. PSO reduces significantly the time spent in moisture coefficient determination. Also, with the PSO algorithm, the statistical analysis required when the optimization process based on the GA is used is unnecessary, this is because all particles are accelerated towards those particles within their communications grouping which have better fitness values, so that the values of the parameters are considered valid for the diffusion model [58]. Therefore, the PSO process can be considered as an improvement to the methodology to determine moisture diffusion coefficients on a transformer's solid insulations.

The aim of this chapter is to use and compare two optimization techniques widely used in the engineering and mathematics area for the determination of moisture diffusion coefficients in cellulose insulation of transformers. It is not the intent of this work to modify any of the optimization methods neither to question its efficiency since they may vary depending on the problem to be solved.

4.2 Particle Swarm Optimization (PSO)

PSO was proposed in 1995 by Kennedy and Eberhart [59]. It is an optimization technique, inspired by flocks of birds and schools of fish to fly or swim synchronously; such animal behaviour is used to search for solutions in optimization problems. PSO is similar in some ways to the GA, but requires less computational bookkeeping and generally fewer lines of code.

PSO comprises individuals, called **particles** that follow a trajectory with stochastic components to find a solution in the search space of an objective function. Each

particle represents a possible solution to the problem and its trajectory is defined iteratively with a velocity that has three major components:

- **Social component:** the effect of the best position found by all particles until the current iteration; that is called the current global best position (G_{best}).
- **Cognitive component:** the effect of the best position found by each particle until the current iteration, called the current best for the i-th particle (P_{best}), where i is the index of each particle.
- **Momentum component:** introduces the effect of the previous velocity of each particle; this is a modification of the original PSO, which was introduced by Shi and Eberhart [60].

With this component, the PSO evaluates each n particle t times to update the positions with the calculation of the velocity as shown in the following equations.

$$V_{i(t+1)} = \omega \cdot V_{i(t)} + C_1 \cdot R_1 \left(P_{best} - X_{i(t)} \right) + C_2 \cdot R_2 \left(G_{best} - X_{i(t)} \right) \tag{4.1}$$

$$X_{i(t+1)} = X_{i(t)} + V_{i(t+1)} \tag{4.2}$$

where C_1 and C_2 are parameters to modify the weight of the social and cognitive components, ω is the inertial coefficient and the learning coefficients, R_1 and R_2, are random vectors drawn from a uniform distribution. When the algorithm finishes, all particles converge on one solution. The appropriate choice of this inertial weight provides a balance between global and local exploration, and results in fewer iterations, on average, to find a sufficiently optimal solution [61].

PSO has had wide acceptance in the research and engineering community due to its easy implementation; when each particle has a simple behaviour and few operations to show the complexity of the whole particle swarm [62], every particle evaluates

the objective function so making the computational load and run time depend on the complexity of that function [63].

PSO works based on the social adaptation of knowledge, and all individuals are considered to be of the same generation. One of the disadvantages of PSO is the fast search causing the algorithm to become trapped in the local optimum [64].

4.3 Genetic Algorithm (GA)

As mentioned earlier Genetic Algorithms belong to the larger class of evolutionary algorithms (EA), which generate solutions to optimization problems using techniques inspired by natural evolution, such as mutation, selection, and crossover. The GA works based on evolution from generation to generation, so the changes of individuals in a single generation based on swarm attitude are not considered [65]. As genetic algorithms are not deterministic methods, there is no guarantee that the optimum result found is not a local minimum. The probability of finding a local minimum can be minimized by introducing a high degree of randomness in the optimization process, mainly during the generation of the initial population.

4.4 Diffusion coefficients

The methodology to determine the moisture diffusion coefficient of impregnated pressboard insulation involves three steps: the first consists of undertaking a drying experiment in which the pressboard samples are subjected to a drying process by exposing them to a hot and dry fluid flow. This drying method is called the hot-oil (HO) drying method. The fluids used as the drying agents are the same as those used to impregnate the pressboard samples.

The second step of the methodology is to simulate the drying experiment; this is carried out by means of a drying model based on Fick's second law (equation 4.3), as explained in chapter 2, and solved by the FEM.

$$\frac{\partial c}{\partial t} = \frac{\partial}{\partial x}\left(D \cdot \frac{\partial c}{\partial x}\right) \tag{4.3}$$

where c is the local moisture concentration in the material (expressed in %) and D is the moisture diffusion coefficient of the cellulosic insulation (expressed in m^2/s).

Finally, the third step of the methodology for determining the moisture diffusion coefficient consists of finding the parameters (k and D_0) to the general expression of D shown in equation (4.4), this general equation also has been mentioned in previous chapters. This can be done by fitting the estimated drying curves obtained from the FEM model to the experimental ones. This can be addressed as an optimization problem. As mentioned above, in the present chapter a basic PSO method and GAs were developed.

$$D_{(c,T)} = D_0 \cdot e^{k \cdot c} \tag{4.4}$$

where D is the moisture diffusion coefficient, D_0 (expressed in m^2/s) is a pre-exponential factor that determines the dependence of the moisture diffusion coefficient with certain variables, for example, temperature, and k is a dimensionless parameter relating the moisture diffusion coefficient with c.

As in the chapter 2, the agreement of the estimated average moisture concentration values of the drying curves calculated with the FEM model (c_{m-est}) and the experimental (c_{m-exp}) depends on the value of the parameters k and D_0 used in the FEM drying model, t_i is the instant of the drying experiment when the i-th measurement was performed. This condition was used to define the objective function (OF) of the optimization process, which is the $RMSD$ calculated from the following expression.

$$RMSD = \sqrt{\frac{1}{n}\sum_{i=1}^{n}\left[c_{m-est(t_i)} - c_{m-exp(t_i)}\right]^2} \tag{4.5}$$

The same optimization scheme was used to calculate the $RMSD$ with the two types of algorithms studied. Figure 4.1 shows the general optimization scheme used.

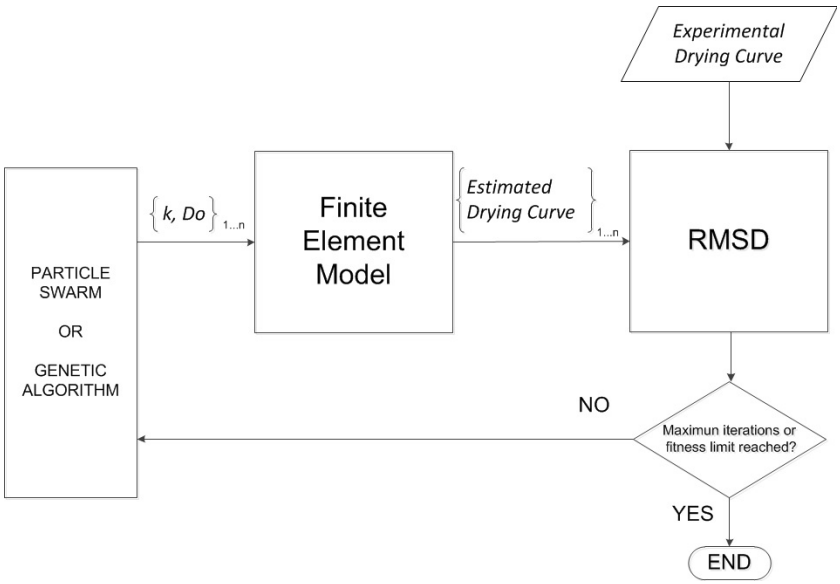

Figure 4.1: General scheme of the optimization process.

On addition, figure 4.2 shows a flow chart of the basic optimization process based on particle swarm. The parameters used in the basic PSO algorithm are shown below in table 4.1. The ω, C_1 and C_2 values used in this work are those proposed by Trelea in [66], ω = 0.729, C_1= C_2=1.494.

Table 4.1: Parameters used for PSO.

Parameters	**Value**
Number of particles	30
Iterations	50
Inertia weight	0.729
C_1 and C_2	1.494
Velocity max.	ω^{-1}
Velocity max.	- V_{max}

Despite the high robustness of PSO to obtain the k and D_0 parameters of the moisture diffusion coefficient using PSO ten optimizations following the procedure

described in figure 4.2 were carried out for each experimental drying curve to avoid local minimums in searching of the OF.

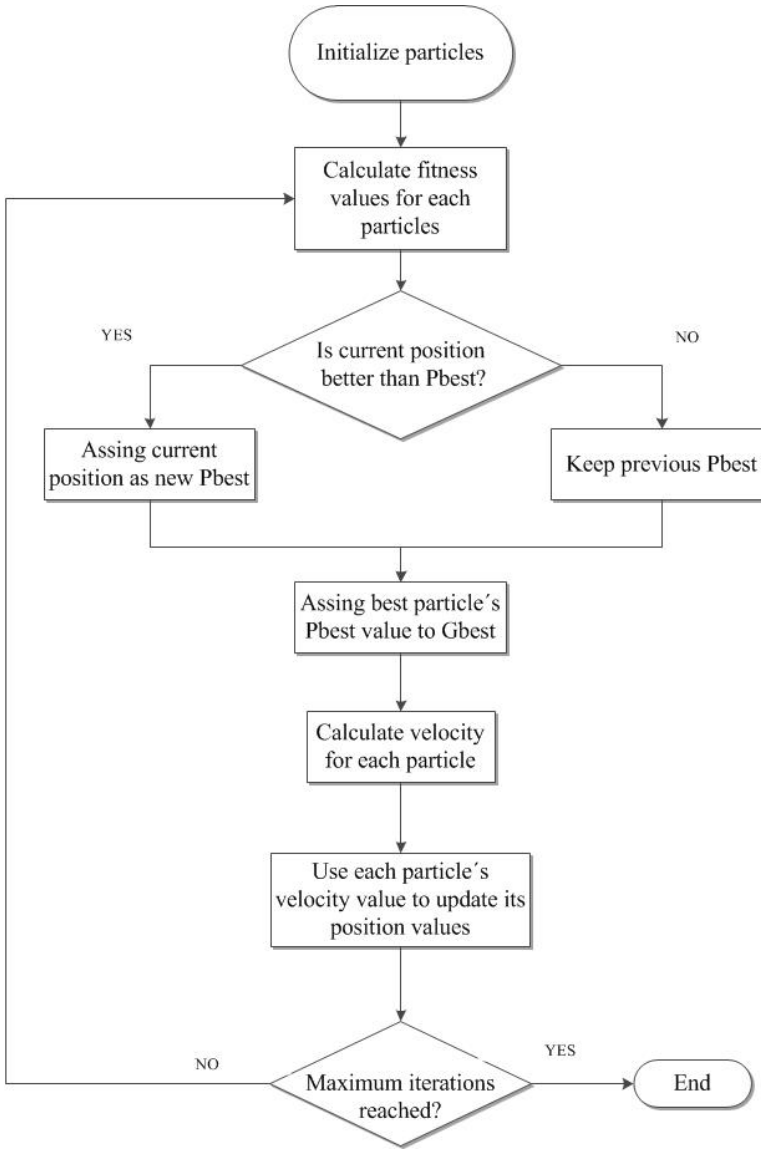

Figure 4.2: Diagram of PSO algorithm.

Figure 4.3 shows a flow chart of the optimization process based on GA's. The parameters used for the GA algorithm are shown in table 4.2.

Due to the low robustness of the optimization method based on GA, evidenced in the scattering of the OF outputs from all the individuals in any generation, repetition of the process several times is required for each experimental data, increasing the

time spent on the optimization. Furthermore, to obtain a valid set of the parameters k and D_0 by using the optimization based on GAs, a subsequent statistical analysis is necessary.

To obtain the k and D_0 parameters of the moisture diffusion coefficient using GA thirty optimizations following the procedure described in figure 4.3 were carried out for each experimental drying curve.

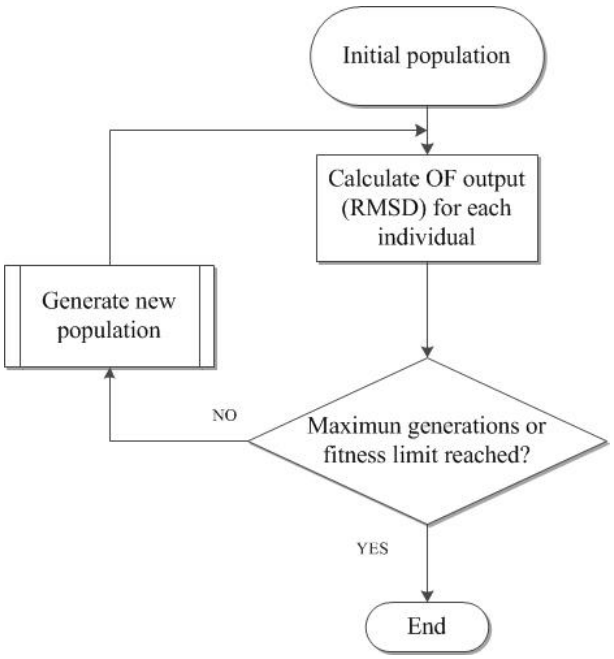

Figure 4.3: General scheme of the optimization process.

Table 4.2: Parameters used for GAs.

Parameters	**Value**
Population size	500
Generations	10
Fitness limit	0.5
Elitecount	5
Crossover Fcn.	crossoverpoint
Mutation Fcn.	mutationadaptfeasible
TolFun	FitnessLimit/10

4.5 Experimental results and discussions

In this section, the results obtained by applying the GA and PSO to find the parameters k and D_0 of the moisture diffusion coefficient are shown. Both optimization processes were employed to find the parameters k and D_0 corresponding to 39 drying curves obtained from the experimental conditions summarized in table 4.3. Type 1 were pressboard samples impregnated with the mineral oil Nytro Taurus by Nynas, type 2 were pressboard samples impregnated with the natural ester Bioelectra by Repsol and type 3 were samples impregnated with the natural ester Biotemp by ABB.

Table 4.3: Summary of the conditions used in the experiments.

Samples	**Drying temperatures (°C)**	**Thicknesses (mm)**
Type 1	60, 70 and 80	0.5 and 3
Type 2 and Type 3	40, 50, 60, 70 and 80	

4.5.1 Optimization times

Table 4.4 shows the optimization times required when applying both optimization methods. It can be seen that the times required when the GA optimization method is used, are considerably higher than those using PSO. This is because the GA requires the optimization process to be applied at least 30 times, to find a set of valid values of the parameters k and D_0 for each experimental data. Unlike the GA, in PSO all the particles are guided by the best global position, moving towards the minimum value of the Objective Function. Therefore, the PSO process is required to be applied only once, decreasing the time spent in finding the moisture diffusion parameters. Also, when PSO is used, statistical analysis is not required.

Table 4.4: Optimization times using PSO and GA.

		Optimization times (minutes)					
		Sample type 1		Sample type 2		Sample type 3	
Temperature	**Thickness**	**PSO**	**GA**	**PSO**	**GA**	**PSO**	**GA**
40 °C	1 mm	—	—	30.78	634.21	46.31	880.80
	2 mm	—	—	36.51	743.39	52.32	1090.42
	3 mm	—	—	38.80	908.53	53.96	1071.3
50 °C	1 mm	—	—	35.79	543.13	39.57	637.98
	2 mm	—	—	31.73	471.02	44.26	900.79
	3 mm	—	—	33.45	444.10	47.46	996.50
60 °C	1 mm	50.48	1032.29	31.81	694.00	45.01	1192.46
	2 mm	42.02	1026.13	33.98	780.22	45.65	1037.68
	3 mm	43.57	1074.95	33.73	754.06	48.37	1207.65
70 °C	1 mm	38.83	903.43	32.52	801.34	43.16	634.39
	2 mm	40.47	982.50	36.67	769.70	40.67	553.44
	3 mm	44.40	848.13	45.82	854.13	44.41	571.10
80 °C	1 mm	35.79	721.66	35.35	786.80	40.47	604.58
	2 mm	34.96	780.66	26.20	672.56	33.18	506.50
	3 mm	34.40	621.17	26.83	1071.30	32.27	456.90
Average times		40.55	887.88	34.00	728.52	43.80	822.63

4.5.2 Root mean square deviation (*RMSD*)

Figure 4.4 shows two experimental drying data and the corresponding estimated drying curves obtained from the FEM model when the diffusion coefficient is calculated using the parameters k and D_0 obtained by using the GA and PSO methods.

In both cases, it can be seen that the estimated curves using the diffusion coefficient from the parameters k and D_0 obtained by particle swarm fit better to the experimental curves than those obtained when the diffusion coefficient was obtained by the GA. The quality of the agreement is quantified based on the $RMSD$ values. Validations were undertaken for all the experiments summarized in table 4.3. Some of the $RMSD$ values obtained are show in figure 4.5.

As mentioned above, the PSO method is more robust than the GA method because, during the exploration of the search space, all particles guided by the best global

position move towards the minimum value of the OF. This behaviour may be demonstrated by the standard deviation which quantified the dispersion of the $RMSD$ values obtained for each particle in each iteration. A low standard deviation indicates that the $RMSD$ values tend to be very close to the mean; a high standard deviation indicates that they are spread out over a large range of values. Therefore, by choosing an appropriate number of particles and iterations, the PSO method does not need statistical analysis, as is the case with the GA.

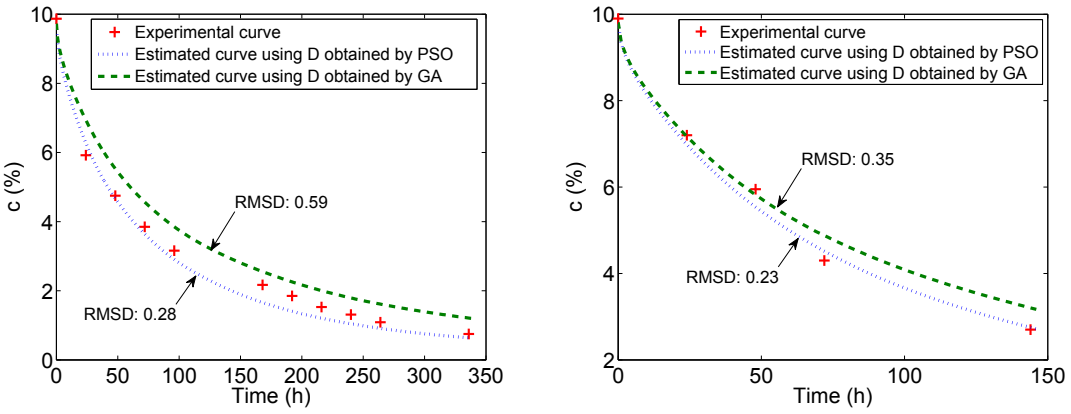

(a) 70 °C and 2 mm sample thickness.

(b) 80 °C and 3 mm sample thickness.

Figure 4.4: Experimental drying curves and estimated drying curves using D obtained by PSO and GA.

According to the $RMSD$ values shown in figure 4.5, PSO proved a better estimation of the parameters k and D_0 than GAs, because the values are lower than those obtained using GAs. This trend continued in all experiments.

Figure 4.6 shows the standard deviation and the best $RMSD$ of each iteration or global best (G_{best}) for the optimization process by PSO over the experimental data of pressboard samples of 3 mm thick, dried at 60 °C using the three studied fluids.

Figure 4.6 (a) clearly shows the tendency of the value of the standard deviation to decrease to the mean, increasing the number of iterations. This means that, for all iterations, the particles follow a leader and approach the minimum value of the OF.

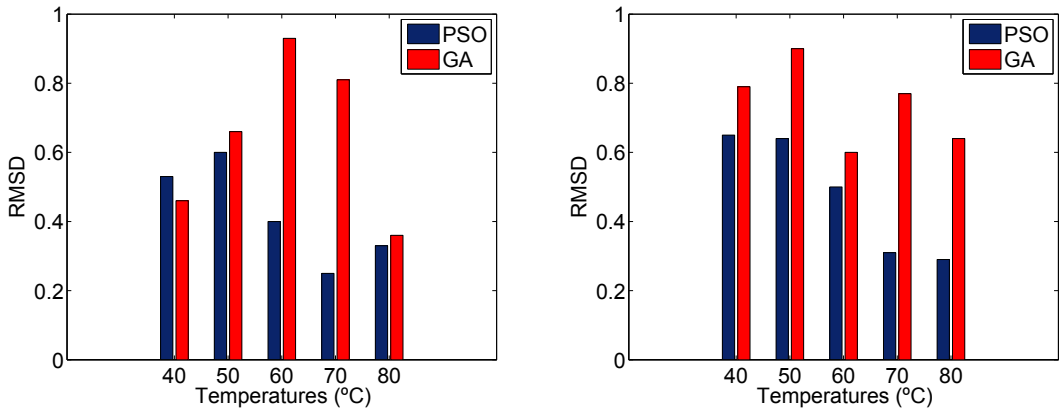

(a) Type 2. (b) Type 3.

Figure 4.5: *RMSD* using moisture diffusion coefficient for both optimization methods determined.

Likewise, figure 4.6 (b) shows that the best position of the swarm improves with increasing iterations. This means that the particles have a social behaviour and follow a leader with the best position, also providing evidence that the minimum function value with few iterations is reached (between 10 and 15). This behaviour was observed for all thicknesses and temperatures studied in this chapter.

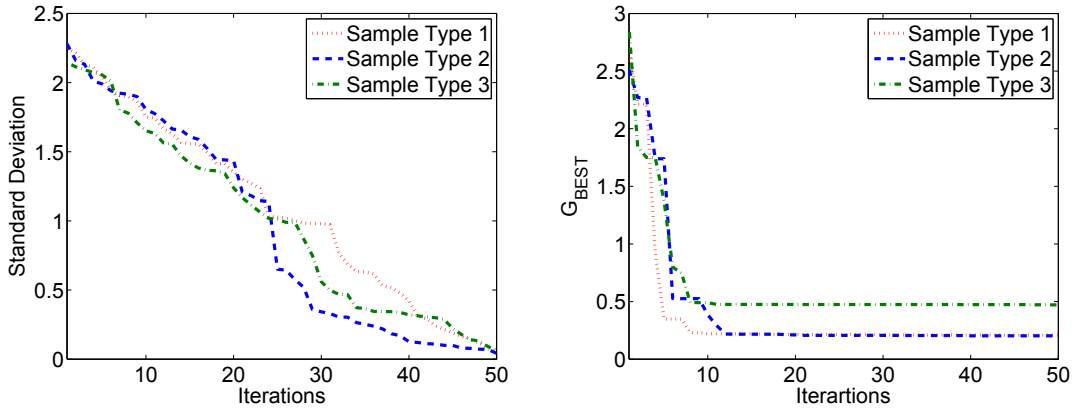

(a) Standard deviation. (b) 80 °C and 3 mm sample thickness.

Figure 4.6: PSO results from 3 mm thick samples dried at 60 ºC.

4.6 Conclusions

In this chapter, a new optimization process based on the particle swarm algorithm was implemented and used to determine the moisture diffusion coefficients of impregnated pressboard insulations.

The parameters of the moisture diffusion coefficient of three types of impregnated pressboard insulations, obtained by the optimization method implemented in this chapter, were validated by comparing the estimated and experimental drying curves.

During validation, good agreement between the estimated and the experimental drying curves was observed, which is evidence that the proposed optimization method based on PSO is suitable for use in determining the moisture diffusion coefficients for pressboard insulations.

The proposed optimization method was compared with the previous optimization method based on GAs. The results show that, in all cases, the optimization times using the particle swarm method are considerably lower than those using the GA method.

The decrease in time when using PSO can be explained by the high robustness of the particle swarm which is due to the social component of this technique.

The $RMSD$ values obtained when the moisture diffusion coefficient was determined using PSO are, in most cases, lower than those obtained when the moisture diffusion coefficients calculated by GAs are used. This means that the moisture diffusion coefficients determined from the PSO method, are more accurate than those obtained using GAs.

Another advantage of the particle swarm method with respect to GAs is that, when the PSO is used, it is not necessary to apply any statistical analysis to ascertain the parameters of the moisture diffusion coefficient.

Decreasing the time spent on optimization and the better estimation of the moisture diffusion parameters makes the proposed PSO method most suitable for the determination of the moisture diffusion coefficients of pressboard insulations.

Chapter 5

Diffusion coefficient in transformer mineral-oil impregnated pressboard

5.1 Introduction

The different elements of the solid insulation of a transformer are usually classified into thick and thin structures. Thick structures comprise about the 50% of the total mass of the cellulose in the transformer [13], but they have a minor contribution to moisture migration among the total insulation system because of the large time constant for the diffusion processes at their typical operating temperatures. On the other hand thin cold structures, which are those that operate at bulk oil temperatures (pressboard barriers, end caps, etc) comprise 20 - 30% of the total mass of the cellulosic materials [13] and retain large amounts of water. These elements are considered the main storage area of water available for migration to oil.

Pressboard impregnation is important to ensure the minimum number of cavities are left inside the cellulose insulation and thereby dangerous partial discharges avoided.To achieve this purpose, mineral oil has been used for many decades with excellent results.

Being able to model moisture migration processes is important to optimize the maintenance investments and to improve the reliability of the equipments. As was explained, moisture migration inside cellulosic insulation is governed by a diffusion process that can be modeled by Fick's second law [27, 28, 39] and whose basic parameter is the diffusion coefficient.

Some authors have reported moisture diffusion coefficients for Kraft paper which have been widely accepted [26, 32, 55], but much less work has been done to characterize the coefficients in pressboard [6, 30].

Although discrete values of the moisture diffusion coefficients have been reported valid in oil-impregnated pressboard at some specific temperatures and moisture concentrations, no general equation for the coefficient is available [15]. The experimental determination of the coefficients is complex, since it requires making moisture diffusion experiments at different temperatures and insulation thickness involving large experimental times.

The aim of this chapter is to determine a specific equation for the moisture diffusion coefficient valid for a wide range of operating temperatures and moisture concentrations. The coefficient will be useful to simulate the moisture behaviour in the thin cold structures of in-service transformers. This new coefficient has been determined by using the methodology proposed in [26] and [6]. The experimental validation of the proposed coefficient is also described in this chapter.

5.2 Drying experiments

Experiments were done on samples of pressboard impregnated with mineral oil. The pressboard used during the experiments can be classified according to the international standard IEC 641-3-1[67] as type B.3.1 and has a density of 1.19 g/cm^3. Samples of

thicknesses 1, 2 and 3 mm were tested. The test specimens, consisting in one layer of pressboard, were cut to dimensions $40x100$ mm, as is shown in figure 5.1.

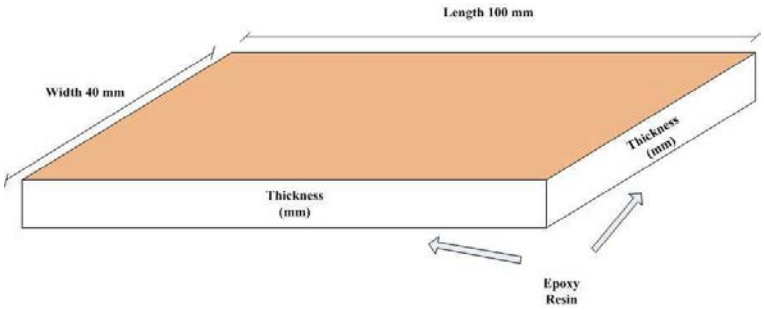

Figure 5.1: Pressboard sample single layer

The four edges of each specimen were sealed with epoxy resin to prevent desorption of moisture through these sides during the drying process and ensure a one-directional desorption through the top and bottom surfaces. Pressboard samples were prepared with specific initial moisture content by placing them in a climatic chamber under a temperature of 35 °C and 70% of relative humidity. Wetting conditions were established according to Jeffries's curves [40] to get equilibrium moisture around 9%. After that, the test specimens were impregnated with oil by submerging the insulation specimens in oil at room temperature at atmospheric pressure for a period of not less than one week. Finally, the oil-impregnated test specimens were introduced again into the climatic chamber to re-wet the insulation until the beginning of the drying experiment.

The mineral oil used in this work was Nytro Taurus that conforms the IEC 60296 [68] whose technical characteristics are shown in table 3.3.

5.2.1 Experimental process

To carry out drying experiments on oil-impregnated samples, a drying plant was used to achieve moisture desorption by circulating hot dry oil. Figure 5.2 shows the general scheme and a photograph of the drying plant.

Test specimens were subjected to experiments in the drying plant to obtain the pressboard insulation drying curves under different conditions of temperature. This experimental methodology has been proposed by García [7]. Several oil temperatures and pressboard thickness were used as summarized in table 5.1 below.

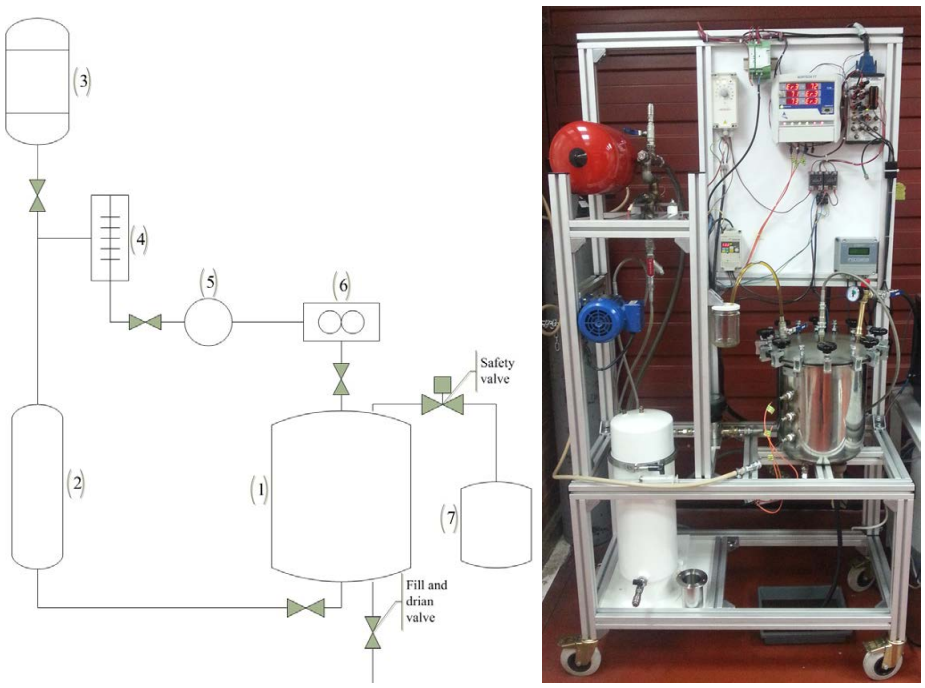

(a) General scheme. Sample container (1), oil filter (2), expansion vessel (3), heater (4), circulating pump (5), flowmeter (6) and security deposit (7).

(b) Photograph.

Figure 5.2: Drying plant.

Table 5.1: Summary of the conditions used in the experiments.

Samples	**Temperatures (°C)**	**Thickness (mm)**	**Density (g/cm^3)**
Pressboard	60, 70 and 80	1, 2 and 3	1.19

The drying experiments consisted of subjecting the test specimens, previously wetted and impregnated with mineral oil, to a constant flow of hot dry oil (figure 5.3). During all drying processes the oil flowing through the drying plant at a rate of 60 l/h, this is to ensure that within one hour all the oil that can be contained in the plant passes through the oil filter.

Before starting the experiments, one sample of each thickness was extracted from

a test specimen and analyzed in the laboratory by Karl-Fischer (KF) titration described in [46], to determine the initial moisture content throughout the thickness of the insulation sample. Later on, one sample of each thickness of pressboard were daily extracted from test specimens and analyzed to determine the evolution of the moisture concentration during the drying process ($c_{m-exp}(t)$).

(a) Sample support.

(b) Oil circulation drying plant, sample container.

Figure 5.3: Sample support and sample container of the drying plant.

During the drying process the moisture content in oil was monitored by an **EE381** sensor, from ***ELEKTRONIKA®***. Additionally, samples of mineral oil were analyzed daily by KF titration. Figure 5.4 shows some measurements of moisture in oil registered during the different drying experiments [1].

5.2.2 Drying curves

Figure 5.5 (a) shows the drying curves obtained from samples of 3 mm thick subjected to different oil drying temperatures (between 60 and 80 ^{o}C) and figure 5.5 (b) shows the drying curves obtained on samples of different thickness at 60 ^{o}C. As expected, higher oil temperature dries pressboard more quickly and thicker pressboard takes longer to dry.

[1] The spikes in the curves correspond to the stops of the oil recirculation during the sample extraction.

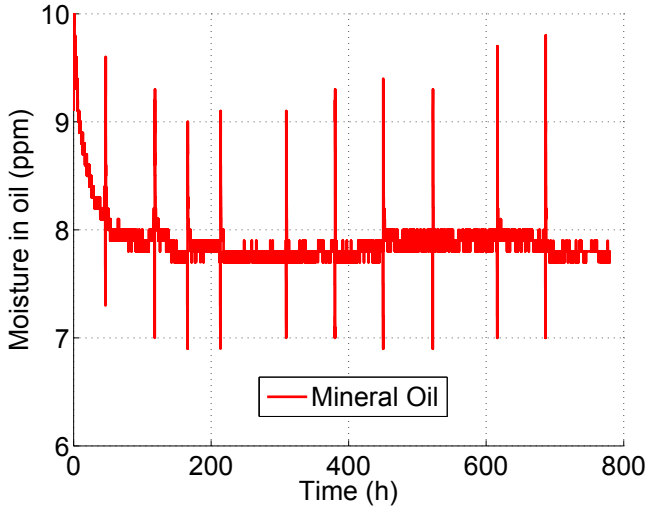

Figure 5.4: Moisture content in oil during the drying experiments.

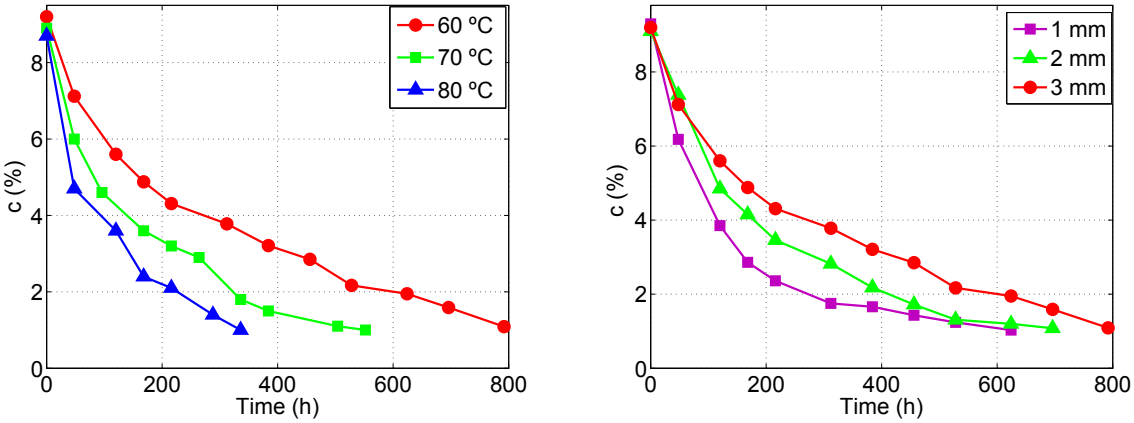

(a) 3 mm thick at different temperatures.

(b) At 60 °C determined over specimens of different thickness.

Figure 5.5: Experimental drying curves at different thickness and temperatures.

5.3 Determination of the moisture diffusion coefficient

The diffusion coefficient was assumed to be expressed by a general equation 5.1. This general expression has been used to describe the process of moisture migration in different materials [36, 69, 70].

$$D_{(c,T)} = D_0 \cdot e^{k \cdot c} \tag{5.1}$$

where c is the local moisture concentration of the insulation (expressed in % of the cellulose dry weight), D_0 is a preexponential factor (expressed in m^2/s) that determines the dependence of the moisture diffusion coefficient with different parameters e.g temperature, and k is a dimensionless parameter relating the moisture diffusion coefficient with the local moisture concentration.

To simulate the drying experiments, a diffusion model based in Fick's second law (equation 5.2) was assumed. Both equations below have been widely explained in the previous chapters.

$$\frac{\partial c}{\partial t} = \frac{\partial}{\partial x}\left(D \cdot \frac{\partial c}{\partial x}\right) \tag{5.2}$$

where c is the local moisture concentration in the material and D is the moisture diffusion coefficient.

5.3.1 Moisture diffusion modelling

The dependence of the diffusion coefficient of cellulosic materials on moisture concentration makes the equation 5.2 non-linear and thus is recommendable to apply a numerical method to solve it.

As said before, the edges of each test-specimen were sealed with epoxy resin to prevent moisture desorption through the sides during the drying process and ensure a one-directional desorption in transverse direction. Thereby, to simulate such process a one-dimensional geometry was assumed to represent the simulated insulation thickness (figure 5.6), as was explained in section 2.2.1.

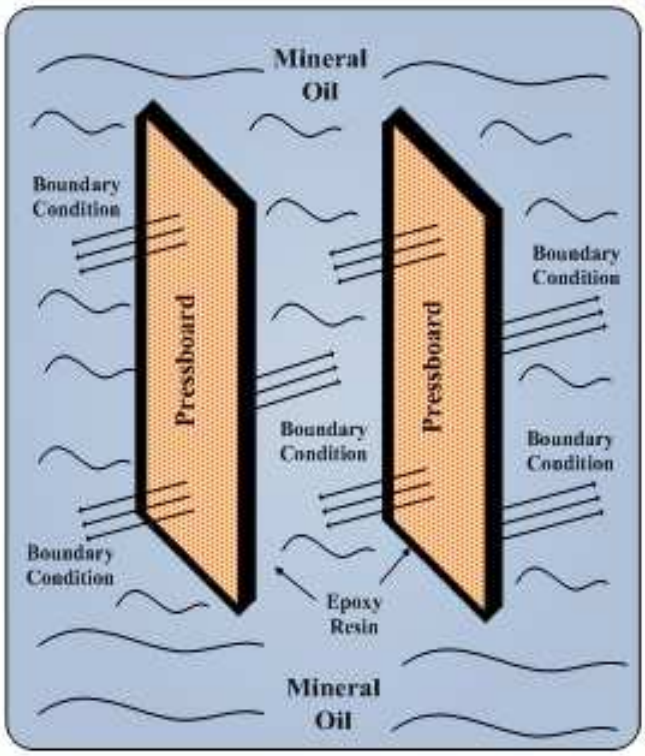

Figure 5.6: Geometry used in the Finite Element Model (FEM).

For the FEM simulation the pressboard was characterized by its moisture diffusion coefficient. Model inputs were the pressboard sample temperature (T), the initial moisture concentration (c_0) of the pressboard sample, and the boundary conditions. As aforementioned in chapter 3, the boundary conditions of the model were calculated in both pressboard surfaces from Fessler's approach (equation 5.3).

$$C_{equil} = 2.173 \cdot 10^{-5} \cdot p_v^{0.6685} \cdot e^{\left(\frac{42,725.6}{T}\right)} \tag{5.3}$$

where C_{equil} is the equilibrium moisture in pressboard, expressed in %, T is the temperature in oil-pressboard interface, and p_v is the partial pressure of water vapour, expressed in atmospheres, whose determination was explained in section 3.5.

To evaluate the diffusion coefficient used in the simulations, the estimated moisture content ($c_{est(t_i)}$) must be compared with the experimental values. It must be noted

that the Karl Fischer determines the average moisture content in the whole thickness of the insulation ($c_{m-exp(t_i)}$). In consequence, to proceed with the comparison the estimated moisture should be averaged within the insulation thickness by means of equation (5.4).

$$C_{m-est(t_i)} = \frac{1}{l} \int_{x=0}^{x=1} C_{est(x,t_i)} \cdot dx \tag{5.4}$$

where l is the pressboard thickness in metres.

As was done in chapters 2 and 4, the difference between the measured and estimated values was quantified by the root- mean square deviation ($RMSD$) (equation 5.5).

$$RMSD = \sqrt{\frac{1}{n} \sum_{i=1}^{n} \left[c_{m-est(t_i)} - c_{m-exp(t_i)} \right]^2} \tag{5.5}$$

The proximity of the estimated average concentration values calculated with the FEM model $c_{m-est(t_i)}$ and the experimental ones $c_{m-exp(t_i)}$ depends on the value of the diffusion coefficient used in the simulation.

To obtain the equation which best describes the moisture diffusion coefficient, the parameters k and D_0 of equation (5.1) that achieve a better agreement between the experimental drying curves and their corresponding estimated curve should be determined. This can be done by means of an optimization process.

According the results obtained in chapter 4, an optimization process based on Particle Swarm Optimization (PSO) was applied to obtain the parameters k and D_0 of the equation 5.1.

5.4 Parameters calculation

In this section, the results obtained by applying the PSO method to find the parameters k and D_0 of the moisture diffusion coefficient are shown, the range of these values are: for k between 0.1 and 0.5, and for D_0 between $1 \cdot 10^{-15}$ and $1 \cdot 10^{-10}$. These values have been widely studied in previous works by several authors as was explained in chapter 2. The optimization process was applied to the drying curves obtained from the experimental conditions summarized in table 5.1.

5.4.1 k parameter

After applying the PSO method fifteen times to the experimental curves, the values obtained for the parameter k did not show dependency on insulation temperature and thickness, so it was considered to be constant. A value of 0.2, obtained as the average of the individual k values, was assumed. This behaviour was also found in [42, 25, 6].

5.4.2 D_0 parameter

Figure 5.7 shows D_0 average values obtained for each temperature and insulation thickness. D_0 shows an exponential dependence with temperature. A dependence of D_0 with insulation thickness is also evidenced, as can be seen in figure 5.7.

Dependence of D_0 with temperature can be expressed by equation 5.6, which is a general expression relating the moisture diffusion coefficient dependence of different hygroscopic materials with temperature [26].

$$D_0 = D_1 \cdot e^{\left(-\frac{D_2}{T}\right)} \tag{5.6}$$

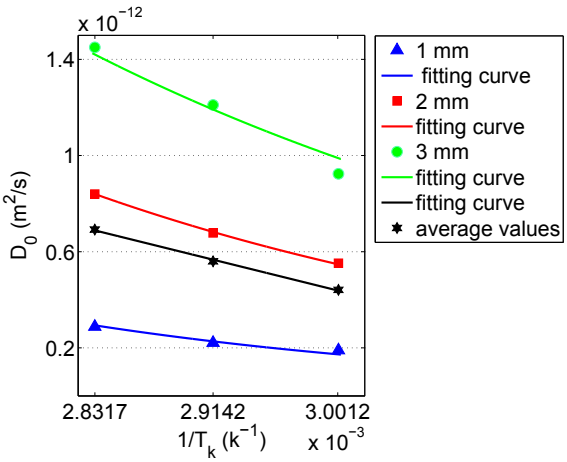

Figure 5.7: Plotted D_0 average values

Table 5.2 shows a summary of the values of the coefficientsD_1 and D_2 obtained by fitting the D_0 curve (figure 5.7) to equation 5.6 for each thickness. An additional curve fitting was performed considering the average value for the three tested thickness. The regression coefficients R^2 of the different fitting processes are shown in table 5.2.

Table 5.2: D_1 and D_2 values obtained by fitting curves.

Thickness (mm)	$D_1(m^2/s)$	D_2**(K)**	R^2
1	$2.34 \cdot 10^{-9}$	3,168	0.98
2	$4.47 \cdot 10^{-8}$	3,857	0.97
3	$2.89 \cdot 10^{-7}$	4,349	0.98
Average	$1.12 \cdot 10^{-7}$	3,791	0.98

5.5 Proposed diffusion coefficients

Taking the average values in table 5.2 and substituting the values in equation 5.6, we obtain an expression for D_0, dependent on temperature but independent of the insulation thickness (equation 5.7).

$$D_{0(T)} = 1.12 \cdot 10^{-7} \cdot e^{\left(-\frac{3,791}{T}\right)} \tag{5.7}$$

Substituting the values of k and D_0 (equation 5.7) in equation 5.1, an expression

can be obtained (equation 5.8), which allows calculating the moisture diffusion coefficient in pressboard including the dependence with temperature and moisture concentration but neglecting the dependence of this parameter with the insulation thickness.

$$D_{(c,T)} = 1.12 \cdot 10^{-7} \cdot e^{\left(0.2 \cdot c - \frac{3{,}791}{T}\right)} \tag{5.8}$$

The dependence of D_0 with thickness was already observed in Kraft paper [25] and non-impregnated pressboard [6]. In appendix B, a deeper study is presented that investigates the reasons of such dependence [43].

To take into account the influence of the insulation thickness in the expression of the diffusion coefficient, the obtained values for D_1 and D_2 (table 5.2) were fitted as a function of that variable.

Equations 5.9 and 5.10 were found to represent the dependence of D_1 and D_2 with the insulation thickness.

$$D_1 = 2.5 \cdot 10^{-9} \cdot l^{4.3} \tag{5.9}$$

$$D_2 = 3164 \cdot l^{0.29} \tag{5.10}$$

In these equations, insulation thickness (l) is expressed in millimetres.

Substituting the values of D_1 and D_2 from equations (5.9) and (5.10) in equation 5.6, an expression can be obtained (equation 5.11) that includes the dependence of D_0 on temperature and insulation thickness.

$$D_{0(T,l)} = 2.5 \cdot 10^{-9} \cdot l^{4.3} \cdot e^{\left(-\frac{3{,}164 \cdot l^{0.29}}{T}\right)} \tag{5.11}$$

Substituting the values of k and D_0 (equation 5.11) in equation 5.1, an expression can be obtained (equation 5.12), which allows calculating the moisture diffusion coefficient in oil impregnated pressboard including the dependence with temperature, moisture concentration and insulation thickness. Equations 5.8 and 5.12 are valid to describe the moisture behaviour inside the pressboard insulation.

$$D_{(c,T,l)} = 2.5 \cdot 10^{-9} \cdot l^{4.3} \cdot e^{\left(0.2 \cdot c - \frac{3{,}164 \cdot l^{0.29}}{T}\right)} \tag{5.12}$$

where (l) is the insulation thickness expressed in millimetres, c is the concentration of moisture in paper in (%), and T is the temperature in K.

5.6 Validation of the coefficients

The proposed expressions for the moisture diffusion coefficient were validated by comparing the experimental data with the simulated ones when considering expressions 5.8 and 5.12 to characterize the diffusion processes in the pressboard.

As mentioned, no other author has reported any study to obtain the moisture diffusion coefficient in oil impregnated pressboard, for this reason no comparison with other coefficients can be carried out in this case.

The validation of the proposed diffusion coefficients were tackled in two stages. Firstly the previous experimental drying curves (figure 5.5) used to determine the moisture diffusion coefficients were simulated by using both proposed diffusion coefficients (equations (5.8) and (5.12)). The $RMSD$ (equation 5.5) between the experimental and the estimated drying curves were calculated to quantify the accuracy of the estimations when the different proposed moisture diffusion coefficients are used.

Then, additional drying curves were experimentally determined on samples of

different thickness and subjected to different temperatures than those applied during the coefficient obtaining process. The drying curves were again simulated using both proposed coefficients.

5.6.1 Validation using experimental drying curves involved in the parameter determination process.

Figure 5.8 shows an example of the results obtained on a 2 mm thick sample subjected to drying at 80 °C. As can be seen the moisture diffusion coefficient proposed that takes into account the dependence on sample thickness fits much better to the experimental drying curve. This trend is evident in all the performed validations.

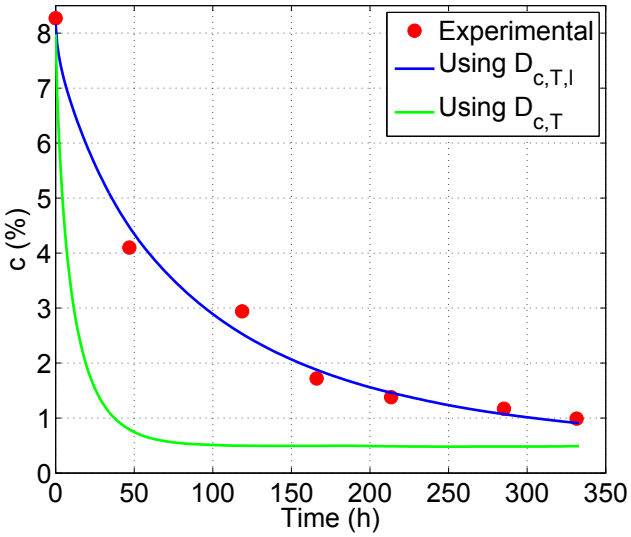

Figure 5.8: Experimental and estimated drying curves obtained at 80 °C and 2 mm sample thickness.

Figure 5.9 shows the RMSD obtained when the previous experimental drying curves were simulated by using the different moisture diffusion coefficients. As can be seen the RMSD is low for all the cases.

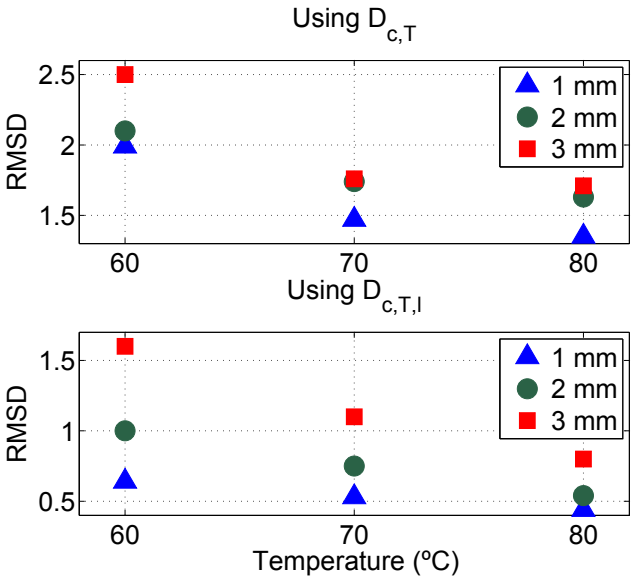

Figure 5.9: RMSD using the different moisture diffusion coefficients proposed in this work.

5.6.2 Validation of the diffusion coefficients with other temperatures and insulation thickness.

Validations were also performed with four additional experimental drying curves registered on samples with different thickness and subjected to drying temperatures that were not used in the determination of the moisture diffusion coefficients (table 5.3).

Table 5.3: Summary of the conditions used in the validation experiments.

Samples	Temperatures (ºC)	Thicknesses (mm)
Pressboard	60	0.5
	70	0.5
	85	1.5 and 3

Figure 5.10 shows the validation results performed on (a) 0.5 mm samples thickness at 70 ºC, (b) 3 mm samples thickness at 85 ºC, (c) 0.5 mm samples thickness at 60 ºC, and (d) 1.5 mm samples thickness at 85 ºC.

As can be seen in figure 5.10, the drying curves simulated with the moisture diffusion coefficient with dependence on thickness proposed in this work (equation (5.12)) fit better to the experimental drying curves than the curves simulated using the mois-

ture diffusion coefficient without thickness dependency also proposed in this work (equation (5.8)).

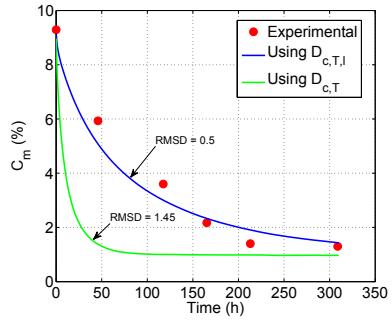

(a) 70 °C and 0.5 mm sample thickness.

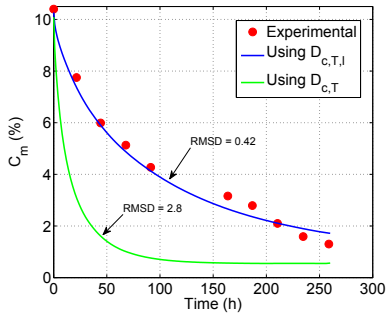

(b) 85 °C and 3 mm sample thickness.

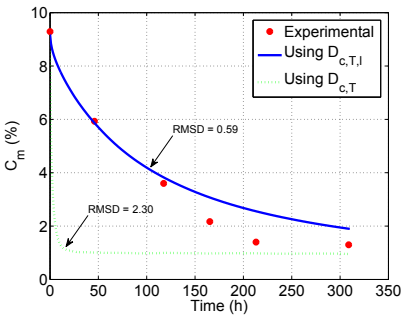

(c) 60 °C and 0.5 mm sample thickness.

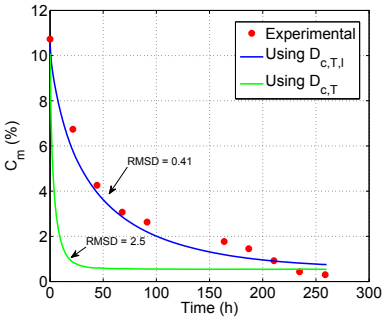

(d) 85 °C and 1.5 mm sample thickness.

Figure 5.10: Experimental and estimated drying curves obtained at different temperatures and sample thicknesses.

5.6.3 Comparison of the coefficients with the values reported by other authors.

Although no other equations have been proposed for the diffusion coefficient of water in oil-impregnated pressboard, Foss determined discrete values for temperatures 70 ^{o}C and 20 ^{o}C in an insulation of thickness 1 mm and moisture concentration 0.5% [15]. These values would not be useful to make simulations of moisture dynamics, since D depends on moisture content, and they are only valid for a concentration of 0.5% in weight. However, these values have been compared with those of the proposed

coefficient (equation (5.12)), obtained when it is particularized for the considered temperatures, insulation thickness and moisture concentration. The obtained values are shown in table 5.4.

Table 5.4: Comparison of Diffusion Coefficients proposed by Foss and Diffusion Coefficients proposed in this work for mineral oil impregnated pressboard for 1 mm sample thick and C=0.5%.

Temperature	$D_{(c,T,l)}(m^2/s)$	$D_{Foss}(m^2/s)$
20 ºC	$9.8 \cdot 10^{-15}$	$8.5 \cdot 10^{-14}$
70 ºC	$2.4 \cdot 10^{-13}$	$4.7 \cdot 10^{-12}$

As can be seen, the values of the coefficient given by Foss in pressboard are higher than those proposed in this work. In a previous work [7], the coefficients proposed by this author on Kraft paper, impregnated and non-impregnated with oil, were validated experimentally obtaining a similar result. The coefficients estimate a too fast desorption of moisture from cellulose to oil. It is not easy to explain the reasons of these discrepancies, as that work was developed by a company and poor information about it is available in scientific journals.

5.7 Conclusions

In this chapter the moisture diffusion coefficient of mineral-oil-impregnated pressboard has been experimentally determined.

No equation of moisture diffusion coefficient for this material have been reported before, in spite of the importance of this material in the moisture migration processes in the transformer.

The coefficients proposed in this work can be used to determine the time required to complete a drying process in the field, as well as to simulate the moisture dynamics during transformer operation.

The coefficients were validated under different temperatures and using samples of different thickness, demonstrating a great accuracy. They were also compared with some experimental values referenced in the bibliography, finding that the new coefficients has a greater accuracy in the estimation of the experimental data.

Considering the influence of the insulation thickness on the diffusion coefficient is fundamental to obtain accurate calculations of the moisture diffusion processes in samples of different thickness.

Chapter 6

Moisture diffusion coefficients of pressboard impregnated with natural esters

6.1 Introduction

Most power transformers nowadays rely on liquid dielectrics as an insulating medium and for heat transfer. The dielectric liquid more widely used is the mineral oil, which is produced from the middle range of petroleum-derived distillates [71]. The use of mineral oil has been justified for decades by its wide availability, good properties, good combination with cellulose and low cost. In recent years, the use of natural esters as an alternative to mineral oil has increased considerably in distribution transformers and, although less usual, some experiences are starting to be reported on its use in power transformers as well. Vegetable insulating oils are almost fully biodegradable (> 95 %) and have low toxicity; they have high flash points > 300 ^{o}C and fire point > 350 ^{o}C, they are considered environmentally friendly and fire-resistant substitutes of insulating mineral oils for power transformers.

Natural esters have greater hydrophilicity than mineral insulating oils due to the fact of hydrogen bonds existing on molecules of natural esters [9]. Moisture has a

strong influence on the performance of pressboard-oil systems in power and distribution transformers. The presence of moisture accelerates the ageing processes of the cellulosic insulation and also decreases its dielectric strength [47].

Moisture migration inside cellulosic insulation is governed by a diffusion process that can be modeled by Fick's second law and whose basic parameter is the diffusion coefficient [56], this method has been widely tackled during previous chapters of this thesis. The diffusion coefficient of moisture in a certain material depends on its physical properties. Different expressions can be used to simulate diffusion processes in Kraft paper or pressboard impregnated or non-impregnated with oil.

The objective of this chapter is to find an expression for the moisture diffusion coefficient of pressboard impregnated with natural ester.

Natural esters are synthesized from a vegetable base, e.g. seeds of soya, sunflower, rapeseed, etc. The different natural esters commercially available have different origin and so they may have their own physical and chemical characteristics and in consequence, the moisture diffusion coefficient could be different for each type of oil.

In this chapter the coefficients of pressboard impregnated with two different commercial natural esters have been obtained. As will be proved, the moisture diffusion coefficients are very similar because both natural esters have a sunflower seed basis.

In this chapter expressions for the moisture diffusion coefficients of pressboard impregnated with two different natural esters have been obtained. The natural esters included in the study are Bioelectra by Repsol and Biotemp by ABB, which are currently widely used by transformer manufacturers.

The coefficients proposed were obtained by means of the experimental methodology used previously in [56, 28, 41], and that has been widely described in previous chapters. In addition, for determining the moisture diffusion coefficient parameters,

the optimization process based in Particle Swarm Optimization (PSO) proposed in chapter 4 has been used.

The obtained expressions are valid on a wide range of temperatures, moisture concentrations and insulation thickness. The coefficients were validated and compared with the ones proposed by Zhang in [21], which is the only reference available to date about this topic.

6.2 Experimental methodology

As in the case of the study presented in chapter 5, the diffusion coefficients on ester impregnated insulations were obtained on pressboard samples of type B.3.1 100% (Wood Pulp Sulfated) [67] with density of 1.19 g/cm^3. The samples consisted of a single layer of pressboard cut to dimensions $40x100$ mm.

The edges of each test-specimen were sealed with ***Epoxy*** resin aiming to emulate the behaviour of the pressboard insulation pieces on transformers, in which the moisture diffusion occurs mainly on thickness direction [27]. (see figure 5.6)

The samples were firstly humidified in an environmental chamber and then they were impregnated with ester fluids. The experiments were repeated for two different ester fluids whose technical characteristics are shown in table 3.2.

6.2.1 Experimental process

As was explained before, to calculate the moisture diffusion coefficient of any material it is necessary to use experimental data of diffusion processes carried out at different conditions.

The experimental data used in this work were derived from hot-oil drying experiments (HO). Pressboard samples of different thickness, prepared with high moisture contents were subjected to drying in the plant schematized in figure 5.2 and the evolution of their average moisture content (drying curve) was determined. The drying fluid that filled the deposit of the drying plant during the tests was the one used to impregnate the samples.

The drying experiments consisted of subjecting the test specimens, previously wetted and impregnated with natural ester, to a constant flow of hot and dry ester. During all the drying processes the ester fluid flowed through the drying plant described in section 5.2.1 at a rate of 60 l/h. That flow rate ensures that the whole amount of fluid inside the plant passes through the filter within one hour. The drying plant was designed to avoid contact of the natural esters with oxygen and thus to limit oxidation processes. To this end a security deposit was included with a membrane that avoided any contact between oil and air.

Before starting the experiments, one sample of each thickness was extracted from a test specimen, and analyzed in the laboratory by Karl-Fischer (KF) titration, to determine the initial moisture content throughout the thickness of the insulation sample.

To determine the moisture diffusion coefficient of pressboard impregnated with natural esters, ten drying experiments were performed. Different fluid temperatures and sample thicknesses were considered as shown in table 6.1. The average time spent in each experiment was one month.

Table 6.1: Summary of the conditions used in the experiments.

Natural ester	**Temperatures (^{o}C)**	**Thickness (mm)**
Biotemp and Bioelectra	40, 50, 60, 70 and 80	1, 2 and 3

The experimental average moisture content in the pressboard samples (c_{m-exp}), was also determined using the Karl-Fischer titration method. One sample of each thickness of pressboard was daily extracted from sample container and analyzed to

determine the drying curve of the sample during the drying process.

Oil samples were also extracted and analyzed every day. Additionally, the moisture content of oil was monitored with a moisture-in-oil sensor. Figure 5.4 shows the evolution of moisture in oil during three whole drying process performed with both natural esters and with mineral oil. As can be seen the moisture in oil remains relatively constant because of the good performance of the filter incorporated by the drying plant.

6.2.2 Drying curves

Drying curves for all thicknesses and temperatures summarized in table 6.1 were obtained for both kinds of natural esters. As an example, figure 6.1 shows the drying curves for pressboard samples of 1 mm thick subjected to different drying temperatures. These curves show drying occurs more quickly at high oil temperature, the same effect is visible in the other thickness.

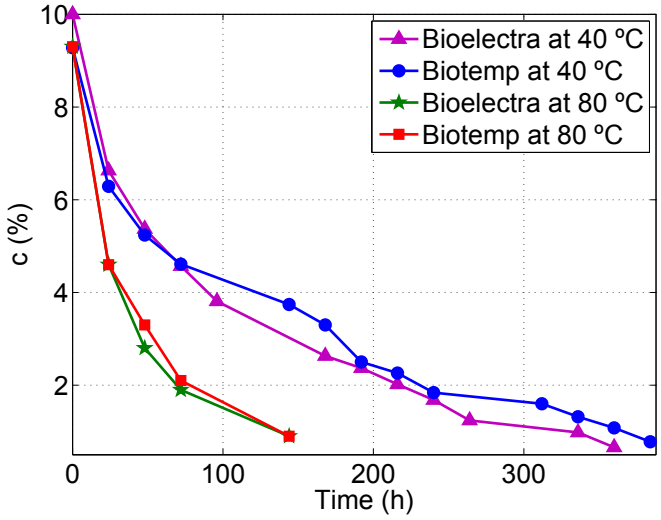

Figure 6.1: Experimental drying curves of 1 mm thick pressboard for both kinds of natural ester.

6.3 Theoretical model for determining moisture diffusion coefficient

The same procedure used in section 5.3 was applied for determining of moisture diffusion coefficients in esters-impregnated pressboard, this coefficient was assumed to be expressed by the general equation (6.1).

$$D_{(c,T)} = D_0 \cdot e^{k \cdot c} \tag{6.1}$$

where c is the local moisture concentration of the insulation (expressed in % of the cellulose dry weight), D_0 is a preexponential factor (expressed in m^2/s) that determines the dependence of the moisture diffusion coefficient with different parameters e.g temperature, and k is a dimensionless parameter relating the moisture diffusion coefficient with the local moisture concentration.

The model inputs are the pressboard sample temperature (T), its initial moisture concentration (c_0), and the boundary conditions. As was explained in chapter 3, the boundary conditions of the model for natural esters are different than the mineral oil, and were calculated using equation (6.2). This equation represent the moisture equilibrium conditions for ester-paper systems.

$$\begin{aligned} C_{equil\_vegetal} = {} & 1.18 \cdot 10^{-18} \cdot {p_v}^3 \cdot e^{\left(\frac{16,570}{T}\right)} - 5.39 \cdot 10^{-12} \cdot {p_v}^2 \cdot e^{\left(\frac{10,960}{T}\right)} \\ & + 9 \cdot 10^{-6} \cdot p_v \cdot e^{\left(\frac{5,418}{T}\right)} + \frac{1,004}{T} - 3 \end{aligned} \tag{6.2}$$

where $C_{equil\_vegetal}$ is the equilibrium moisture in pressboard impregnated with natural ester, expressed in %, T is the temperature in oil-pressboard interface, and p_v is the partial pressure of water vapour (atm), whose determination was explained in section 3.5.

The output of the FEM model is the evolution of the local moisture concentration (c_{est}) during the whole drying process. To compare the simulation results with the experimental data, is necessary to calculate the average moisture concentration of the sample (c_{m-exp}), this can be done by using equation (5.4).

6.4 Parameters calculation

To obtain the equation of the moisture diffusion coefficients (5.1), the parameters k and D_0 should be determined. To this end, the PSO based optimization method proposed in chapter 4 was applied. The objective function used was the root- mean square deviation ($RMSD$) (equation (5.5)), that quantifies the difference between the experimental and estimated drying curves.

As was discussed in chapter 4, the application of the PSO optimization method proposed in the thesis provides a single value of every parameter for each experimental condition. This fact simplifies the analysis significantly and allows to skip the statistical study, that was required when GA were applied.

6.4.1 k parameter

After applying the optimization process to the 15 experimental drying curves, 15 values of the parameter k were obtained. The analysis of these values did not suggest any dependence of k with the temperature or insulation thickness. In consequence, as was done in the case of mineral-oil impregnated pressboard, a representative value of k was taken as the average of the 15 results obtained through PSO.

The obtained values for the parameter k are 0.20 for Bioelectra and 0.25 for Biotemp, with a maximum standard deviation of 0.10 for both natural esters.

6.4.2 D_0 parameter

The average values obtained for the parameter D_0 for Biotemp and Bioelectra, showed dependence with the temperature and the insulation thickness. This dependence was widely shown in previous works [6, 7, 41, 56]. Figure 6.2 shows D_0 temperature dependence for pressboard impregnated with Biotemp, similar behaviour occurs with Biolectra.

The dependence of D_0 with temperature can be fitted to equation (5.6), which is a general expression that relates the moisture diffusion coefficient dependence of different hygroscopic materials with temperature [7].

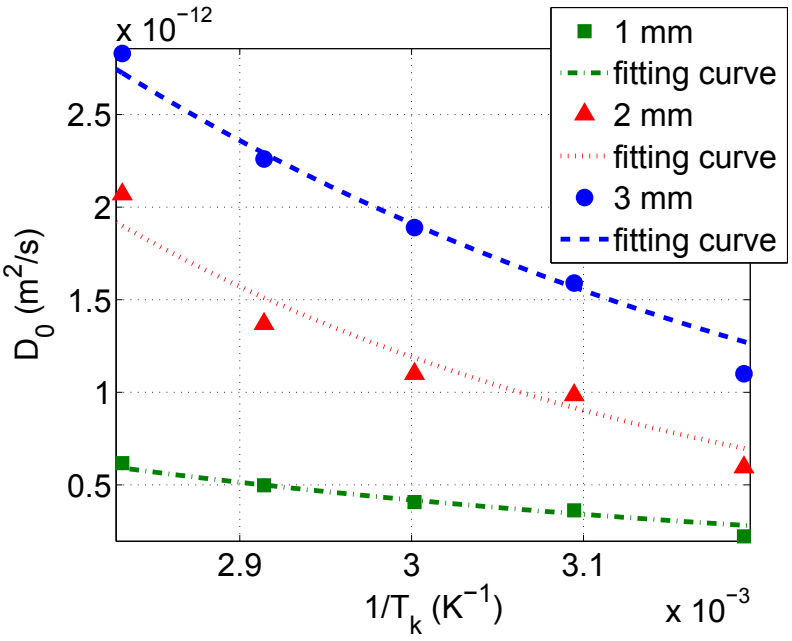

Figure 6.2: Plotted D_0 average values for Biotemp.

Table 6.2 shows a summary of the values of the coefficients D_1 and D_2 obtained by fitting the D_0 values obtained by PSO for both kinds of natural esters. As can be seen, a clear dependence with the thickness is once again found.

Table 6.2: D_1 and D_2 values obtained by fitting curves for both natural esters.

	Biotemp		**Bioelectra**	
Thickness (mm)	D_1 **(**m^2/s**)**	D_2 **(K)**	D_1 **(**m^2/s**)**	D_2 **(K)**
1	$1.90{\cdot}10^{-7}$	4,450	$1.70{\cdot}10^{-7}$	4,440
2	$2.20{\cdot}10^{-6}$	4,520	$1.20{\cdot}10^{-6}$	4,462
3	$2.90{\cdot}10^{-6}$	4,570	$3.84{\cdot}10^{-6}$	4,481

6.5 Proposed diffusion coefficients

To obtain the equations of the moisture diffusion coefficient, D_1 and D_2 were expressed as a function of thickness from the values of table 6.2. These equations are shown in table 6.3, where insulation thickness (l) is expressed in millimetres.

Substituting D_1 and D_2 equations in (5.6) and then in (5.1), expressions for moisture diffusion coefficient can be obtained. These equations are dependent on local moisture concentration, temperature and insulation thickness.

Table 6.3: D_1 and D_2 as a function of thickness.

	Biotemp	**Bioelectra**
D_1	$1.2{\cdot}10^{-7} \cdot l^{-3.7}$	$1.7{\cdot}10^{-7} \cdot l^{-4.5}$
D_2	$4{,}491{\cdot}l^{-0.5}$	$4{,}450{\cdot}l^{-0.5}$

Equation (6.3) is valid in the case of pressboard impregnated with Biotemp while equation (6.4) is applicable for pressboard impregnated with Bioelectra.

$$D_{Biotemp} = 1.2 \cdot 10^{-7} \cdot l^{-3.7} \cdot e^{\left(0.25 \cdot c - \frac{4{,}491 \cdot l^{-0.5}}{T}\right)} \tag{6.3}$$

$$D_{Bioelectra} = 1.7 \cdot 10^{-7} \cdot l^{-4.5} \cdot e^{\left(0.2 \cdot c - \frac{4{,}450 \cdot l^{-0.5}}{T}\right)} \tag{6.4}$$

where (l) is the insulation thickness expressed in millimetres, c is the concentration of moisture in paper, and T is the temperature in K.

As can be observed, both equations are very similar; this is because both natural esters have the same origin based on sunflower seed.

Figure 6.3 compares the moisture diffusion coefficients of the pressboard impregnated with the two natural esters and also the coefficient of pressboard impregnated with mineral oil that was proposed in chapter 5. In Figure 6.3 samples of thickness 3 mm subjected to a temperature of 70 ºC and variable moisture concentration between 1% and 8% were considered. As can be seen moisture diffusion coefficients increase with moisture concentration and temperature, as was expected. It should be noted that the coefficients of pressboard impregnated with both natural esters present a similar behaviour, but this behaviour is very different to the moisture diffusion coefficient of pressboard impregnated with mineral oil.

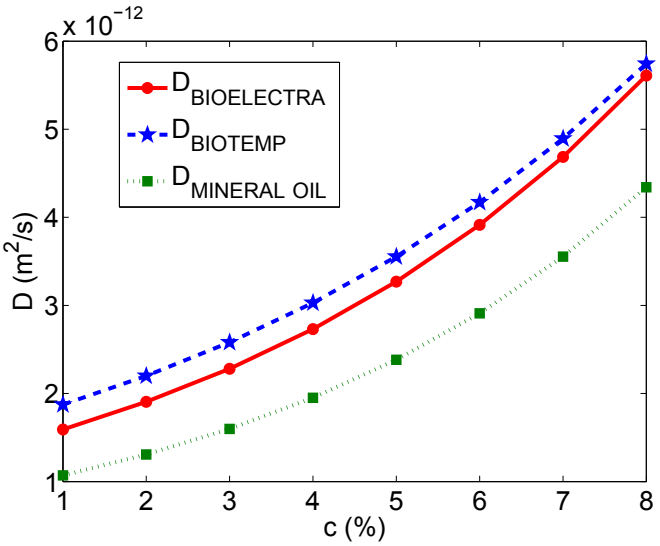

Figure 6.3: Moisture diffusion coefficient for vegetables and mineral oil, 3 mm sample thickness, 70 ºC and variable concentration.

A higher moisture diffusion coefficient means that the oil can extract the moisture with a higher rate from the sample of pressboard, which means that the sample is dried faster in natural esters than in the mineral oil. As an example of the previous results, table 6.4 has been included to compare the drying times for Biotemp and mineral oil in several particular cases. It can be observed how the drying times in pressboard impregnated with natural oil are lesser that those of pressboard impregnated with mineral oil. Similar behaviour occurs with Bioelectra. A deeper study on the drying times of mineral-oil-impregnated and ester-impregnated pressboard is presented in appendix A.

Table 6.4: Drying times for different samples thickness at 70 °C, 8% initial moisture content, 0.5% final moisture content, and 10 ppm in oil.

Thickness (mm)	Biotemp	Mineral Oil
1	192 h	379 h
2	344 h	427 h
3	438 h	499 h

6.6 Validation of the coefficients

Equations (6.3) and (6.4), proposed for the moisture diffusion coefficient calculation, were validated by comparing the experimental drying curves with the simulated ones.

The proposed moisture diffusion coefficients were also validated with additional drying curves which were experimentally determined on samples of different thicknesses and subjected to different drying temperatures to those used during the coefficient determination. The estimated drying curves of these samples were obtained from the FEM model, using the coefficients proposed in this chapter and also the coefficient for Kraft paper proposed by Zhang et al in [21].

6.6.1 Validation with temperatures and insulation thickness involved in the coefficient determination process.

Figure 6.4 shows two examples of the results obtained when the drying experiments were simulated. Case 1 corresponds to samples 2 mm thick impregnated with Bioelectra subjected to drying process at 80 °C. In the same way, case 2 corresponds to samples 1 mm thick impregnated with Biotemp subjected to a drying process at 40 °C. As can be seen the estimated drying curves fits very well the experimental ones when the proposed moisture diffusion coefficients are used.

All experiments summarized in table 6.1 were simulated obtaining a low $RMSD$ for all cases. The best and the worst results obtained in the whole study are shown in

figure 6.4 (i.e $RMSD$ = 0.23 and $RMSD$ = 0.82).

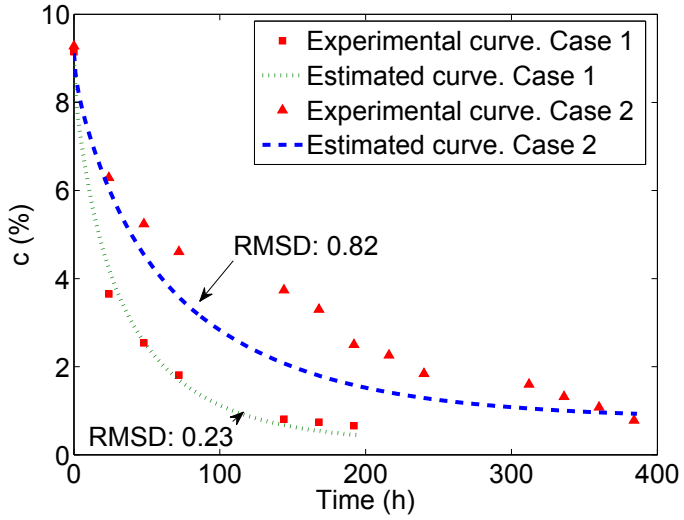

Figure 6.4: Experimental and estimated drying curves obtained for case 1 and case 2.

6.6.2 Validation with temperatures and insulation thickness not considered in the coefficient determination process

Validations were also performed with experimental drying curves determined on samples of thickness and drying temperatures that were not used in the determination of the moisture diffusion coefficients. The conditions of these additional experiments are shown in table 6.5.

Table 6.5: Summary of the conditions used in the validation experiments.

Natural ester	Temperatures (°C)	Thickness (mm)
Biotemp	85	1.5, 2.5, 3.5 and 5
Bioelectra	50	1.5, 2.5 and 4

Validation for all the experiments summarized in table 6.5 was also performed. The case with the minimum $RMSD$ is shown in figure 6.5. The $RMSD$ obtained in the simulation of the whole set of experiments was into a range of 0.30 to 0.65 which means that the moisture diffusion coefficients proposed in this work are valid and allow obtaining accurate simulation values.

Figure 6.5 shows the simulated and experimental data of the drying process of a sample 2.5 mm thick dried with Biotemp at 85 ºC.

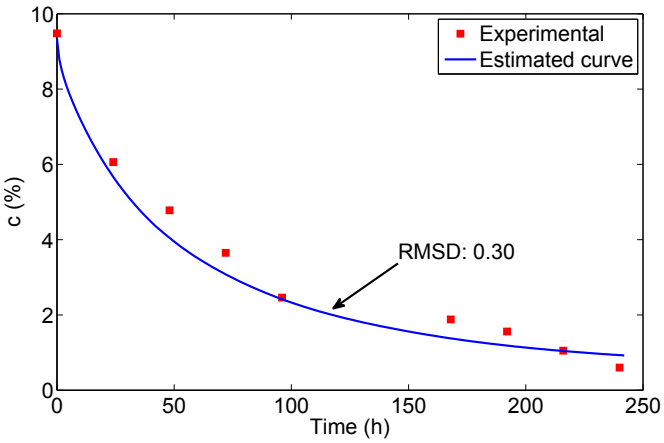

Figure 6.5: Experimental and estimated drying curves obtained on samples 2.5 mm thick dried with Biotemp at 85 °C.

6.6.3 Comparison of the coefficient with the values reported by other authors

So far, no moisture diffusion coefficient for natural ester impregnated pressboard has been reported in the literature. In [21], Zhang et al proposed an expression for the moisture diffusion coefficient of Kraft paper impregnated with a kind of natural ester. Zhang's equation is based on the empirical equation proposed by Guidi in [23] and considers the dependence of the coefficient with temperature and moisture concentration (equation (6.5)).

$$D = D_G \cdot e^{\left[k \cdot c + E_a\left(\frac{1}{T_0} - \frac{1}{T}\right)\right]} \tag{6.5}$$

where T_0 is the reference temperature (298 K), T is the insulation temperature (also expressed in K) and c is the moisture concentration of the insulation (in % of dry weight).

Zhang carried out experiments on Kraft paper samples 3 mm thick (composed of 60 paper layers of 0.05 mm each) impregnated with a type of rapeseed insulating oil. The evolution of moisture distribution in time was determined with an adsorption experiment. The values for E_a, D_G and k parameters of moisture diffusion coefficient proposed by Zhang were: $k = 0.497$, $D_G = 7.34 \cdot 10^{-14}\ m^2/s$ and $E_a = 6{,}940$ (K)

Zhang's coefficient has been evaluated by simulating our experimental drying curves. It is important to note that the coefficient proposed by Zhang does not consider the dependence on thickness. To skip the effect of this variable in the validation of the coefficient, the simulations have been limited to the experiments performed on samples of 3 mm, the same as used by Zhang in his experiments.

Figure 6.6 shows the results obtained when the drying curves of a 3 mm sample impregnated with Bioelectra and Biotemp dried at 60 ºC and 50 ºC respectivily are estimated using Zhang's coefficient (equation 6.5), and also using both proposed coefficients (equations (6.3)(6.4)). As can be seen the estimations obtained with Zhang's coefficient are far from experimental data, while the predictions when equations (6.3)(6.4) were used are more precise. Further simulations were conducted to evaluate Zhang's coefficient at different temperatures obtaining similar results.

The bad behaviour of Zhang's coefficient in the simulation of drying processes of pressboard can be due to the fact that it was determined using a different cellulosic material (Kraft paper instead of pressboard) and also with a different ester fluid (a type of rapeseed) to those used in our experiments.

Another possible cause of the discrepancies may be that Zhang's coefficient was determined from adsorption experiments while the validations were done on moisture desorption processes. As it is well known, a certain hysteresis exists between adsorption and desorption of moisture in cellulosic materials, although it does not seem to be the explanation to such a big discrepancy.

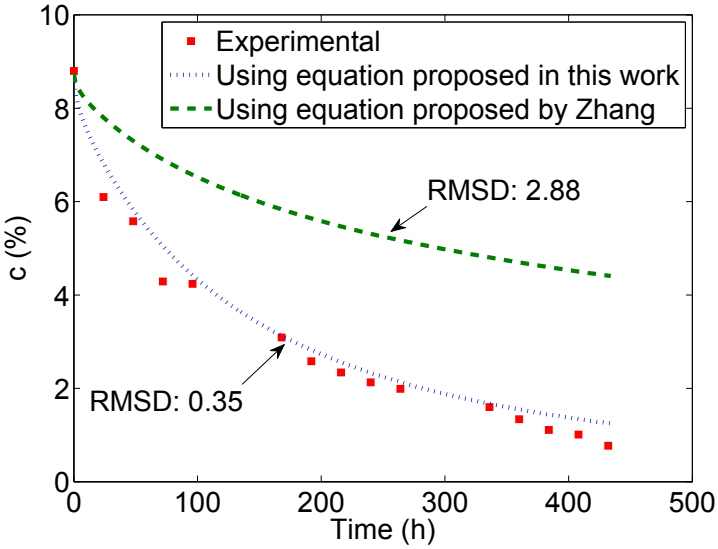

(a) 60 °C and 3 mm sample thickness. Using Bioelectra

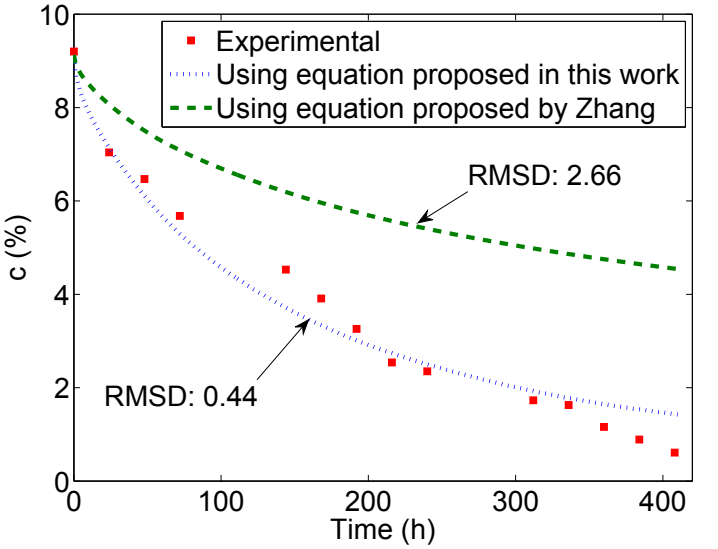

(b) 50 °C and 3 mm sample thickness. Using Biotemp

Figure 6.6: Experimental and estimated drying curves of a 3 mm pressboard impregnated with both natural esters and dried by HO.

6.7 Conclusions

In this chapter the moisture diffusion coefficient for pressboard impregnated with two different natural esters has been determined and validated. This work was carried out on two natural esters widely used for transformer manufacture.

A new optimization process, based in particle swarm, was applied that is fast and accurate in determining the parameters of the diffusion coefficients.

The obtained expressions were similar for both esters, this is because the similarities of the physical and chemical properties of the fluids. However, for better estimation of the moisture migration process, it is desirable to use a coefficient specifically obtained for the material under study.

The moisture diffusion coefficients proposed in this chapter consider a dependency with temperature, moisture concentration and thickness of the samples. Although considering thickness in the diffusion coefficient equation may be not so rigorous from the physical point of view, it allows modelling the studied phenomena with much more accuracy than when this variable is skipped.

The coefficients were validated under different temperatures and using samples of different thickness, demonstrating a great accuracy. It was also compared with the equation proposed by another author, demonstrating the effectiveness of the coefficients and the methodology used to derive them.

The coefficients proposed in this chapter can be used to determine the time required to complete a drying process in the field, as well as to simulate the moisture dynamics during transformer operation.

Natural ester is much more hydrophilic than mineral oil, it leads the fluid to absorbing more moisture in the drying experiments and therefore they were performed in less time. Additionally it can be concluded that due to this same condition, diffusion coefficient is greater when using natural esters.

Chapter 7

Moisture dynamics model

7.1 Introduction

In the last years the use of natural and synthetic esters is becoming habitual in distribution transformers. These fluids are biodegradable and present some other good properties, as their high fire temperatures, that make them a valuable alternative to mineral oils. These fluids have recently started to be applied to power transformers, although their use is still sporadic mainly because of their cost and some disadvantageous properties presented by them, as their high viscosity and their oxidation rates [2].

One of the differential properties of these fluids is that they are able to absorb a much greater amount of water than mineral oils, as was proved in chapter 3, one of the variables that deserves more attention in power transformers, as its presence accelerates the paper ageing rates and increases the equipment risk of failure. However, as the application of ester fluids to power transformers is still scarce, not much work has been addressed about the moisture behaviour in cellulose-ester systems.

Cellulose and oil have a very different behaviour with regard to moisture; cellu-

losic materials are hydrophilic while oil is highly hydrophobic. In consequence most of the moisture in a mineral-oil filled transformer is absorbed in its cellulosic insulation. However the distribution of moisture between paper and oil is not static, but depends on the transformer operating condition, and mainly on the temperature reached by the different materials.

In order to make a good estimation of the moisture dynamics inside transformers in operation, it is necessary to take into account those parameters that could affect its behaviour; specially the operating temperatures and the moisture content inside cellulosic materials. In this chapter, a moisture dynamics model has been developed which includes the thermal and moisture dynamics phenomena within the transformer.

7.2 Moisture dynamic model

The moisture dynamic model proposed in this work is an integration of the thermal model described in Annex G of the IEEE standard C57-91-2011 [8] and a moisture model based in the solution of Fick's second law imposing a set of dynamic boundary conditions [56, 73]. For the integration of these two models. the computational Finite Elements (FEM) tool Comsol Multiphysics and the software Matlab were used.

7.2.1 Thermal model

The thermal model of the Annex G of IEEE C57-91-211 [8], considers that the distribution of temperature on the transformer winding is linear (Figure 7.1).

As is well known the transformer winding hot-spot temperature is one of the most critical parameters when defining the power transformer thermal conditions and overloading capability beyond the nameplate rating.

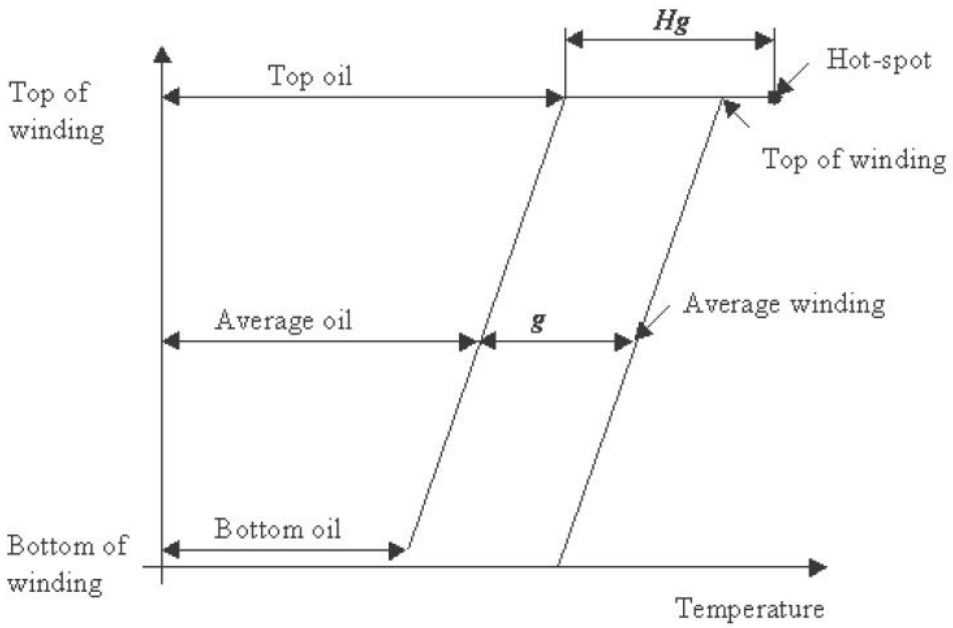

Figure 7.1: Transformer thermal diagram that shows the temperature distribution along the winding height and the oil temperature distribution inside the transformer tank. g is the rated average winding to average oil temperature gradient, and H_g is the Hot-spot factor. Taken from [74].

According to the IEEE standard C57-91-2011 [8], the hot-spot temperature in a transformer can be calculated as the addition of three components: the ambient temperature rise, the top-oil temperature rise, and the hot-spot temperature rise over the top-oil temperature, figure 7.1 [74] It is assumed that during a transient period the hot-spot temperature rise over the top-oil temperature varies instantaneously with transformer loading and independently of time.

Figure 7.2, taken from [8], shows a load fluctuations throughout the day. For normal loading or planned overloading above nameplate, a multi-step load cycle calculation method is usually used.

An equivalent two step overload cycle as shown in figure 7.3, taken from [8], may be used for determining emergency overload capability. The equivalent two-step load cycle consists of a prior load and a peak load. This figure is also used for the purpose of describing calculations to determine equivalent load cycles.

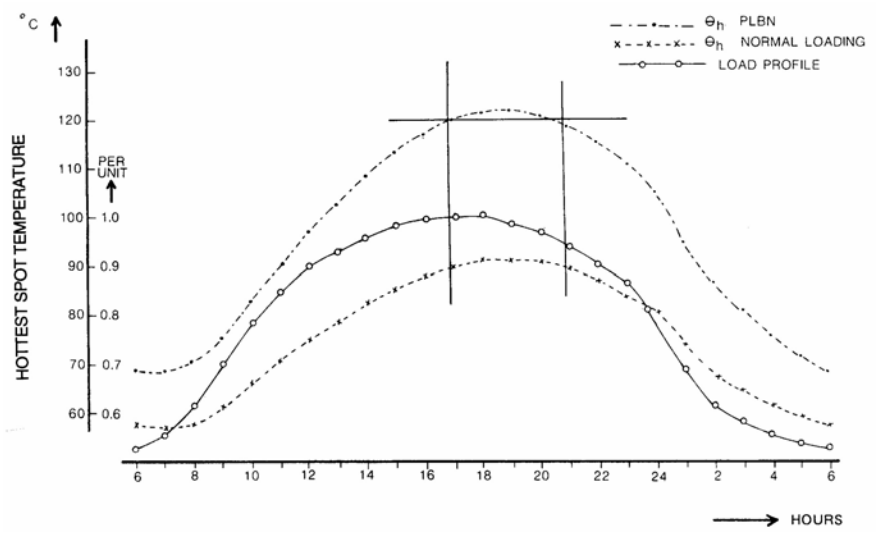

Figure 7.2: Load cycles for normal loading and planned loading beyond nameplate. Taken from [8]

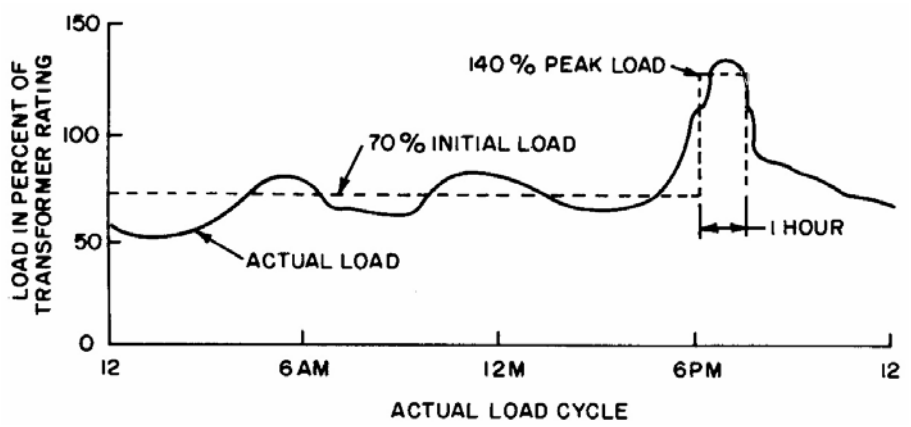

Figure 7.3: Example of actual load cycle and equivalent load cycle. Taken from [8]

Calculation of temperatures

IEEE standard C57-91-2011 [8] proposes two different methodologies to calculate the temperatures throughout the transformer for a certain load profile. The simplest one, given in the clause 7 of that standard, is based in solving a first order differential equation that models the increase or decrease of temperature for a certain load. To determine the time constant of the oil and the winding, the model considers the exponents m and n, that approximately account for changes in load loss and oil viscosity caused by

changes in temperature. Values for the exponents used in these equations are shown in table 7.1 [1].

Table 7.1: Exponents used in temperature determination equations.

Cooling modes	**m**	**n**
ONAN	0.8	0.8
ONAF	0.8	0.9
Non-directed OFAF or OFWF	0.8	0.9
Directed ODAF or ODWF	1.0	1.0

An alternate method, which requires more complex computer calculation procedures, is given in Annex G in [8]. This method is more exact in accounting for changes in load loss and oil viscosity caused by changes in resistance and oil temperature, respectively. The effect of a variable ambient temperature is also considered.

This method was used in this work because it has a greater accuracy in the calculation of the temperatures during transient loading [8].

Equations

The winding hottest-spot and oil temperatures are obtained from equations for the conservation of energy during a small period of time, Δt. The system of equations constitutes a transient forward-marching finite difference calculation procedure. The equations were formulated so that temperatures obtained from the calculation at the prior time t_1 are used to compute the temperatures at the next instant of time $t_1 + \Delta t$ or t_2. The time is incremented again by Δt, and the last calculated temperatures are used to calculate the temperatures for the next time step. At each time step, the losses were calculated for the load and corrected for the resistance change with temperature. Corrections for fluid viscosity changes with temperature were also incorporated into the equations. With this approach, the required accuracy is achieved by selecting a

[1] ONAN: Natural convection flow of oil, and natural convection flow of air. ONAF: Natural convection flow of oil, and forced convection flow of air. OFAF: Forced convection flow of oil, and Forced convection flow of air. ODAF: Directed convection flow of oil, and Forced convection flow of air.

small value for the time increment Δ_t and the programming approach is very simple.

The equations shown in this chapter are those that represent the temperatures of the most critical points of the transformer. In order to calculate these temperatures, all the equations proposed in the Annex G of IEEE standard C57-91-2011 [8] have been used. The complete set of equations is not reproduced here because of the great number of expressions and symbols that would need to be displayed. This thesis have not contributed to improve the thermal model or has made any change on it, but has just implemented it according to the recommendations of the Annex G of IEEE standard C57-91-2011 [8]. However, the full description of the model and the whole system of equations used can be seen in [8].

The hottest-spot temperature

The hottest-spot temperature is made up of the following components.

$$\Theta_H = \Theta_A + \Delta\Theta_{BO} + \Delta\Theta_{\frac{WO}{BO}} + \Delta\Theta_{\frac{H}{WO}} \tag{7.1}$$

where:

- Θ_H is the winding hottest-spot temperature, ^{o}C.
- Θ_A is the average ambient temperature during the load cycle to be studied, ^{o}C.
- $\Delta\Theta_{BO}$ is the bottom fluid rise over ambient, ^{o}C.
- $\Delta\Theta_{\frac{WO}{BO}}$ is the temperature rise of oil at winding hot-spot location over bottom oil, ^{o}C.
- $\Delta\Theta_{\frac{H}{WO}}$ is the winding hot-spot temperature rise over oil next to hot-spot location, ^{o}C.

The top and bottom oil temperatures

The temperatures of the top and bottom oil are determined from following equations:

$$\Theta_{BO} = \Theta_{AO} - \frac{\Delta\Theta_{\frac{T}{B}}}{2} \tag{7.2}$$

$$\Theta_{TO} = \Theta_{AO} + \frac{\Delta\Theta_{\frac{T}{B}}}{2} \tag{7.3}$$

- Θ_{BO} is the bottom fluid temperature, ^{o}C.
- Θ_{TO} is the top fluid temperature, ^{o}C.
- Θ_{AO} is the average fluid temperature in tank and radiator, ^{o}C.
- $\Delta\Theta_{\frac{T}{B}}$is the temperature rise of fluid at top of radiator over bottom fluid, ^{o}C.

The thermal model calculates the top-oil, hot-spot and bottom-oil temperatures for the specified load profile. Additionally, it is able to calculate the temperature at any specified height of the winding.

7.2.2 Moisture diffusion modelling

As is widely mentioned in previous chapters, the desorption of moisture from cellulose to oil can be modelled as a diffusion phenomenon by means of Fick's second law (equation 7.4).

$$\frac{\partial c}{\partial t} = \frac{\partial}{\partial x}\left(D \cdot \frac{\partial c}{\partial x}\right) \tag{7.4}$$

where D is the effective moisture diffusion coefficient in the solid insulation, c is the local total moisture concentration, t is the time and x is the distance into the material in the direction of moisture movement.

As was explained in chapter 2, the transport of moisture inside the cellulose proceeds in the form of vapor and condensed water through the fibres and void spaces that constitute the cellulose. The diffusion coefficient increases with moisture concentration and decreases when moisture is reduced [26].

To solve Fick's equation, the FEM commercial software Comsol Multiphysics 3.5a was used. The initial moisture concentration and temperature of the insulation were used as independent inputs to the moisture model.

The FEM diffusion model can consider either Kraft paper or pressboard as cellulosic insulation, including different expressions of the diffusion coefficient to characterize the different materials. It can also consider several insulating fluids, as mineral oils or natural esters that are represented by adequate boundary conditions. Taking into account that moisture dynamics occurs in a unidirectional way, a one-dimensional model was assumed. As will be explained latter, to estimate the moisture dynamics at different heights of the winding, different simulations could be run.

Figure 7.4 shows a schematic of the implemented model. In the case represented in this figure, one of the sides of the insulation is considered to be in contact with the winding, and then no diffusion takes place on this side. However different situations and geometries could also be easily studied by the model.

As was mentioned, the diffussion coefficients used in the model were those obtained in chapters 5 and 6 of this thesis. This parameter characterizes the material that is being studied by the model, and in particular determines the moisture diffusion rate within the material for each operating condition.

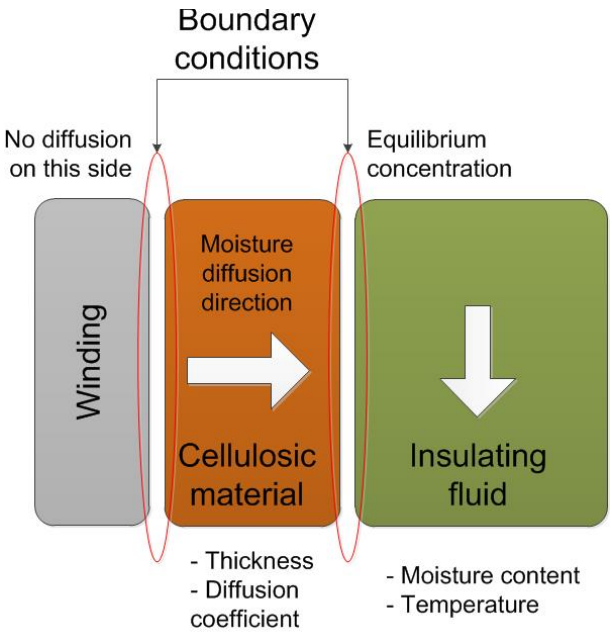

Figure 7.4: Outline of the diffusion model.

To simulate the moisture dynamics in mineral-oil-paper systems, the diffusion coefficient was taken as equation 7.5, while to simulate natural-ester-paper systems, equations 7.6 and 7.7 were considered.

$$D_{Mineral} = 2.5 \cdot 10^{-9} \cdot l^{4.3} \cdot e^{\left(0.2 \cdot c - \frac{3{,}164 \cdot l^{0.29}}{T}\right)} \tag{7.5}$$

$$D_{Biotemp} = 1.2 \cdot 10^{-7} \cdot l^{-3.7} \cdot e^{\left(0.25 \cdot c - \frac{4{,}491 \cdot l^{-0.5}}{T}\right)} \tag{7.6}$$

$$D_{Bioelectra} = 1.7 \cdot 10^{-7} \cdot l^{-4.5} \cdot e^{\left(0.2 \cdot c - \frac{4{,}450 \cdot l^{-0.5}}{T}\right)} \tag{7.7}$$

where c is the local moisture concentration of the insulation (expressed in % of dry weight), D is the moisture diffusion coefficient (expressed in m^2/s), and T is the operation temperature.

7.2.3 Development of the moisture dynamic model

The moisture dynamic model proposed is an integration of a thermal model set out in IEEE standard C57-91-2011 [8] and the moisture diffusion model based on Fick's second law described in section 7.2.2. Figure 7.5 shows the flow chart of the model.

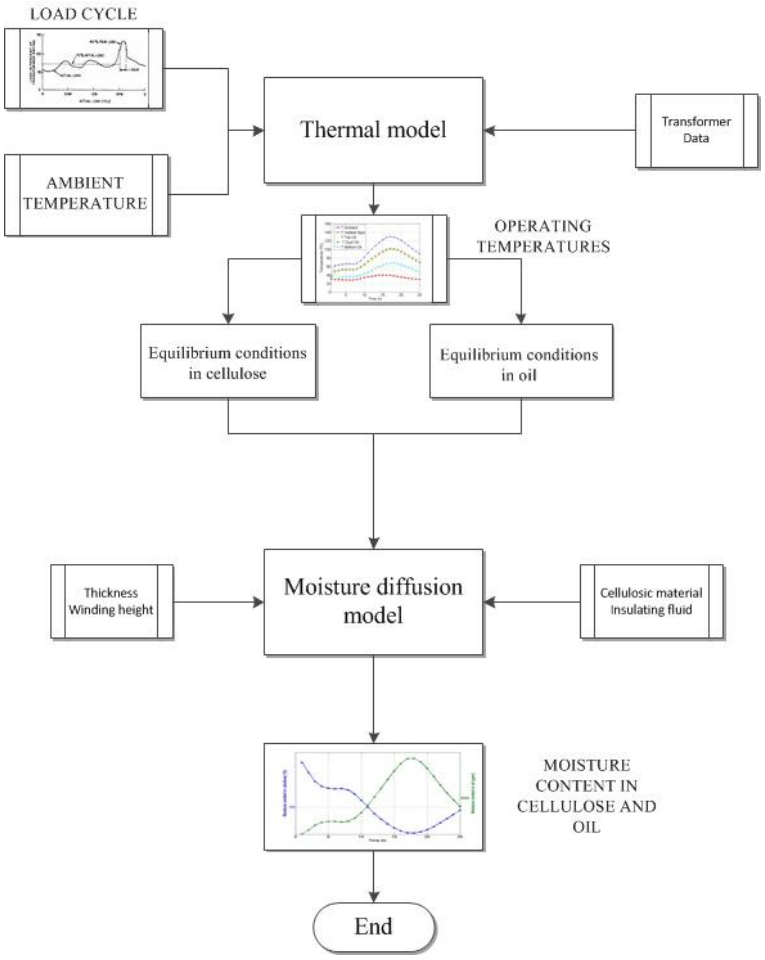

Figure 7.5: General scheme of the moisture dynamic model.

The transformer operating temperatures calculated with the thermal model will be used as a starting point to calculate the evolution of the moisture inside the transformer, what will be done by solving Fick's second law 7.4. The thermal model is capable of estimating oil operating temperatures at different heights of the transformer, at different heights of the windings and also at the hottest-spot of the transformer.

As was explained before, the moisture model considers a one-dimensional geometry to study the solid insulation. To calculate the moisture distribution at different points of the transformer, several simulations must be run in parallel considering the temperatures calculated for different parts of the winding, and specifying adequate insulation thicknesses.

The instantaneous temperatures are used as an input of the moisture diffusion model. They are used to calculate the instantaneous diffusion coefficient at each instant of the simulation, and also to determine the boundary condition.

The boundary condition of the model should set the moisture content on the surface of the solid insulation at each time. To establish the superficial moisture, the model assumes that the surface of the paper reaches the equilibrium instantaneously for any time.

The equilibrium condition, states how water would be splitted between paper and oil at each working temperature and is established by the equilibrium curves that were calculated in chapter 3. The curves are used in the model in their parametrized form (equation 7.8 for mineral oil and equation 7.9 for natural esters).

$$C_{equil} = 2.173 \cdot 10^{-5} \cdot p_v^{0.6685} \cdot e^{\left(\frac{42{,}725.6}{T}\right)} \tag{7.8}$$

where C_{equil} is the equilibrium moisture in cellulose, expressed in %, T is the temperature in oil-cellulose interface and p_v is the partial pressure of water vapour, expressed in atmospheres.

$$\begin{aligned} C_{equil\_vegetal} = {} & 1.18 \cdot 10^{-18} \cdot {p_v}^3 \cdot e^{\left(\frac{16{,}570}{T}\right)} - 5.39 \cdot 10^{-12} \cdot {p_v}^2 \cdot e^{\left(\frac{10{,}960}{T}\right)} \\ & + 9 \cdot 10^{-6} \cdot p_v \cdot e^{\left(\frac{5{,}418}{T}\right)} + \frac{1{,}004}{T} - 3 \end{aligned} \tag{7.9}$$

where $C_{equil\_vegetal}$ is the equilibrium moisture in pressboard impregnated with

natural ester, expressed in %, T is the temperature in oil-pressboard interface, and p_v is the partial pressure of water vapour.

An additional mass balance equation is necessary to determine the equilibrium condition for a particular temperature. The equation 7.10, proposed by Frimpong in [75] was used to this end, which assume that the total weight of water in the transformer does not vary although it is split between paper and oil in different proportions as temperature changes.

$$W_{total} = M_{cellulose} \cdot \frac{C_{equil}}{100} + M_{oil} \cdot \frac{PPM_{oilequil}}{1,000,000} \tag{7.10}$$

where W_{total} is the total water in the transformer, expressed in kg, $M_{cellulose}$ is the weight of cellulose, expressed in kg, M_{oil} is the weight of oil, expressed in kg, C_{equil} is the final % weight of water in cellulose, and $PPM_{oilequil}$ is the moisture content in oil.

The equilibrium moisture in paper and oil (C_{equil}, $PPM_{oilequil}$) calculated by solving the system of equations formed by 7.8 and 7.10, would be only reached if the transformer operates at constant temperature for a very long time. However, the determination of these variables is basic to establish the boundary condition required to solve the dynamic model.

At every iteration, the paper surface is considered to have a moisture content equal to the C_{equil} obtained for the temperature of this particular time instant, i.e. the model assumes that the surface of the paper reaches the equilibrium in an instantaneous way. The model solves Fick's equation using the finite element method, and with the aforesaid boundary condition, and calculates the moisture distribution throughout the solid insulation at every iteration. The average moisture in paper C_m, is then calculated using equation 7.11.

$$C_{m-est(t_i)} = \frac{1}{l} \int_{x=0}^{x=1} C_{est(x,t_i)} \cdot dx \tag{7.11}$$

where l is the pressboard thickness in metres.

Once calculated C_m, the instantaneous moisture content in oil can be also calculated using equation 7.10.

7.3 Moisture dynamics on a transformer insulated with vegetable oil. Case studies

The moisture dynamic model proposed in this work has been tested in three different cases that will be described next. Different loading profiles were simulated in a 52,267 KVA transformer, whose properties are shown in table 7.2. The data were taken from [8]. Table 7.3 shows the transformer insulation system weights used in this model.

Table 7.2: Data of the transformer.

Parameters	**Value**
Refrigeration	ONAN/ONAF
Power	52,267 KVA
Core and coil weight	75,600 lb
Tank and radiators	31,400 lb
Gallons of oil	4,910
No load loss	36,986 W
Load loss	72.768 W
Total loss	109.755 W

Table 7.3: Transformer insulation system weights.

Parameters	**Value**
Total cellulose insulation weight (kg)	3,023
Total mineral oil weight (kg)	31,500
Total natural ester weight (kg)	32,208
Initial moisture in solid insulation (% by weight)	4

In first place, the transformer was considered to be filled with the natural ester Biotemp. It is important to mention that the thermal model applied to the study of the ester-filled transformer is the one proposed in the annex G of the IEEE Std C.57.91-2011 [8] and has not been changed to consider the different properties of the fluid. This will

probably introduce some error in the calculation of the temperatures from the load profiles. A thermal model for ester-insulated transformers will be developed in the future, as is explained in section 8.3.

In this case the solubility curve determined in chapter 3 for the ester Biotemp was taken as equation 7.12.

$$LogW_S = 5.67 - \frac{791}{T} \tag{7.12}$$

The insulation thickness considered in the simulations is 3 mm, although the multi-physical model can be applied to other insulation thickness as well. The model can also simulate the temperature and moisture dynamics at any height of the winding, but all the simulations were done considering the temperature of the top oil.

7.3.1 Case 1. Load step

The first case considers the load profile and ambient temperature shown in figure 7.6. During the first five hours the transformer is considered to be out of service (load 0), and then it worked at rated load for 19 hours. The ambient temperature had a constant value equal to 25 ^{o}C for the whole simulated period.

Figure 7.7 shows the evolution of the temperatures in different points of the transformer during the simulated period. As can be seen, the temperature increases sharply after the load step, and the system needs approximately 7 hours to reach the equilibrium.

Regarding the moisture dynamics, figure 7.8 shows the moisture in paper and moisture in oil that would be attained in steady state condition for every operating temperature. However, the dynamics of moisture in the oil-paper system has a large

time constant, and the instantaneous values of moisture in cellulose and moisture in oil are the ones shown in figure 7.9 and 7.10

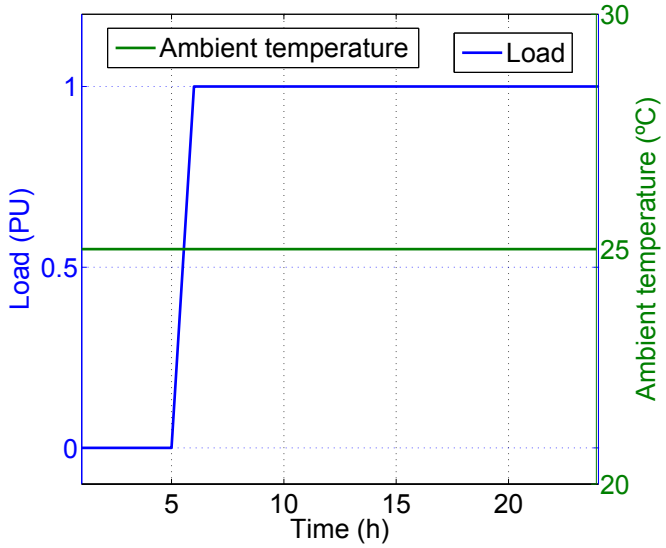

Figure 7.6: Load cycle and ambient temperature used in case 1.

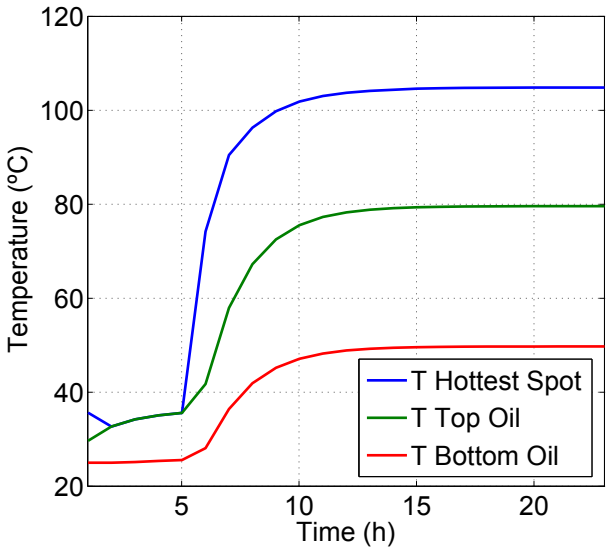

Figure 7.7: Temperatures distribution calculated for case 1.

Additionally, figure 7.9 shows the instantaneous moisture content inside the cellulose during the operation cycle, which will be called from this section c_m, and the moisture content that would be attained for each temperature if the system would be in steady state, which will be called from this section c_e. The behaviour observed is

while the temperature is increasing the moisture content in cellulose is decreasing until reaches the equilibrium. To achieve this, the temperature must be constant during a long time to reach the equilibrium.

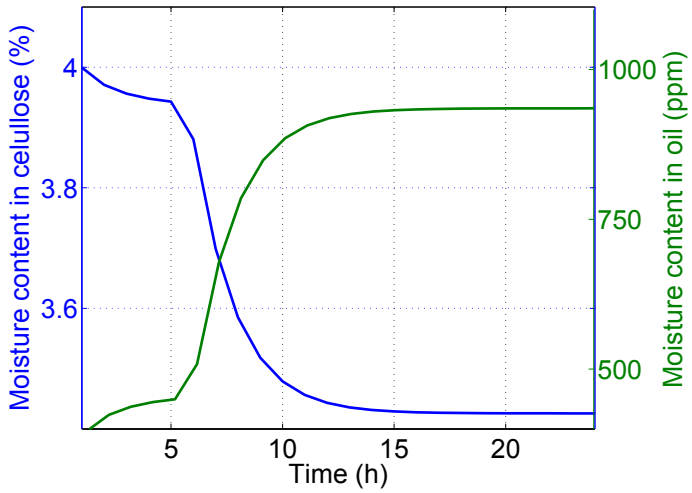

Figure 7.8: Moisture content in Biotemp and cellulose in steady state obtained from moisture dynamic model in case 1.

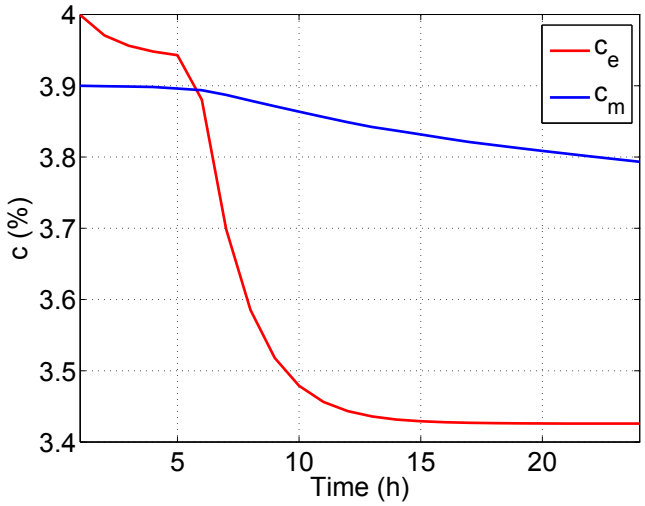

Figure 7.9: Moisture content in cellulose in operation (c_m) and steady state (c_e) obtained from moisture dynamic model in case 1.

On the other hand, figure 7.10 shows the moisture content in Biotemp during the operation cycle and the moisture content in oil in steady state. Opposite to the cellulose, the moisture content in oil increases with the temperatures.

According with the figure 7.10, the moisture content in oil keeps increasing until reaching the equilibrium. If the temperature remains constant for a long time, the moisture content in oil in operation could be the same that the equilibrium one.

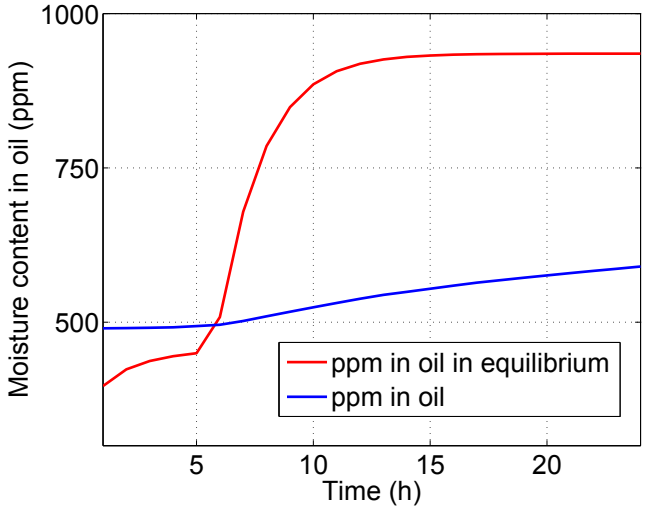

Figure 7.10: Moisture content in oil (considering the insulating fluid Biotemp) in operation and steady state obtained from moisture dynamic model in case 1.

7.3.2 Case 2. Cycle load proposed in IEEE Std C.57.91-2011

In the second case, the load profile and ambient temperature shown in figure 7.11 was considered. These profiles are provided in the Annex G of IEEE Std C.57.91-2011 as an example of cyclical short term overload.

As can be seen in figure 7.12, the temperatures in the transformer follow the same cyclical behaviour as the load, with an approximated time delay of two hours. The hottest spot temperatures reached at some points of the simulation are higher than 100 ^{o}C, and so the loss of life of the insulation during these periods would be significant.

Figure 7.13, shows the moisture contents that would be attained in oil and paper for each working temperature if the system would be in steady state. As can be seen these steady state moistures varies in a cyclical manner as well. If the peaks. If

the peaks of the temperatures and the instantaneous values of moisture contents in Biotemp are compared, it can be stated that the time delay between both variables is approximately 5 hours, figures 7.14 and 7.16.

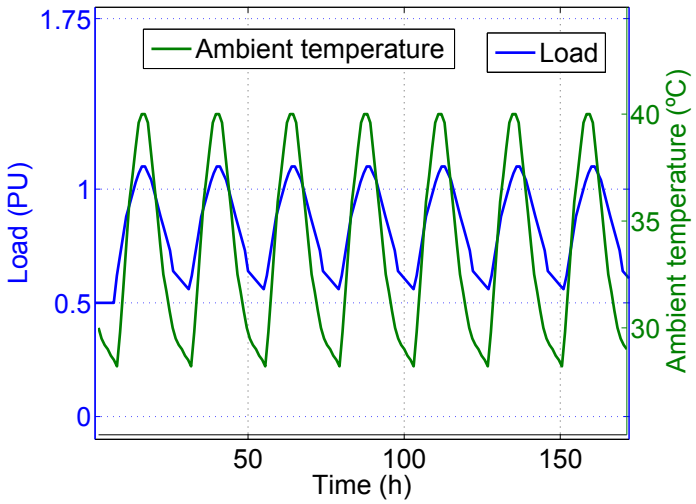

Figure 7.11: Load cycle and ambient temperature used in case 2.

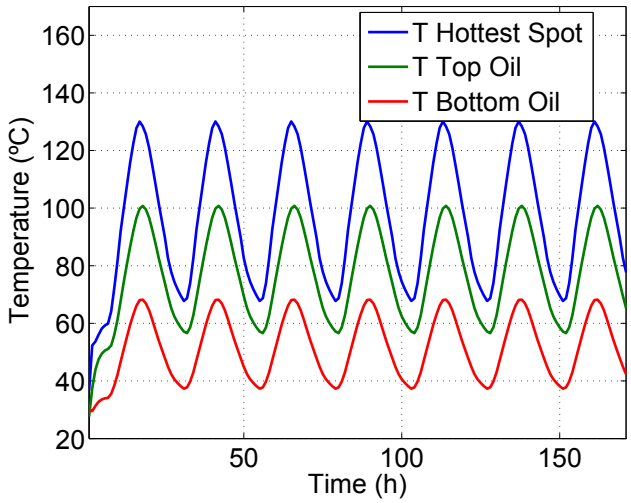

Figure 7.12: Temperatures distribution calculated for case 2.

In figure 7.14, the value of the instantaneous average moisture of the cellulose changes cyclically with the temperatures, however, as can be seen it presents a downward trend, due to the fact that the diffusion coefficient depends on temperature, and in consequence the desorption of moisture from paper to oil (that occurs when the

temperature increases) takes place at a higher rate than the process of adsorption of moisture by cellulose that takes place when temperature decreases.

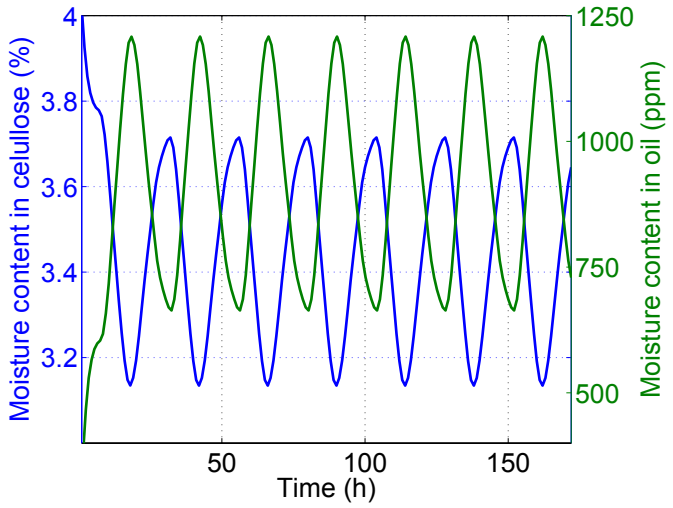

Figure 7.13: Moisture content in Biotemp and cellulose in steady state obtained from moisture dynamic model in case 2.

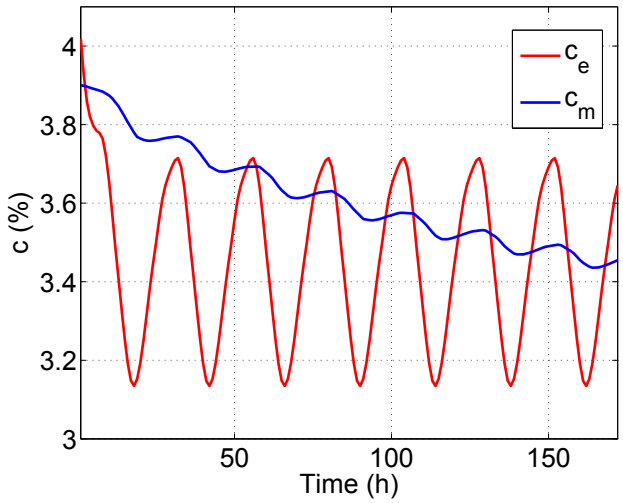

Figure 7.14: Moisture content in cellulose in operation (c_m) and steady state (c_e) obtained from moisture dynamic model in case 2.

Figure 7.15 shows the values of the instantaneous average and the steady state of moisture in the cellulose changing cyclically with the temperatures after one month of operation, during this time the instantaneous average value of moisture in cellulose reaches a stable condition.

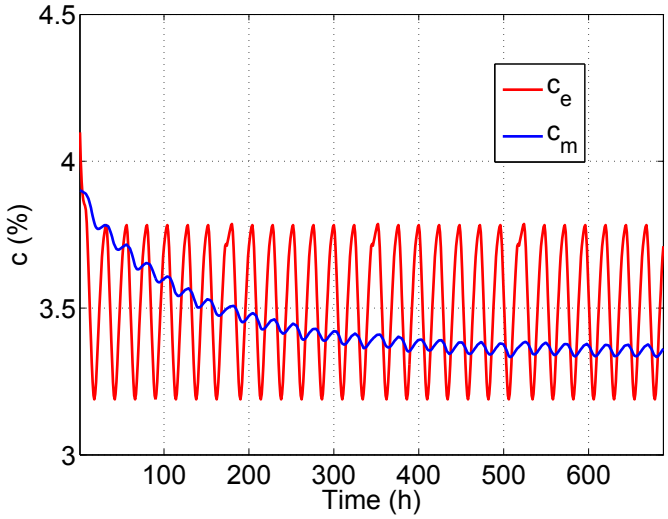

Figure 7.15: Moisture content in cellulose in operation (c_m) and steady state (c_e) after one month obtained from moisture dynamic model in case 2.

Likewise, figure 7.16 compares the instantaneous moisture content in Biotemp during the operation cycle and the moisture content of oil in steady state. Despite the moisture content is changing cyclically with temperature, it has a trend to increase because the rate of the absorption in oil is higher than the rate of return to cellulose. This trend keeps constant until the equilibrium is reached.

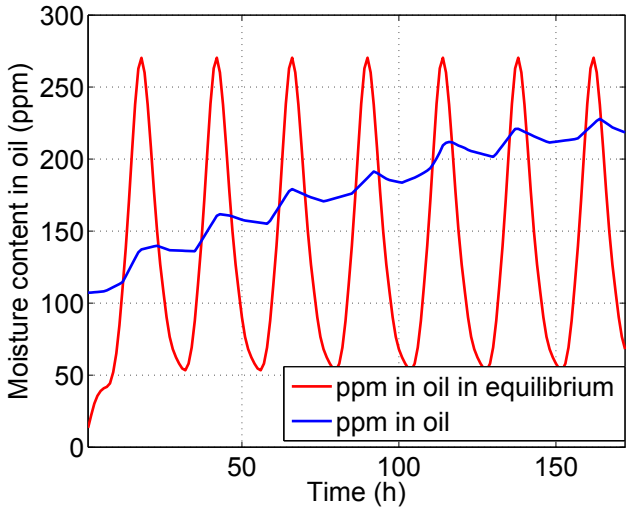

Figure 7.16: Moisture content in Biotemp in operation and steady state obtained from moisture dynamic model in case 2.

Similar behaviour can be found in figure 7.17, after one month of operation the

instantaneous moisture content in Biotemp reaches a stable condition.

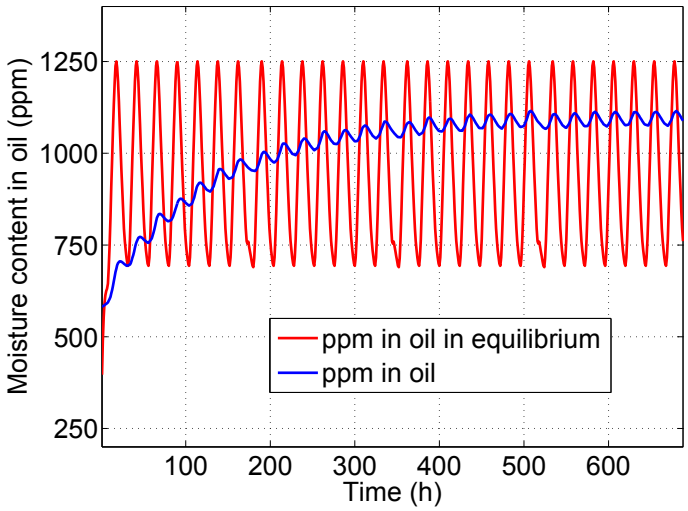

Figure 7.17: Moisture content in Biotemp in operation and steady state after one month obtained from moisture dynamic model in case 2.

7.3.3 Case 3. Overload and further disconnection

In the third and last case, a long term overload was considered, followed by a sudden disconnection of the transformer. This case has been reported to be specially critical when wet transformers are operated at low ambient temperatures. The load profile and ambient temperature are shown in figure 7.18. As can be seen, a constant ambient temperature of 5 ^{o}C was considered during the simulation. It is very difficult to find load profiles as high as this in operating transformers, however the criteria to simulate this case were based in the importance to know more about the saturation phenomena.

As can be seen in figure 7.19, when the transformer is overloaded, the temperature of the insulation rises to very high values. At the same time, oil becomes more hydrophilic, i.e. its solubility increases, and part of the moisture of paper migrate towards it. The migration rate is governed by the diffusion coefficient, that is high, and the oil becomes able to admit a big amount of water. In consequence water will migrate from paper to oil with a relatively fast migration rate, as the diffusion coefficient

depends exponentially on temperature.

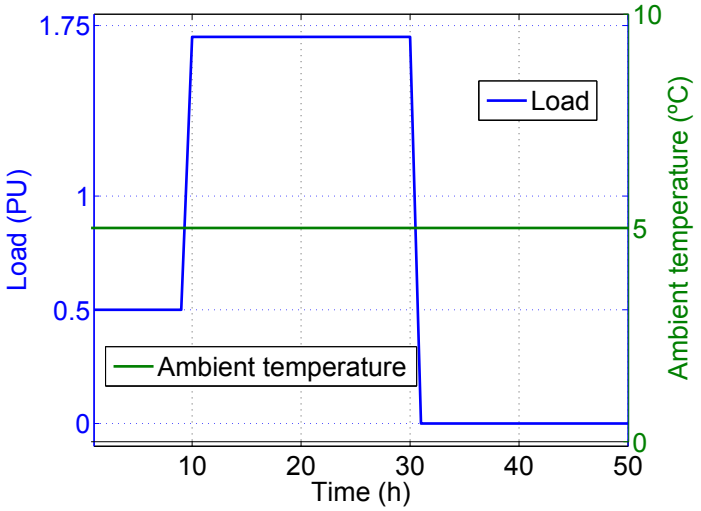

Figure 7.18: Load cycle and ambient temperature used in case 3.

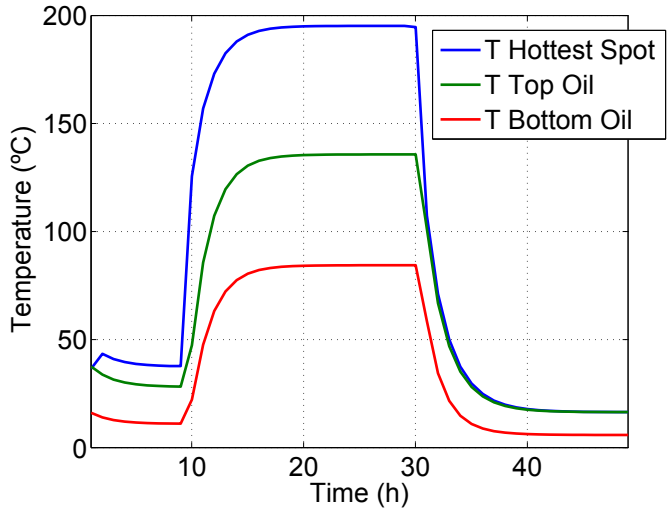

Figure 7.19: Temperatures distribution calculated for case 3.

As with the previous cases, in figure 7.20, the steady state moisture in oil increases according with the temperatures while the moisture content in paper decreases. For the three load levels shown in this case, the behaviour of moisture content in oil as cellulose were as expected. It is important to note that due the high load value (1.7 PU) the temperatures are too high during ten hours of operation and therefore the migration of moisture from cellulose to the oil is higher than previous cases, figures 7.21 and 7.22.

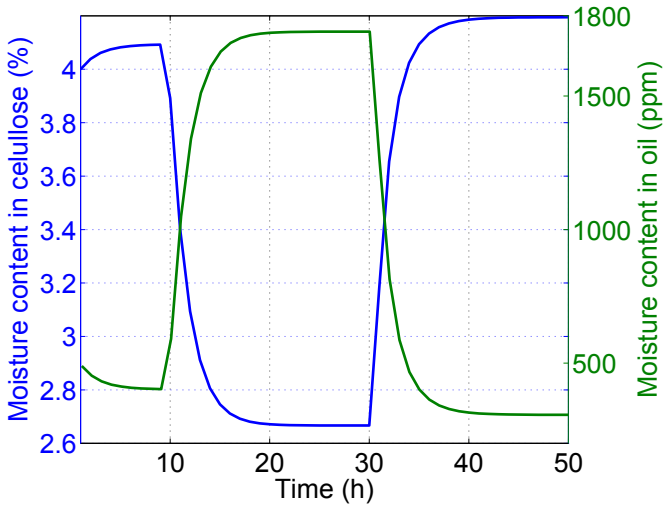

Figure 7.20: Moisture content in Biotemp and cellulose in steady state obtained from moisture dynamic model in case 3.

Similar to previous cases, in figure 7.21, when the load changed after ten hours the value of the average moisture of the cellulose also has changed keeping a downward trend always looking to reach equilibrium, after thirty hours of operation, the load changed to 0 PU then the temperatures start to decrease and the moisture content in paper starts to increase. For the load profile used in this case neither the moisture content in paper nor moisture content in oil can reach the equilibrium.

As in cases 1 and 2, figure 7.22 shows the moisture content in Biotemp during the operation cycle and the moisture content in steady state, the moisture content in oil increases with the temperatures and viceversa looking for reach the equilibrium, as it is explained above for the load profile used in this case neither the moisture content in paper nor moisture content in oil can reach the equilibrium.

Figure 7.23 shows the instantaneous moisture in oil and the saturation limit (i.e. the maximum amount of moisture accepted by oil without being satured). The saturation limit depends on temperature and can be calculated according to equation 7.12. As can be seen, after disconnection of the transformer, there is a certain risk of saturation of the oil. This would cause the presence of water in liquid phase within the

transformer tank [13].

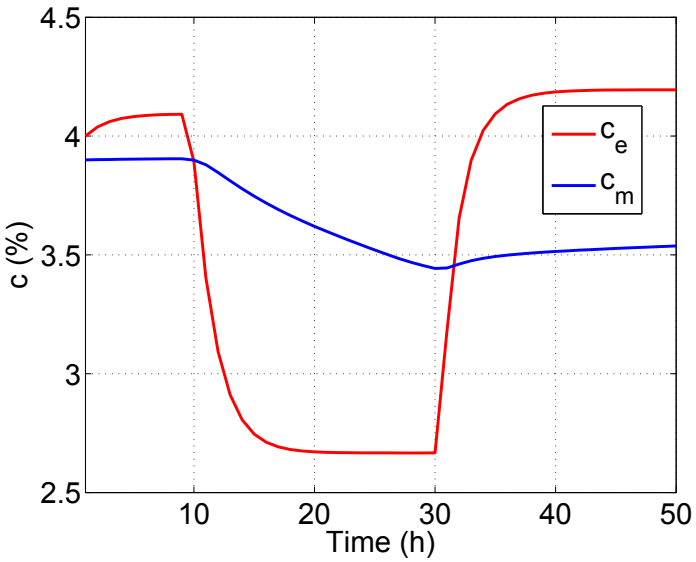

Figure 7.21: Moisture content in cellulose in operation (c_m) and steady state (c_e) obtained from moisture dynamics model in case 3.

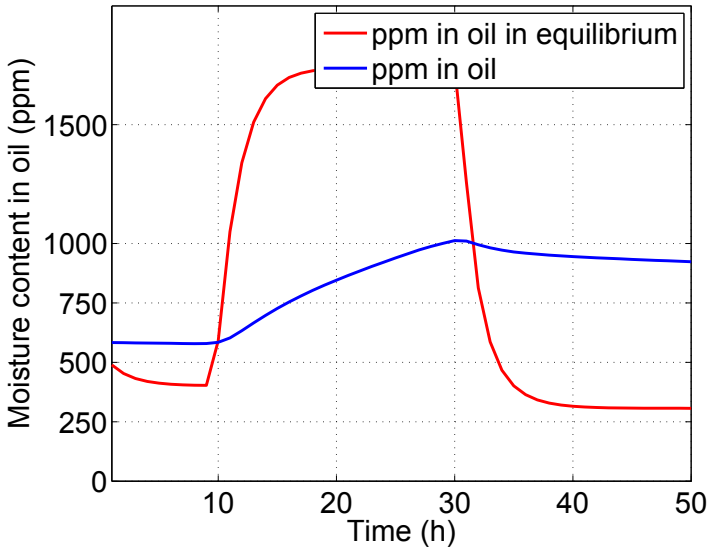

Figure 7.22: Moisture content in Biotemp in operation and steady state obtained from moisture dynamics model in case 3.

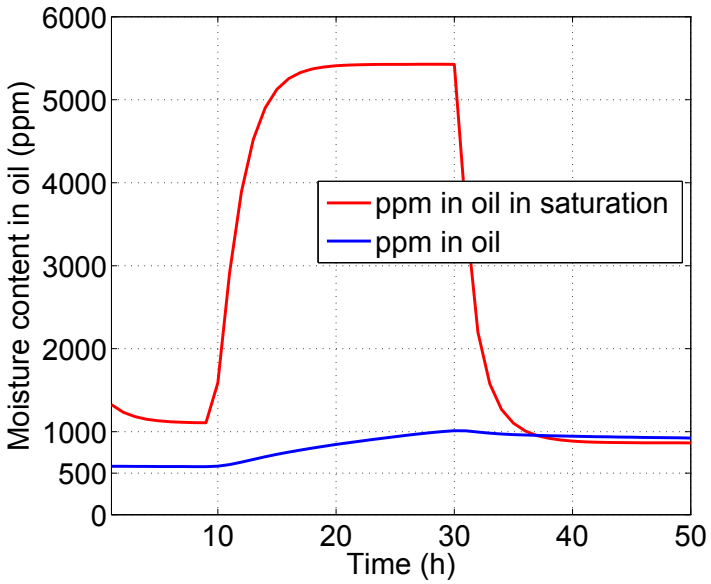

Figure 7.23: Moisture content in Biotemp in saturation vs instantaneous moisture. Case 3.

7.4 Moisture dynamics in a transformer insulated with mineral oil

The simulations done in the previous section were repeated considering that the transformer is filled with mineral oil. This section intends to do a comparison of the moisture dynamics inside the transformer using Biotemp and Mineral oil as insulating liquids, based in the studied cases.

For mineral oil the solubility curve was taken as equation 7.13, , while for Biotemp equation 7.12 was applied as was explained before.

$$LogW_S = 7.44 - \frac{1,686}{T} \tag{7.13}$$

7.4.1 Case 1

The same load conditions as for case 1, described in section 7.3.1, were applied to a transformer insulated with mineral oil.

The main difference to highlight in this case is the high absorption capacity of Biotemp against the Mineral oil. Figure 7.24 shows the moisture content in Biotemp and Mineral oil in steady state. As can be seen, the values of moisture are more than nine times higher in Biotemp than in mineral oil at high temperatures. Due that the solubility of these kinds of oils increase with the temperatures, natural esters can extract much more water from cellulose at the same temperature than a mineral oil.

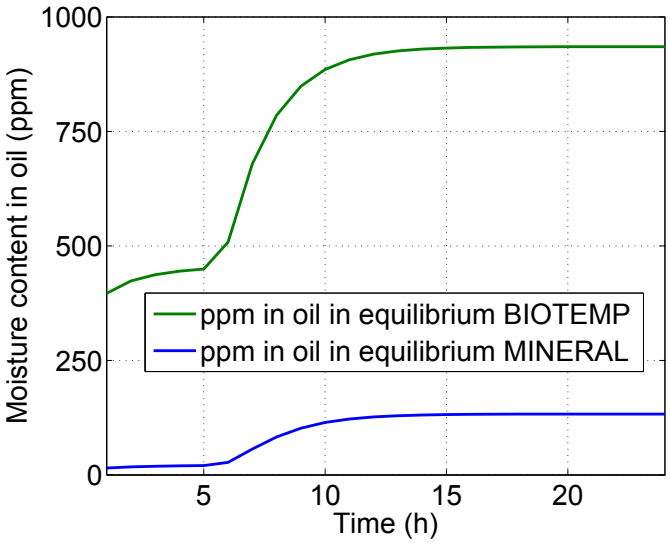

Figure 7.24: Comparison of moisture content in steady state in Biotemp and in Mineral Oil. Case 1.

On the other hand, all the explained above can be evidenced with the moisture content in cellulose using both kinds of oils. At higher moisture content in oil, the moisture content in cellulose must be lower and vice versa. Figure 7.25 shows the moisture content in cellulose with a clear trend to stay in equilibrium during the load cycle. It should also be noted, that the moisture migration rate, which is reflected by the slope of the curves, is higher in the system insulated with Biotemp. This is due to the

differences on the diffusion coefficients of both materials that where widely described in previous chapters.

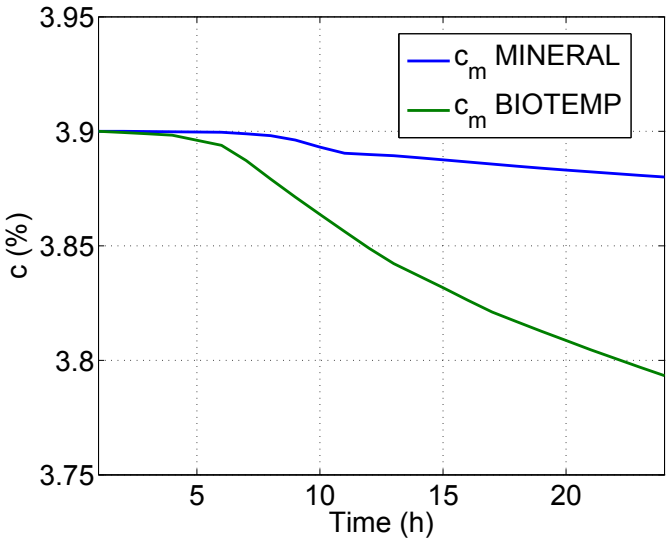

Figure 7.25: Instantaneous moisture content in cellulose (c_m) in Biotemp and in Mineral oil. Case 1.

7.4.2 Case 2

The same load conditions as for case 2, described in section 7.3.2, were applied to a transformer insulated with mineral oil.

Similar behaviour to case 1 can be observed in case 2. The main difference between the two kinds of oils are the cyclical changes, again the moisture content in Biotemp is higher than that mineral oil. The moisture content in cellulose is also changing with temperatures. Figures 7.26 and 7.27 show the moisture content in oil and cellulose respectively.

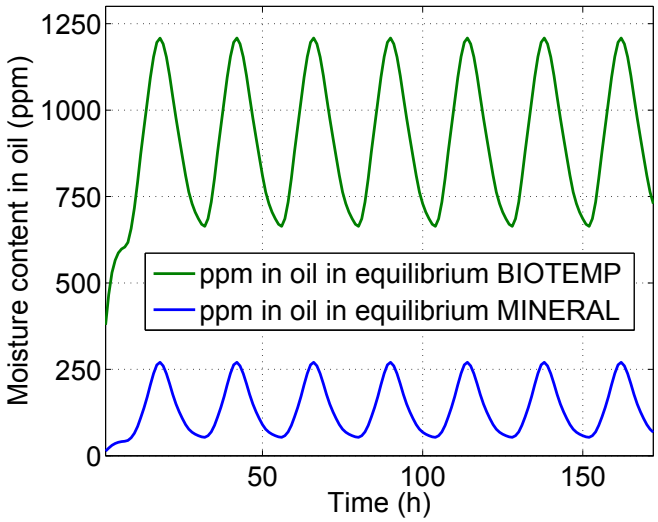

Figure 7.26: Comparison of moisture content in steady state in Biotemp and in Mineral Oil. Case 2.

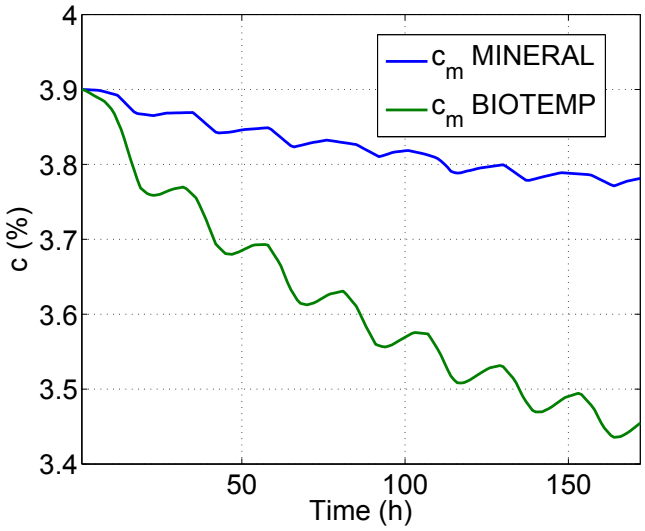

Figure 7.27: Instantaneous moisture content in cellulose (c_m) in Biotemp and in Mineral oil. Case 2.

7.4.3 Case 3

The same load conditions as for case 2, described in section 7.3.3, were applied to a transformer insulated with mineral oil.

Similar behaviour to case 1 and case 2 can be observed in case 3. The moisture content in the two kinds of oils and cellulose can be observed in figures 7.28 and 7.30 respectively.

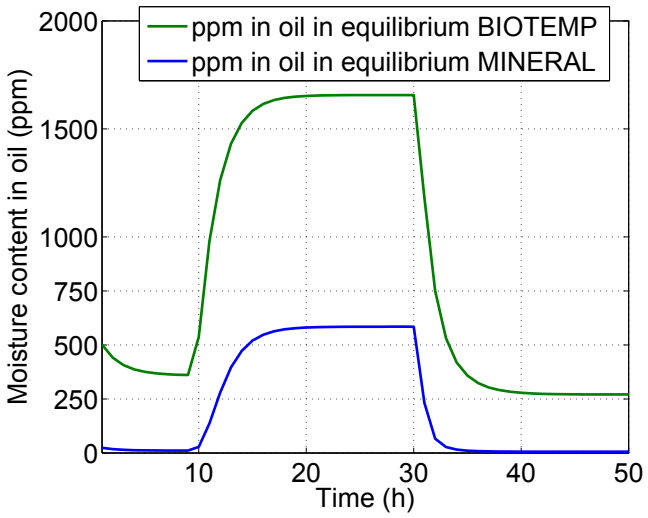

Figure 7.28: Comparison of moisture content in Biotemp and Mineral Oil. Case 3.

Figures 7.23 and 7.29 show the saturation condition for the two kinds of oils used in this chapter.

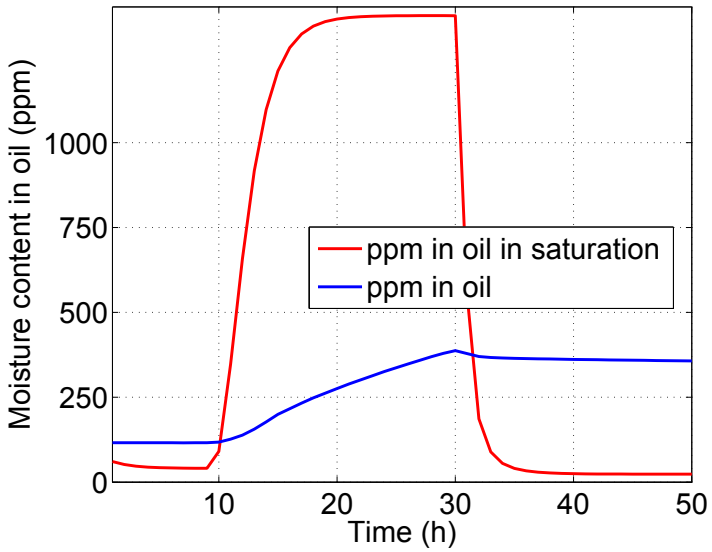

Figure 7.29: Moisture content in Mineral oil in saturation. Case 3.

In all cases, the moisture content in Biotemp is higher than in mineral oil. How-

ever, in this case is interesting to observe the difference in the saturation conditions of both kinds of oils. After the disconnection (30 hours), the mineral oil reaches saturation levels higher than those of the natural ester (figure 7.23). This is due to a double effect. On the one hand, the saturation limits of natural esters are much bigger that those of natural oils (see equations 7.12 and 7.13).

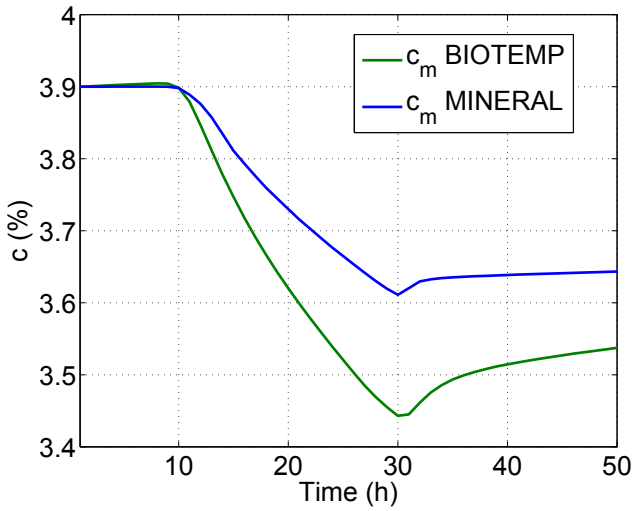

Figure 7.30: Instantaneous moisture content in cellulose (c_m) in Biotemp and in Mineral oil. Case 3.

Additionally, the diffusion coefficient is lower in mineral-oil impregnated insulation, and the return of water to the cellulose is, in consequence more slow, which increases the risk of saturation of the oil in this kind of situation.

7.5 Conclusions

In this chapter, a moisture dynamics model is developed, which allows the study of the behaviour of moisture in cellulose insulation and insulating liquid. During the real operation of a transformer, the moisture content of oil and paper is estimated in a dynamic mode taking into account the temperature profile. No other dynamic model of these characteristics has been proposed to date.

The model proposed in this chapter is based on the integration of the thermal model proposed in the Annex G of the IEEE loading guide C.57.91-2011 [8], and a moisture model based on Fick's second law.

This model has been used to simulate different operating conditions as overload of the transformers, ambient temperature changes and different insulating liquids.

To implement the model, the specification of liquid transformer insulation is required, and also the moisture diffusion coefficients for different types of cellulose insulation presented in this chapter.

Chapter 8

Conclusions

This chapter presents the general conclusions of the thesis. In addition, the chapter summarises the work's main contributions and makes suggestions for future research. Finally, the chapter lists the published articles based on the thesis research and acknowledges the projects that have supported the research and the international stays.

8.1 General conclusions

This work shows a study about the moisture dynamics in transformers. A model was developed to calculate the dynamic behaviour of water in transformer insulation. The main parameter of this model is the diffusion coefficient.

Firstly a summary about the previous works regarding moisture diffusion coefficients on different materials, and the experimental methodologies used in those works was done. The results obtained in this search have been used as reference or starting point of this work. Few references were found for the moisture diffusion coefficient of pressboard impregnated with mineral oil and with a natural ester, which were the materials characterized in the thesis.

Moisture diffusion coefficients for pressboard impregnated with two different natural esters have been proposed and validated under different temperatures and using samples of different thickness, demonstrating a great accuracy. No other author has proposed any moisture diffusion coefficient in pressboard impregnated with natural ester considering the effect of the thickness of the samples. An expression for the diffusion coefficient of mineral-oil impregnated pressboard has been obtained as well allowing the comparison of the dynamic behaviour of moisture in both materials.

A new optimization method was proposed to be used in the determination of the parameters of the coefficients. The method is based in the Particle Swarm algorithm and has been proved to be more efficient than the Genetic Algorithms method that was used in previous works. The results obtained using PSO were better than the results obtained using GAs in all the evaluated cases. The optimization times using the particle swarm method were considerably lower than those using the GA method. In addition, the root-mean-square-deviation values obtained when the moisture diffusion coefficient was determined using PSO were, in most cases, lower than those obtained when the moisture diffusion coefficients calculated by GAs were used.

The moisture equilibrium curves of natural ester and mineral oil with cellulosic insulation have been experimentally determined. A comparison between these curves was done, finding that the moisture content in natural esters is much greater than that in mineral insulating oil for the same temperature and the same moisture content in cellulose. This is due to the fact that the ester group in the molecules of ester fluids has a strong ability to participate in hydrogen bonding. The equilibrium curves were used as a boundary condition of the moisture dynamics model.

Finally a multi-physical model has been developed that allows simulating the coupled effects of temperature and moisture dynamics for a certain load profile. Different cases have been studied to compare the behaviour of these variables on mineral oil insulated transformers and on natural ester insulated units. The model could also be used in transformer maintenance (i.e. to determine the drying times of the trans-

formers) or for life management purposes.

8.2 Main contributions

During this work different experimental and theoretical methodologies have been developed to study moisture dynamics inside transformers insulated with natural esters, the original contributions of the work can be found below:

- An experimental methodology to determine solubility curves in dielectric fluids has been developed and validated, involving experiments under controlled temperature and relative humidity. The methodology has been applied to the determination of the moisture solubility curves of natural esters and mineral oil.
- New moisture equilibrium curves have been obtained for cellulose-mineral oil systems and cellulose-natural ester systems.
- A new optimization method has been proposed based in Particle Swarm that has been demonstrated to be more efficient than other previously used methodologies.
- An expression for the moisture diffusion coefficients of mineral-oil impregnated pressboard have been proposed and validated experimentally. As far as the author of the thesis knows, no other expressions for the moisture diffusion coefficient of mineral-oil-impregnated pressboard were proposed before.
- An expression for the moisture diffusion coefficients of natural-ester-impregnated pressboard have been proposed and validated experimentally. Only one author had proposed a coefficient for these materials before.
- A multi-physical model has been developed to study the dynamic behaviour of the moisture in transformers impregnated with natural esters under real operation. The model has been applied to the investigation several cases, performing a

comparison of the results when transformers are insulated with mineral oil and when they are insulated with natural ester fluids.

8.3 Beyond PhD Thesis

The results and experience gained through this project suggest the following lines of future research.

- Conduct an experimental validation of the moisture dynamics model on transformer prototypes subjected to variable load.
- Development of a model to estimate the temperature profiles in transformers insulated with natural esters with more accuracy.
- Complete the model to include the calculation of the aging rate of the solid insulation by the effect of the temperature and moisture under different loading profiles.
- Apply the moisture dynamics model to the development of a moisture monitoring system.
- Research the moisture dynamics on aged transformers.
- Apply the developed methodologies to the study and characterization of new insulating materials.

8.4 Publications, research projects and international stays

Several of the results of this thesis have appeared in the following journal papers:

8.4.1 Publications in scientific journals

1. R. Villarroel, D.F. Garcia, Maria A. Davila, Eduardo F. Caicedo. Particle Swarm Optimization and Genetic Algorithm, application and comparison to determine the moisture diffusion coefficients of pressboard transformer insulation. IEEE Transactions on Dielectrics and Electrical Insulation, In press, (2015).

2. D. F. Garcia, R. Villarroel, B. Garcia, and J. C. Burgos. Effect of the Thickness on the Water Mobility inside Transformer Cellulosic Insulation. IEEE Transactions on Power Delivery, In press, (2015).

3. R. Villarroel, D.F. Garcia, B. Garcia, and J.C. Burgos. Moisture diffusion coefficients of transformer pressboard insulation impregnated with natural esters. IEEE Transactions on Dielectrics and Electrical Insulation, 22(1):581-589, 2015.

4. R. Villarroel, B. Garcia, D.F. Garcia, and J.C. Burgos. Assessing the use of natural esters for transformer field drying. IEEE Transactions on Power Delivery, 29(4):1894-1900, 2014.

5. R. Villarroel, D.F. Garcia, B. Garcia, and J.C. Burgos. Diffusion coefficient in transformer pressboard insulation part 2: mineral oil impregnated. IEEE Transactions on Dielectrics and Electrical Insulation, 21(1):394-402, 2014.

6. R. Villarroel, D.F. Garcia, B. Garcia, and J.C. Burgos. Diffusion coefficient in transformer pressboard insulation part 1: non impregnated pressboard. IEEE Transactions on Dielectrics and Electrical Insulation, 21(1):360-368, 2014.

7. D.F. Garcia, R. Villarroel, B. Garcia, and J.C. Burgos. A review of moisture diffusion coefficients in transformer solid insulation - part 2: Experimental validation of the coefficients. IEEE Electrical Insulation Magazine, 29(2):40-49, 2013.

The results of the thesis have been presented at the following conferences:

1. R. Villarroel, D.F. Garcia, B. Garcia and J.C. Burgos. Studying the moisture dynamics in transformers insulated with natural esters. IEEE International Conference on Solid Dielectrics (ICSD). Bologne-Italy, 2013.

2. D.F. Garcia, B. Garcia, R. Villarroel and J.C. Burgos. A new methodology for determining the moisture diffusion coefficient of transformer solid insulation. IEEE International Conference on Solid Dielectrics (ICSD). Bologne-Italy, 2013.

3. R. Villarroel, D.F. Garcia, B. Garcia and J.C. Burgos. Comparison of the drying times for kraft paper and pressboard in transformers factory drying. International Conference on Electrical Machine. Marseille-France, 2012.

4. D.F. Garcia, B. Garcia, J.C. Burgos and R. Villarroel. Transformer field drying improvement by applying low-frecuency-heating. Bogotá-Colombia, 2012.

This PhD. thesis has been supported through the following research projects:

- Moisture dynamics in transformers insulated with natural esters, (DPI2012-35819). 2013-2015.
- Optimization of the drying processes of power transformers in field (DPI2009-07093). 2010-2012.

During the thesis, the following research stays have been done:

- Institution: University of Valle. School of Electrical and Electronic Engineering. Cali, Colombia. Start date: 17/11/2013. End date: 14/02/2014 (3 months). Supported by Univerisdad Carlos III de Madrid. Name of the grant: Mobility aids for researchers in foreign or national research centres.

- Institution: University of Valle. School of Electrical and Electronic Engineering. Cali, Colombia. Start date: 28/04/2014. End date: 30/06/2014 (2 months). Supported by Santander Bank. Name of the grant: Latin America Scholarship, Young Professors and Researchers.

- Institution: University of Manchester. School of Electrical and Electronic Engineering. Manchester, UK. Start date: 15/09/2014. End date: 06/03/2015 (6 months). Supported by Univerisdad Carlos III de Madrid. Name of the grant: Mobility aids for researchers in foreign or national research centres.

Bibliography

[1] A Bandyopadhyay, H Radhakrishnan, BV Ramarao, and SG Chatterjee. Moisture sorption response of paper subjected to ramp humidity changes: Modeling and experiments. *Industrial & engineering chemistry research*, 39(1):219–226, 2000.

[2] WG Cigre. A2. 18. *Guide for life management techniques for power transformers*, 2003.

[3] IEEE guide for acceptance and maintenance of natural ester fluids in transformers, 2008.

[4] D.F. Garcia, B. Garcia, and J.C. Burgos. A review of moisture diffusion coefficients in transformer solid insulation-part 1: coefficients for paper and pressboard. *IEEE Electrical Insulation Magazine*, 29(1):46–54, 2013.

[5] R Jeffries. The sorption of water by cellulose and eight other textile polymers. *Journal of the Textile Institute Transactions*, 51(9):T339–T340, 1960.

[6] R. Villarroel, D.F. Garcia, B. Garcia, and J.C. Burgos. Diffusion coefficient in transformer pressboard insulation part 1: non impregnated pressboard. *IEEE Transactions on Dielectrics and Electrical Insulation*, 21(1):360–368, 2014.

[7] D.F. Garcia, R. Villarroel, B. Garcia, and J.C. Burgos. A review of moisture diffusion coefficients in transformer solid insulation - part 2: Experimental validation of the coefficients. *IEEE Electrical Insulation Magazine*, 29(2):40–49, 2013.

[8] IEEE guide for loading mineral-oil-immersed transformers and step-voltage regulators - redline, 2012.

[9] Cigre Brochure. 436. *Experiences in service with New Insulating Liquids*, 2010.

[10] Green Power. Transformers. *Inside Housing*, pages 16–17, 2002.

[11] S Tenbohlen, M Koch, D Vukovic, A Weinläder, J Baum, J Harthun, M Schäfer, S Barker, R Frotscher, D Dohnal, et al. Application of vegetable oil-based insulating fluids to hermetically sealed power transformers. In *Cigre session*, volume 42, pages 24–29, 2008.

[12] A Bandyopadhyay, BV Ramarao, and Shri Ramaswamy. Transient moisture diffusion through paperboard materials. *Colloids and Surfaces A: Physicochemical and Engineering Aspects*, 206(1):455–467, 2002.

[13] Cigre Brochure. 349. *Moisture equilibrium and moisture migration within transformer insulation systems*, 2008.

[14] B. Garcia, J.C. Burgos, A.M. Alonso, and J. Sanz. A moisture-in-oil model for power transformer monitoring - part i: Theoretical foundation. *IEEE Transactions on Power Delivery*, 20(2):1417–1422, 2005.

[15] Yanqing Du, Markus Zahn, Bernard C Lesieutre, Alexander V Mamishev, and Stanley R Lindgren. Moisture equilibrium in transformer paper-oil systems. *IEEE Electrical Insulation Magazine*, 15(1):11–20, 1999.

[16] Zhaotao Zhang, Jian Li, S. Grzybowski, and Ping Zou. Moisture equilibrium in vegetable oil and paper insulation system. In *Annual Report Conference on Electrical Insulation and Dielectric Phenomena (CEIDP)*, pages 428–431, 2011.

[17] M. Jovalekic, D. Kolb, S. Tenbohlen, L. Bates, and R. Szewczyk. A methodology for determining water saturation limits and moisture equilibrium diagrams of alternative insulation systems. In *Dielectric Liquids (ICDL), 2011 IEEE International Conference on*, pages 1–5, 2011.

[18] V. Vasovic, J. Lukic, C. Perrier, and M.-L. Coulibaly. Equilibrium charts for moisture in paper and pressboard insulations in mineral and natural ester transformer oils. 30(2):10–16, 2014.

[19] T.V. Oommen. Vegetable oils for liquid-filled transformers. 18(1):6–11, 2002.

[20] C. Perrier and A. Beroual. Experimental investigations on mineral and ester oils for power transformers. In *Electrical Insulation, 2008. ISEI 2008. Conference Record of the 2008 IEEE International Symposium on*, pages 178–181, 2008.

[21] Zhaotao Zhang, Jian Li, Ruijin Liao, and S. Grzybowski. Moisture diffusion in vegetable oil-paper insulation. In *IEEE International Conference on Dielectric Liquids (ICDL)*, pages 1–4, 2011.

[22] Jian Li, Zhaotao Zhang, S. Grzybowski, and Yu Liu. Characteristics of moisture diffusion in vegetable oil-paper insulation. *IEEE Transactions on Dielectrics and Electrical Insulation*, 19(5):1650–1656, 2012.

[23] WW Guidi and HP Fullerton. Mathematical methods for prediction of moisture take-up and removal in large power transformers. In *Proceedings of IEEE Winter Power Meeting*, pages 242–244, 1974.

[24] Diego Fernando García Gómez. Determinación de coeficientes de difusión de humedad en papeles aislantes de transformador. 2012.

[25] DF García, B García, and JC Burgos. Determination of moisture diffusion coefficient for oil-impregnated kraft-paper insulation. *International Journal of Electrical Power & Energy Systems*, 53:279–286, 2013.

[26] Diego F García, Belén García, Juan Carlos Burgos, and Néstor García-Hernando. Determination of moisture diffusion coefficient in transformer paper using thermogravimetric analysis. *International Journal of Heat and Mass Transfer*, 55(4):1066–1075, 2012.

[27] J.A. Almendros-Ibañez, J.C. Burgos, and B. Garcia. Transformer field drying procedures: A theoretical analysis. *IEEE Transactions on Power Delivery*, 24(4):1978–1986, 2009.

[28] Diego F García, Belén García, and Juan Carlos Burgos. Modeling power transformer field drying processes. *Drying Technology*, 29(8):896–909, 2011.

[29] PF Ast. Movement of moisture through a50p281 kraft paper (dry and oil impregnated). *General Electric, Test Report HV-ER-66-41*, 1966.

[30] Yanqing Du. *Measurements and modeling of moisture diffusion processes in transformer insulation using interdigital dielectrometry sensors*. PhD thesis, Massachusetts Institute of Technology, 1999.

[31] SD Foss and L Savio. Mathematical and experimental analysis of the field drying of power transformer insulation. *IEEE Transactions on Power Delivery*, 8(4):1820–1828, 1993.

[32] AS Asem and AF Howe. Drying of power-transformer insulation. In *IEE Proceedings C (Generation, Transmission and Distribution)*, volume 129, pages 228–232. IET, 1982.

[33] Wanquan Li and Changyin Gao. Establishment and application for diffusion model of moisture in drying process of pressboard. In *International Conference on Mechatronics and Automation.*, pages 1422–1426. IEEE, 2009.

[34] HP Gasser, Ch Krause, and Th Prevost. Water absorption of cellulosic insulating materials used in power transformers. In *IEEE International Conference on Solid Dielectrics (ICSD)*, pages 289–293. IEEE, 2007.

[35] BV Ramarao, A Massoquete, S Lavrykov, and S Ramaswamy. Moisture diffusion inside paper materials in the hygroscopic range and characteristics of diffusivity parameters. *Drying technology*, 21(10):2007–2056, 2003.

[36] Arun S Mujumdar. *Handbook of industrial drying*. CRC Press, 2006.

[37] J Zhang and AK Datta. Some considerations in modeling of moisture transport in heating of hygroscopic materials. *Drying Technology*, 22(8):1983–2008, 2004.

[38] John Crank et al. The mathematics of diffusion. 1975.

[39] AF Howe. Diffusion of moisture through power-transformer insulation. In *Proceedings of the Institution of Electrical Engineers*, volume 125, pages 978–986. IET, 1978.

[40] Y. Du, A.V. Mamishev, B.C. Lesieutre, and M. Zahn. Measurement of moisture diffusion as a function of temperature and moisture concentration in transformer pressboard. In *Conference on Electrical Insulation and Dielectric Phenomena*, volume 1, pages 341–344, 1998.

[41] DF Garcia, B Garcia, JC Burgos, and NGarcia Hernando. Experimental determination of the diffusion coefficient of water in transformer solid insulation. *IEEE Transactions on Dielectrics and Electrical Insulation*, 19(2):427–433, 2012.

[42] Diego F García. A new proposed moisture diffusion coefficient for transformer paper. *International Journal of Heat and Mass Transfer*, 56(1):469–474, 2013.

[43] D.F. Garcia, R.D. Villarroel, B. Garcia, and J.C. Burgos. Effect of the thickness on the water mobility inside transformer cellulosic insulation. to be published. Early Access.

[44] Yeong-Sung Park, Hyun Nam Shin, Dong Hyun Lee, Duk Joon Kim, Ji-Heung Kim, Young Kwan Lee, Sang Jun Sim, and Kyong-Bin Choi. Drying characteristics of particles using thermogravimetric analyzer. *Korean Journal of Chemical Engineering*, 20(6):1170–1175, 2003.

[45] Zhanyong Li and Noriyuki Kobayashi. Determination of moisture diffusivity by thermo-gravimetric analysis under non-isothermal condition. *Drying technology*, 23(6):1331–1342, 2005.

[46] IEC insulating liquids. oil-impregnated paper and pressboard. determination of water by automatic coulometric karl fischer titration, 1997.

[47] Cigre Brochure. 323. *Ageing of cellulose in mineral oil insulated transformers*, 2007.

[48] D. Martin, C. Perkasa, and N. Lelekakis. Measuring paper water content of transformers: A new approach using cellulose isotherms in nonequilibrium conditions. 28(3):1433–1439, 2013.

[49] J. Fabre and A. Pichon. Deteriorating processes and products of paper in oil. application to transformers. In *Intern. Conf. Large High Voltage Electric System (CIGRE)*, 1960.

[50] TV Oommen. Moisture equilibrium in paper-oil systems. In *Electrical/Electronics Insulation Conference*, 1983.

[51] PJ Griffin, CM Bruce, and JD Christie. Comparison of water equilibrium in silicone and mineral oil transformers. In *Minutes of the Fifty-Fifth Annual International Conference of Doble Clients*, pages 10–9, 1988.

[52] Maik Koch. Improved determination of moisture in oil-paper-insulations by specialised moisture equilibrium charts. In *Proceedings of the XIVth International Symposium on High Voltage Engineering*, page 508, 2005.

[53] TV Oommen. Moisture equilibrium charts for transformer insulation drying practice. *IEEE Transactions on Power Apparatus and Systems*, (10):3062–3067, 1984.

[54] WA Fessler, TO Rouse, and William J McNutt. *Bubble formation in transformers*. Prepared for Electric Power Research Institute, 1987.

[55] SD Foss. Power transformer drying model. *Report prepared for General Electric Company, Large Transformer Operation, Pittsfield, MA, and Consolidated Edison Corporation, New York, NY, by Dynamic Systems, Pittsfield, MA*, pages 16–19, 1987.

[56] R. Villarroel, D.F. Garcia, B. Garcia, and J.C. Burgos. Diffusion coefficient in transformer pressboard insulation part 2: mineral oil impregnated. *IEEE Transactions on Dielectrics and Electrical Insulation*, 21(1):394–402, 2014.

[57] Qinghai Bai. Analysis of particle swarm optimization algorithm. *Computer and information science*, 3(1):p180, 2010.

[58] M Sadeghierad, A Darabi, H Lesani, and H Monsef. Optimal design of the generator of microturbine using genetic algorithm and pso. *International Journal of Electrical Power & Energy Systems*, 32(7):804–808, 2010.

[59] J. Kennedy and R. Eberhart. Particle swarm optimization. In *IEEE International Conference on Neural Networks*, volume 4, pages 1942–1948, 1995.

[60] Yuhui Shi and Russell Eberhart. A modified particle swarm optimizer. In *IEEE International Conference on Evolutionary Computation Proceedings*, pages 69–73. IEEE, 1998.

[61] JH Heo, MK Kim, and JK Lyu. Implementation of reliability-centered maintenance for transmission components using particle swarm optimization. *International Journal of Electrical Power & Energy Systems*, 55:238–245, 2014.

[62] Xin-She Yang. *Engineering optimization: an introduction with metaheuristic applications*. John Wiley & Sons, 2010.

[63] Maria A Dávila-Guzmán, Wilfredo Alfonso-Morales, and Eduardo F Caicedo-Bravo. Heterogeneous architecture to process swarm optimization algorithms. *Tecno Lógicas*, 17(32):11–20, 2014.

[64] Konstantinos E Parsopoulos, Michael N Vrahatis, and IGI Global. *Particle swarm optimization and intelligence: advances and applications*. Information Science Reference Hershey, 2010.

[65] XH Shi, YH Lu, CG Zhou, HP Lee, WZ Lin, and YC Liang. Hybrid evolutionary algorithms based on pso and ga. In *Congress on Evolutionary Computation (CEC)*, volume 4, pages 2393–2399. IEEE, 2003.

[66] Ioan Cristian Trelea. The particle swarm optimization algorithm: convergence analysis and parameter selection. *Information processing letters*, 85(6):317–325, 2003.

[67] Specification for pressboard and presspaper for electrical purposes. part 3: specifications for individual materials. sheet 1: requirements for pressboard, types b.0.1, b.2.1, b.2.3, b.3.1, b.3.3, b.4.1, b.4.3, b.5.1, b.6.1 and b.7.1, 2012.

[68] EN STN. 60296: Fluids for electrotechnical applications. *IEC Standard: Unused mineral insulating oils for transformers and switchgear.*, 2012.

[69] AAJ Ketelaars, Leo Pel, WJ Coumans, and PJAM Kerkhof. Drying kinetics: a comparison of diffusion coefficients from moisture concentration profiles and drying curves. *Chemical engineering science*, 50(7):1187–1191, 1995.

[70] NP Zogzas and ZB Maroulis. Effective moisture diffusivity estimation from drying data. a comparison between various methods of analysis. *Drying Technology*, 14(7-8):1543–1573, 1996.

[71] Zhongdong Wang, Alan Darwin, and Russell Martin. New insulation fluids: Use of environmentally friendly fluids in power transformers. *Cigre, Brugge*, 2007.

[72] Stefan Tenbohlen and Maik Koch. Aging performance and moisture solubility of vegetable oils for power transformers. *IEEE Transactions on Power Delivery*, 25(2):825–830, 2010.

[73] R. Villarroel, D.F. Garcia, B. Garcia, and J.C. Burgos. Moisture diffusion coefficients of transformer pressboard insulation impregnated with natural esters. *IEEE Transactions on Dielectrics and Electrical Insulation*, 22(1):581–589, 2015.

[74] Dejan Susa. *Dynamic Thermal Modelling of Power Transformers*. PhD thesis, Helsinki University of Technology, 2005.

[75] G.K. Frimpong, T.V. Oommen, and R. Asano. A survey of aging characteristics of cellulose insulation in natural ester and mineral oil. 27(5):36–48, 2011.

[76] N. Lelekakis, D. Martin, Wenyu Guo, J. Wijaya, and Meng Lee. A field study of two online dry-out methods for power transformers. *IEEE Electrical Insulation Magazine*, 28(3):32–39, 2012.

[77] Diego F Garcia, Belen Garcia, and Juan Carlos Burgos. Analysis of the influence of low-frequency heating on transformer drying–part 1: Theoretical analysis. *Electrical power & energy systems*, 38(1):84–89, 2012.

[78] Diego F Garcia, Belen Garcia, and Juan Carlos Burgos. Analysis of the influence of low-frequency heating on transformer drying–part 2: Experiences with a real

transformer. *International Journal of Electrical Power & Energy Systems*, 38(1):90–96, 2012.

[79] V Wasserberg, H Borsi, and E Gockenbach. A new method for drying the paper insulation of power transformers during service. In *IEEE International Symposium on Electrical Insulation*, pages 251–254. IEEE, 2000.

[80] Jian Li, XL Chen, ZT Zhang, RJ Liao, and LJ Yang. Characteristics of moisture diffusion in vegetable oil-paper insulation. *Gaodianya Jishu/ High Voltage Engineering*, 36(6):1379–1384, 2010.

[81] M Ahmet Tütüncü and TP Labuza. Effect of geometry on the effective moisture transfer diffusion coefficient. *Journal of Food Engineering*, 30(3):433–447, 1996.

[82] PN Johnson, JG Brennan, and FY Addo-Yobo. Air-drying characteristics of plantain (musa aab). *Journal of Food Engineering*, 37(2):233–242, 1998.

[83] Şenol I banoğlu and Medeni Maskan. Effect of cooking on the drying behaviour of tarhana dough, a wheat flour–yoghurt mixture. *Journal of food engineering*, 54(2):119–123, 2002.

[84] Aysun Maskan, Sevim Kaya, and Medeni Maskan. Hot air and sun drying of grape leather (pestil). *Journal of Food Engineering*, 54(1):81–88, 2002.

[85] Minh-Hue Nguyen and William E Price. Air-drying of banana: Influence of experimental parameters, slab thickness, banana maturity and harvesting season. *Journal of food engineering*, 79(1):200–207, 2007.

[86] WJN Fernando, HC Low, and AL Ahmad. Dependence of the effective diffusion coefficient of moisture with thickness and temperature in convective drying of sliced materials. a study on slices of banana, cassava and pumpkin. *Journal of Food Engineering*, 102(4):310–316, 2011.

Appendix A

Assessing the use of natural esters for transformer field drying

A.1 Introduction

The presence of water in transformer insulation affects the equipment reliability in addition to its loading capability. On one hand, excessive water content increases the presence of partial discharges (PDs) and decreases the dielectric strength of the insulation.Moreover, water promotes the hydrolysis reactions that are the predominant aging processes of the transformer insulation at working temperatures. Transformers are subjected to the drying processes after manufacturing. However, since cellulosic insulation is a highly hydrophilic material, some amount of water will still be present after that.

The amount of water present in transformer insulation increases through the years of service due to several underlying causes. In free-breathing transformers, the rate of water contamination could be up to 0.2 % per year of service while in membrane-sealed preservation systems, it increases at about 0.03 % to 0.06 % per year [13]. Water contamination may also occur in the presence of poor gaskets or in the case of field repairs involving oil draining that expose active parts to air. In addition, the

aging process of the cellulose generates water, so that the water content of the transformer will increase through the years.

Because of the hydrophobic nature of oil and the hydrophilic character of paper, water is absorbed in the paper in a proportion of 1 % in oil versus 99 % in cellulose, and a greater amount of water is usually concentrated in the thick insulation [13]. According to the IEEE standard C57.91-2011 [8], a transformer with moisture content in its insulation of greater than 4 % is too wet to be operated safely. When high water contents are found in units with a significant remaining service life, it is common to schedule drying treatments that are usually performed in the field.

Different drying methods are available to dry power transformers in the field [76], but all of them involve two basic steps:

- **Step 1:** forcing the water to travel through the insulation thickness until reaching its surface where it is removed by the drying agent.
- **Step 2:** extracting the water away from the transformer usually by a treatment of the drying agent.

The first step is the one that requires more time to be completed. As is well known, the diffusion of water inside the insulation can be accelerated by increasing the temperature of the system. In some cases, the circulation of a hot drying agent (i.e., air or oil) is used to heat the insulation. Sometimes, additional heating is applied to obtain higher drying temperatures and to reduce the drying times. Some commonly used heating methods are low-frequency heating (LFH), based on forcing circulation of current in the transformer windings, or hot-oil spray (HOS), that is usually applied in combination with vacuum.

To remove water from the insulation surface, a dry environment must be created around it. This is usually achieved by the application of the vacuum inside the tank,

or by forcing the circulation of hot and dry oil or air through the transformer active parts. The main differences between the available drying methods lies in the agents that are used to remove the surface moisture, and in how the solid insulation is heated to force the exit of water from its inner part to the surface. Table A.1 summarizes the most relevant methods used presently. Some advantages and disadvantages of each method can be seen in table A.2.

Table A.1: Main methods used to dry transformers in the field.

Method	**Drying agent**	**Heating agent**
Hot oil drying (HO)	Hot dry oil	Hot oil and LFH
Vacuum drying (VD)	Vacuum	Hot oil cycles, LFH and Hot oil Spray
Hot air drying (HA)	Hot dry air	Hot air

Table A.2: Advantages and disadvantages of the different drying methods.

Drying method	**Advantages**	**Disadvantages**
HO	No deimpregnation	Long drying times
VD	Fast removal of surface water	Deimpregnation of oil
HA	Lower drying times	Oxidation of oil

In previous works [27, 77, 78], the HO drying method was theoretically studied; the main finding was that the drying times involved in the process are large and, in consequence, this kind of drying processes is sometimes less effective. Also, experimental studies showed much shorter drying times in the case of hot air (HA) drying although, in this case, there is an increased risk of oil deimpregnation, as well as cellulose oxidation. The improvement in the drying time achieved with HA drying is due to the greater affinity of air for water in comparison to that of oil. This seems to indicate that the use of a more hygroscopic fluid than mineral oil would be a way to increase the efficiency of the HO drying diminishing drying times and obtaining lower moisture contents in the solid insulation at the end of the process.

In recent years, the use of natural and synthetic esters is becoming common in distribution transformers [2]. One of the properties of these fluids is that they are able to absorb much greater amounts of water than mineral oils [72]. Some authors have suggested that the use of this kind of fluid would be useful to reduce the drying times, making the drying process more efficient [72, 11, 79]. In [79], a drying method based

on the use of ester fluids is proposed as an alternative to HO drying. The method consists of using vegetable oil only for drying purposes and, afterwards, the transformer should be refilled with mineral oil for operation, since the transformer was designed to be operated with mineral oil. In that paper, qualitative analysis is presented that compares the equilibrium condition between paper and oil in both cases and reports some preliminary experiments.

In this appendix, the improvement obtained by the use of ester fluids is quantified. To this aim, a theoretical model is used that simulates drying processes at different temperatures considering drying with mineral oil and drying with natural esters. Drying experiments were also performed using both drying agents in the laboratory at different drying conditions. Finally, performances of different ester fluids were compared.

A.2 Theoretical analysis of the process

A.2.1 Theoretical model

As aforementioned throughout this thesis, a model to simulate the HO drying process of a transformer was presented. The model, based on Fickâs second law, is used to study the mass transport problem in the transformer insulation. Because of typical dimensions of the transformer insulation, the process was considered to be 1-D.

In chapter 5, section 5.3.1 the theoretical model used is very well explained. According with this model, the parameters A and B are constants that depend on the oil properties. If mineral oil is used as a drying agent, parameters A and B could be taken as 7.09 and 1,567 [15, 31]. In case of using a different drying agent, parameters A and B corresponding to that fluid must be considered.

IEEE Standard C57.147-2008 [3] provides two sets of values for A and B obtained on two different ester fluids (table A.3). The standard concludes that the properties of both of them regarding moisture solubility are very similar at the temperatures of interest.

Table A.3: Parameters A and B for different insulating fluids provided by IEEE Standard C57.147-2008.

	A	**B**
Ester fluid 1	5.708	802
Ester fluid 2	5.332	684

A.2.2 Simulation of the drying model

Simulations were carried out considering a conventional HO drying process performed with mineral oil as well as a HO drying using an ester fluid. Parameters A and B corresponding to ester fluid 1 in table A.3 have been considered. It is important to note that the only difference introduced to simulate the drying process with mineral oil and with a natural ester fluid was just the change in the boundary condition. The expression of the diffusion coefficient considered in all simulations was (A.1). This equation was experimentally obtained by the authors in a previous work on samples of Kraft paper impregnated with mineral oil [25].

$$D = 0.5 \cdot e^{\left(0.5 \cdot c - \frac{10057 - 133.7 \cdot l}{T}\right)} \tag{A.1}$$

where c is the moisture concentration of the paper in percentage, l is the insulation thickness in millimeters, and T is the insulation temperature in Kelvin.

Presently, experiments are being conducted to calculate the moisture diffusion coefficient in cellulosic insulations impregnated with natural esters. This coefficient may differ from that obtained for mineral-oil-impregnated materials, so the simulated values shown in this section should be taken as approximate results. However, it may

be noted that in the case of drying a transformer immersed in mineral oil with a natural ester fluid, the results of the simulation would be pretty realistic since, in this case, the fluid adsorbed in the insulation would be mineral oil.

First, simulations were done to determine the influence of the drying fluid in deciding the rate of water removal at different temperatures. Drying processes were simulated at temperatures 60 and 80 ºC. The analyzed specimen was a piece of cellulosic insulation 5 mm thick,with a homogeneous initial moisture content of 3 %. Diffusion in just one face of the insulation was considered since it occurs in the insulation of transformer windings or in the bushing leads. The moisture content of the oil during the drying process was assumed to be 10 ppm, which is a typical value when a transformer is being dried with HO in the field.

As can be seen in figure A.1, the use of natural esters improves the rate of drying at both temperatures, although in the case of drying at 80 ºC, the improvement is not so significant (a). More important is the acceleration in water removal in case of drying at 60 ºC (b).

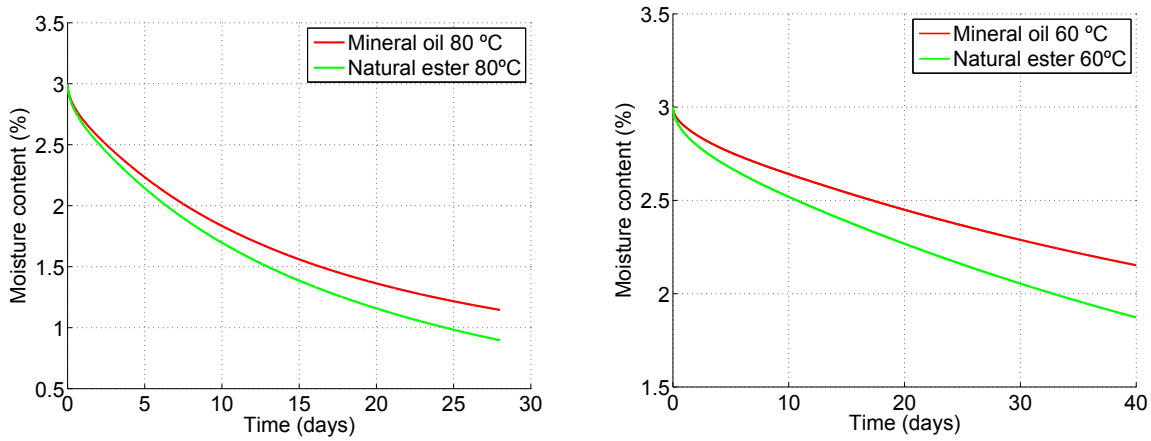

(a) 80 °C using mineral oil and natural ester fluid with moisture content of 10 ppm

(b) 60 °C using mineral oil and natural ester fluid with moisture content of 10 ppm

Figure A.1: Calculated drying curves of a 5 mm insulation considering HO drying.

It is also interesting to note that the improvement obtained by the use of an ester

fluid notably increases when the moisture content of the oil is not so low during the drying process. This may occur during the drying process of large transformers with large quantities of oil, so that the filter is not able to keep moisture at low enough values. In figure A.2, the drying curves at 70 ºC, when drying with mineral and vegetable oil, are shown for moisture contents in oil of 5 and 20 ppm. As can be seen, when the moisture content of oil is very low, little improvement is achieved by substituting the mineral oil by an ester, whereas in case of the drying process where moisture content in oil was 20 ppm, an increase in the drying rate is observed while using an ester fluid.

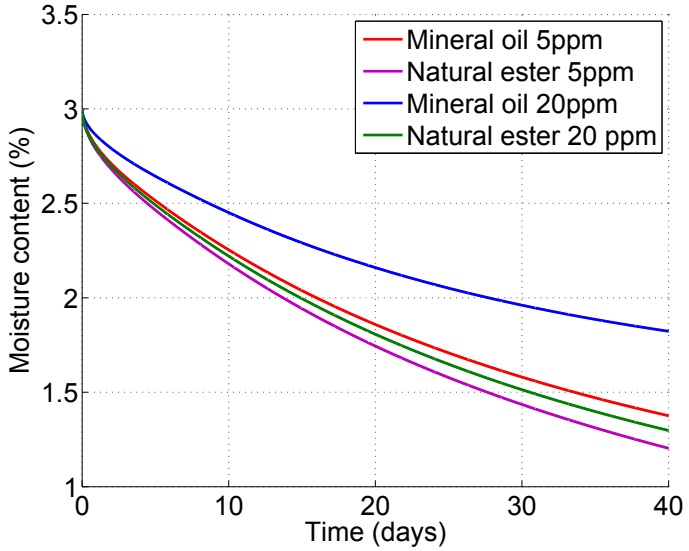

Figure A.2: Calculated drying curves of 5 mm insulation at 70 ºC considering different moisture contents in oil.

A.3 Experimental study

A.3.1 Test plant

The drying plant (figure A.3) was designed to reproduce the conditions of a real hot-oil drying process. The specimen to be dried is introduced into a tank that is filled with oil. Oil is continuously forced to circulate through a drying filter by means of a pump.

The filter dries the oil, extracting the water that is released from the paper during the drying process. Oil also passes through a heater where it is heated to a specified value.

Figure A.3: Drying plant.

The plant is provided with optical sensors to measure the temperatures of the paper and oil, and it also incorporates a capacitive sensor to register oil moisture evolution. The moisture sensor was installed in a pipe at the bottom of the plant that connects the deposit and the drying filter and was recalibrated to determine the ppm in the different fluids using Karl Fischer measurements. All of the variables are registered and controlled by means of an acquisition system allowing control of the oil temperature.

A.3.2 Sample preparation

Dynamics experiments were performed on pressboard samples prepared with a high initial moisture level. The specifications of the evaluated pressboard were according to the international standard IEC 641-3-1, being all of type B.3.1.

The test specimens were obtained from one layer of pressboard sheet. Pieces of thicknesses 0.5, 1, 2, and 3 mm were evaluated during the experimental stage of the work. The four edges of each specimen were coated with epoxy resin to prevent desorption of moisture through these sides during the drying processes and to ensure a unidirectional desorption only through the upper and lower surfaces (figure A.4).

(a) View 1 (b) View 2

Figure A.4: Pressboard samples.

Before being impregnated with oil, samples were humidified by placing them in a climatic chamber under a temperature of 35 ºC and relative humidity of 70 %. Wetting conditions were established according to Jeffries's curves [5] to obtain an equilibrium moisture of about 9 %. After that, the test specimens were impregnated by submerging them in mineral oil or natural ester at room temperature and atmospheric pressure for a period of no less than one week. Finally, the oil-impregnated test specimens were introduced again in the climatic chamber to re-wet them until the beginning of the drying experiment.

A.3.3 Test conditions

A first set of drying experiments was performed on pressboard samples of different thicknesses impregnated with mineral oil. After that, the experiments were repeated using a commercial natural ester fluid, Bioelectra. Temperatures and insulation thickness used in the tests are summarized in table A.4.

Table A.4: Experimental testing conditions.

Fluid	**Temperature (^{o}C)**	**Pressboard thickness (mm)**
Mineral oil	60, 70 and 80	0.5, 1, 2 and 3
Ester		

The samples were dried by hot-oil circulation in the test plant (figure A.3) and during the whole process, pressboard samples were periodically extracted and analyzed with the Karl Fischer method [46]. The experiments were stopped when the moisture determined on all of the samples was less than 1 % in weight.

In the case of experiments carried out with natural ester, the nitrogen atmosphere was used during the extraction process with the aim of avoiding oxidation of oil. Dielectric measurements were also carried out daily on oil samples extracted from the tank to monitor their condition.

A.4 Results

As explained in the previous section, drying experiments were performed on pressboard samples of different thickness subjected to different temperatures (table A.4). The same experimental conditions were applied to the HO drying process carried out with mineral oil and to that using Bioelectra natural ester as a drying agent.

Figure A.5 shows the drying curves obtained on the samples of different thicknesses dried with mineral and vegetable oil at 70 ^{o}C. As expected, the drying times are

greater for the thicker samples. If the drying times are compared for samples of the same thickness, it is found that they are significantly shorter when drying them with natural ester than those when they are dried with mineral oil.

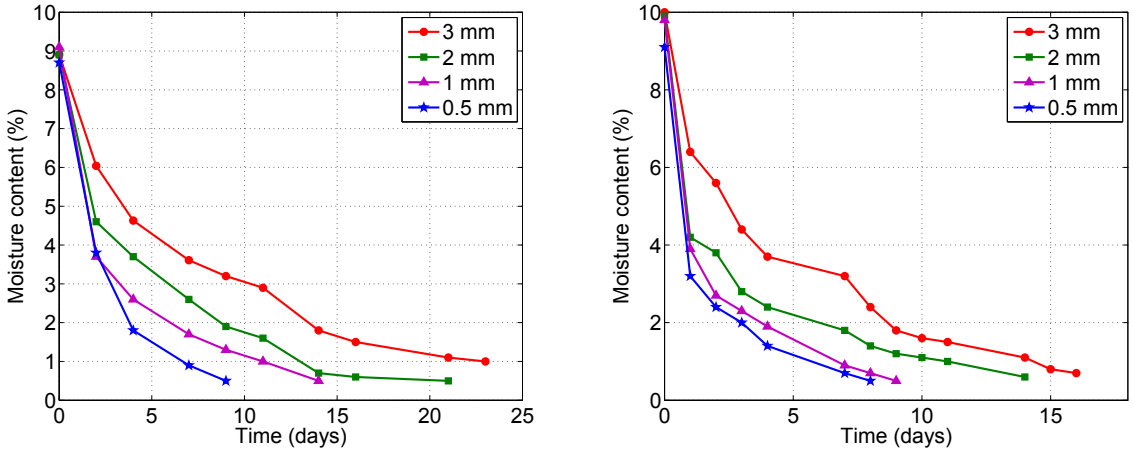

(a) In presence of Mineral Oil.

(b) In presence of natural ester Bioelectra.

Figure A.5: Experimental drying curves of pressboard at 70 ºC.

In addition, it must be remarked that, although the procedure of sample preparation was exactly the same for all samples, the resulting initial moisture contents were slightly different in both cases (i.e., about 10 % in weight for the samples impregnated with natural ester and about 9 % in those impregnated with mineral oil). The explanation for these differences can be found in the rewetting process that the samples were subjected to once impregnated with oil. During this part of the preparation process, the mineral oil avoided adsorption of moisture, but the natural ester absorbed some moisture, increasing the total moisture content of the sample.

To quantify the improvement achieved in the drying times with the change of drying agent, the number of days required to dry the different samples to a level below 1 % in weight were calculated as shown in table A.5.

As can be seen, the drying times diminish in between 20 % and 70 % when drying with the natural ester. Although these data should be taken as an estimation, since they are affected by slight differences in the initial moisture of the samples and be-

Table A.5: Approximate drying times required to achieve moisture content lower than 1 % when using natural ester (E) or mineral oil (M) as drying agents.

	Time to c < 1 % (days)					
	80 ºC		**70 ºC**		**60 ºC**	
Thickness	**E**	**M**	**E**	**M**	**E**	**M**
3 mm	10	14	15	23	17	33
2 mm	6	11	11	14	13	29
1 mm	6	12	7	11	8	26
0.5 mm	3	5	7	9	6	20

cause of the fact that the drying curve is discrete, it is important to note that the greater improvements appear in the case of the drying processes carried out at lower temperatures, as was observed in the simulation stage. The experimental data obtained at 60 and 80 ºC on a 3 mm sample are shown in figure A.6 , where this aspect seems clear.

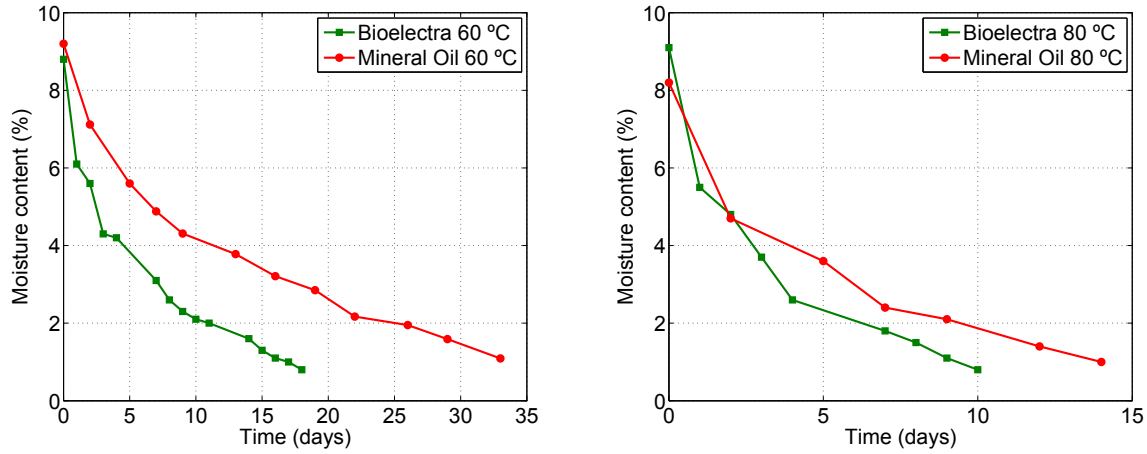

(a) At 60 ºC.

(b) At 80 ºC.

Figure A.6: Comparison between drying a sample 3 mm thick with mineral oil and with natural ester.

It is also interesting to compare the moisture content in the different oils during the drying processes. As can be seen, the water content in both fluids is low because of the action of the filter. The spikes in the curves correspond to the stops of the oil recirculation during the sample extraction operations. Anyhow, it must be noted that the ester fluid presented a higher moisture level, despite using the same kind of filter for water removal (figure A.7).

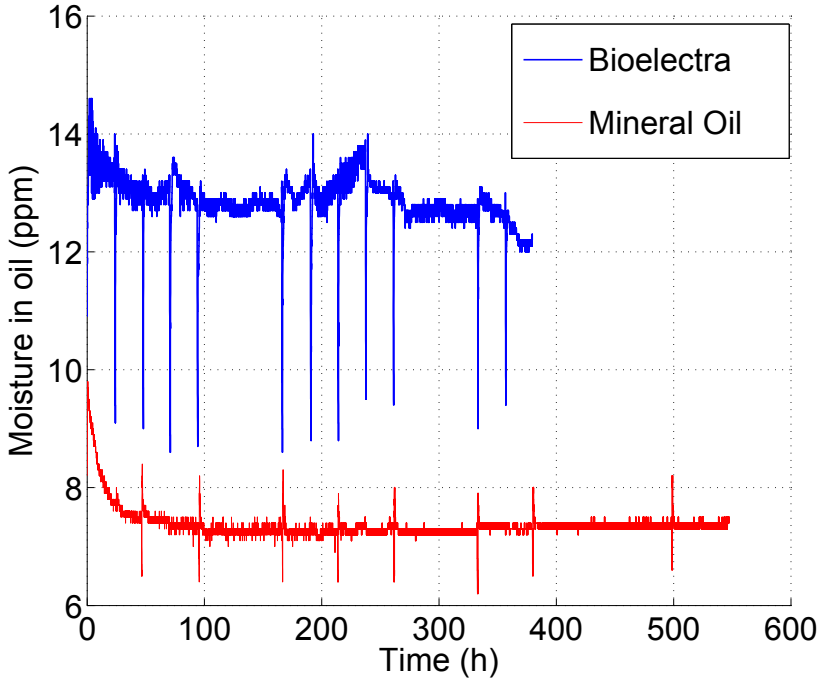

Figure A.7: Moisture content in oil during the drying process at temperature 70 °C.

This seems logical because of much higher solubility of water in these fluids and, consequently, the appreciably different equilibrium conditions between paper and oil. Moreover, it must be remarked that the efficiency of the filter may be lower due to the effect of the lower viscosity of ester fluids.

Finally, an additional drying process was carried out using the natural ester Biotemp with the aim of comparing the effectiveness of different ester fluids for drying purposes. This drying experiment was performed at temperature 70 °C, and for samples of thickness 0.5, 1, 2, and 3 mm. The results of the process are shown in figure A.8. A comparison of the results obtained when drying a 3 mm thick sample using both natural esters is plotted in figure A.9.

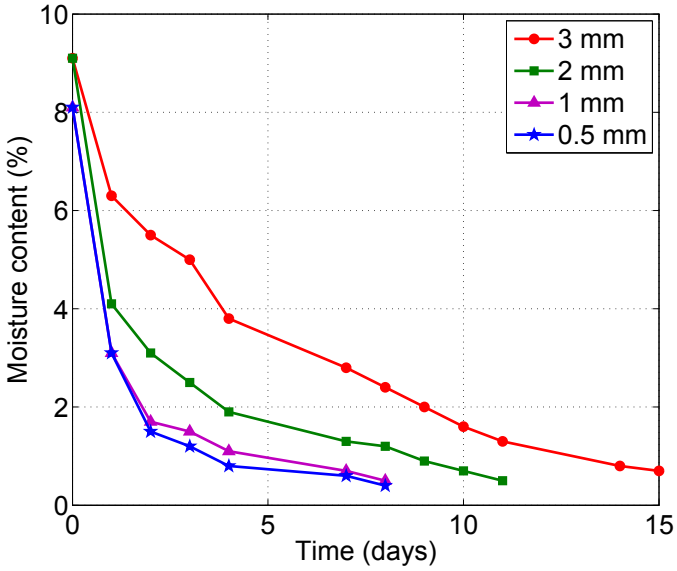

Figure A.8: Drying curves obtained when drying with the natural ester Biotemp at 70 ^{o}C.

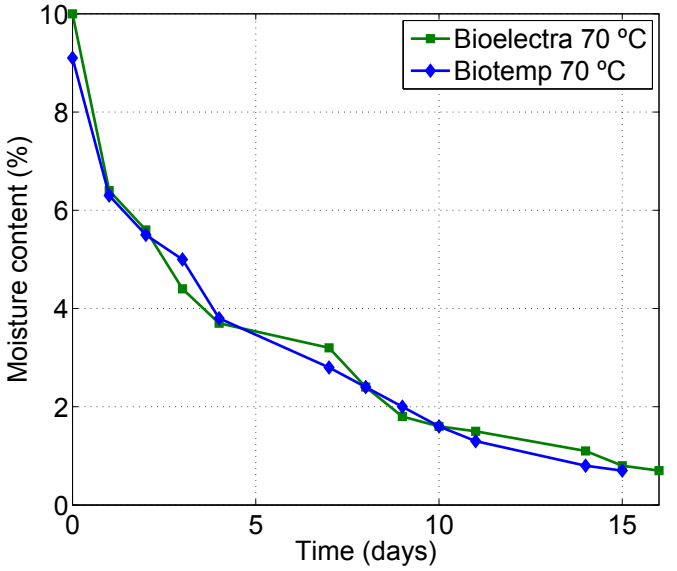

Figure A.9: Comparison of the drying process with two different ester fluids.

A.5 Conclusions

The use of natural esters has been proposed by several authors as a way to reduce the time involved in the drying processes of power transformers in the field. This ap-

pendix quantifies the improvement achieved by this method. Simulations were done by using a theoretical model solved by the finite-element method, and considering the solubility of each fluid as a function of temperature to state the equilibrium condition. In addition, drying experiments were carried out with mineral oil and use two different natural esters. The main conclusions of the study are summarized as follows.

HO drying is a well-known drying method that has been used for years to process transformers in the field. The main disadvantage of the method lies in the fact that mineral oil is very hydrophobic and, consequently, the amount of water extracted in each oil circulation is low and the drying time required is very high. Some authors proposed using ester fluids for drying purposes, since they absorb amounts of water of about 20 times greater than mineral oils.

Currently, the price of ester fluids is high; therefore, before using them for this application, it is necessary to determinate whether the reduction of drying time that may be achieved compensates for the investment that would be required. Moreover, the safety of the method should be guaranteed.

As expected, the theoretical simulations and the laboratory experiments demonstrated that the use of esters makes the drying process more efficient, enabling a reduction in the drying time. However, the improvement achieved is not equal for all tested conditions. When the drying process is carried out at high temperature and low water content in oil, the acceleration of the process seems to not be so significant to justify the application of alternative fluids. On the other hand, when the drying temperature is not so high, or the moisture content in oil cannot be kept within so low values, which sometimes happens when a large transformer is dried in the field, the improvement achieved turns out to be appreciable.

Better results are also obtained on thinner insulations, where the effect of the boundary condition in the entire process is more significant. In the case of very thick insulation, the largest part of the drying process is the removal of water from the inner

part of the insulation to the surface of contact with oil where it is released. The duration of this period mainly depends on temperature and less on the drying agent.

Different commercial natural esters were compared; and very similar behaviors were observed between them.

Natural esters are more oxidation susceptible than mineral oils. The drying procedures must be carefully revised when using these fluids to guarantee that the drying fluid is not degraded by contact with air or excessive temperature, since the presence of sludge and acid in oil could be harmful for solid insulation.

This work should be completed to determine the effect of using different fluids in HO drying in the final condition of the insulation, and to guarantee that the procedure be safely applied. The manufacturers of these kinds of liquids claim that they are compatible with mineral oil and that it would be safe even to operate with mixtures of both kinds of fluids. However, esters have different physical properties (dielectric, viscosity, etc.) compared to mineral oil and the effect of the residual ester trapped in the winding after drying may alter the properties of the insulation. As a continuation of this paper, tests are being developed to determine whether the different drying processes performed at different temperatures and with the different fluids produce a significant degradation of the solid insulation.

Appendix B

Effect of the insulation thickness on the water mobility inside transformer cellulosic insulation

B.1 Introduction

The electrical insulation of most power transformers is composed of two parts: the solid insulation based mainly of cellulosic materials like Kraft paper and pressboard, and the liquid insulation. The fluid most widely used in power transformers is mineral oil. Cellulose is a porous material so when cellulose is impregnated with oil, air in internal cavities is replaced by oil.

Mineral oil is an excellent insulation that improves the dielectric properties of the cellulose insulation when impregnates it. Additionally oil acts as a cooling agent helping to evacuate the heat generated mainly in the transformer active parts (windings and core) to the environment.

Water is harmful for the cellulosic insulation because it accelerates the ageing process, reduces the dielectric margin and decreases the partial discharge inception voltage. For these reasons, the moisture inside the solid insulation increases the prob-

ability of unexpected failures of the transformer, causing a decrease in its reliability. These failures can lead to service interruptions that could involve economic penalties for the companies which add to the cost of transformer repairing and even to the cost of infrastructure replacement if damaged Therefore is important to maintain the moisture levels of the transformer cellulosic insulation within safe values. For this reason, when a transformer is manufactured the active part is subjected to a drying process before its impregnation with oil.

Nevertheless during transformer life, moisture in the transformer insulation increases. The increase of moisture in the thin cellulosic insulation of transformers is due to three mechanisms: The first mechanism is the residual moisture from the bulk cellulosic insulation which is released during transformer operation. The second mechanism is moisture ingress from the atmosphere by direct exposure of the transformer's windings to the external environment, e.g. during repairs of the equipment as well as by molecular flow through micropores in the tank. The third one is the chemical reactions of cellulose degradation and oil oxidation, which provide water as a byproduct.

Because the oil is hydrophobic and the cellulosic insulation is hydrophilic, most water remains in the solid insulation, affecting its life expectancy. The distribution of moisture between the liquid and solid insulation is not static due mainly to the temperature changes that take place during transformer operation. When the moisture content in the transformer is too high the transformer may be subjected to a drying process in field. Different drying technologies are available for field drying. One of these technologies, the so called hot oil drying method, consists in forcing a circulation of hot and dry oil through the transformer active part. The difference in relative saturations, of water in oil and water in paper, forces moisture to exit from paper to oil.

Understanding and properly estimating the moisture dynamics in power transformer insulation is essential for improving the manufacturing process, operation and maintenance of those equipments.

Moisture dynamics inside the cellulose insulation can be estimated by using a mathematical model of diffusion based on Fick's second law [28]. This can be useful to determine the transformer drying times and consequently to estimate the cost of the drying process.

Also, moisture diffusion models, working together with thermal models, could be used in the future as part of an on-line monitoring system, to estimate the moisture distribution inside the transformer, during its operation stage. This information can be useful to estimate the ageing of the transformer's cellulosic insulation, and therefore help to propose better strategies to manage this equipment.

The main parameter of the moisture diffusion model is the so-called moisture diffusion coefficient. The accuracy of the model results depends on the value of moisture diffusion coefficient used in the model [23, 32, 26].

Moisture diffusion coefficients of cellulosic insulation proposed by most authors [30, 31, 39, 80], only consider the dependence with local temperature and local moisture concentration, according to the behaviour of most hygroscopic materials. In these works the influence of the thickness of the material on water mobility was not evaluated. However, the influence of the geometric properties of the material on water mobility inside solid hygroscopic materials has been recently evidenced in some experimental works carried out on foodstuff [81, 82, 83, 84, 85, 86].

This appendix reports some experiments that show that the insulation thickness affects the moisture diffusion inside cellulosic materials as well. Additionally it is shown that, when this variable is incorporated in the expressions of the moisture diffusion coefficient, the estimations of moisture dynamics obtained by means of diffusion models are much closer to the experimental data than the estimations obtained by using the classical approach.

It should be noted that the thickness of the different cellulosic pieces that com-

pounds the transformer solid insulation are widely variable, going from a few tenth of mm, in the case of HV and LV winding insulation, and 70 mm - 80 mm in the case of the pressboard barriers located between the HV and LV windings. In consequence, considering a diffusion coefficient valid for a single thickness would lead to great errors in the simulations of the moisture dynamics.

B.2 Modelling moisture transport inside cellulosic materials

Moisture migration inside cellulosic transformer insulation is a complex process where thermal transfer and mass transport phenomena are interlinked. However, as the thermal time constant is much smaller than the moisture diffusion time constant, moisture migration can be modelled as a diffusion process, using Fick's second law [28].

Moisture migration proceeds in form of liquid and gaseous phases. Unfortunately, it is not easy to determine a particular diffusion coefficient for every phase of water (liquid and gas). Neither is it easy determining the amount of water changing of phase during the process. Moisture diffusion when water is moving in unidirectional way, as in the transformer's solid insulation [27], is given by (B.1).

$$\frac{\partial c}{\partial t} = \frac{\partial}{\partial x}\left(D \cdot \frac{\partial c}{\partial x}\right) \tag{B.1}$$

where D is the effective moisture diffusion coefficient in the solid insulation, c is the local total moisture concentration, t is the time and x is the distance into the material in the direction of moisture movement.

Equation (B.1) models the different mechanisms of water transport inside the solid by using the so-called *effective diffusion coefficient*. That coefficient can be interpreted as a combination of the coefficient corresponding to gaseous water mov-

ing through the cellulose cavities and the one corresponding to liquid water moving mainly through the cellulose fibres.

The value of the moisture diffusion coefficient of cellulosic insulation as Kraft-paper or pressboard has been obtained by several authors employing diverse methodologies [23, 32, 30, 80]. Different values of the moisture diffusion coefficient can be found in the literature represented by mathematical expressions, tables or simple experimental curves, relating the dependence of the diffusion coefficient with the local moisture concentration and the insulation temperature. A review about the main works aimed at determining the moisture diffusion coefficients on cellulosic insulation can be found in [4, 7]. All the authors that studied moisture dynamics in transformer solid insulation have considered an effective diffusion coefficient dependent only on local variables (moisture concentration and temperature). Most authors use the empiric equation for the diffusion coefficient (B.2), proposed by Guidi in [23]. However as above mentioned, in several works about moisture dynamics in foodstuff, moisture mobility was shown to be also influenced by the sample geometry.

$$D = D_0 \cdot e^{\left[k \cdot c + E_a\left(\frac{1}{T_0} - \frac{1}{T}\right)\right]} \tag{B.2}$$

where D is the diffusion coefficient (m^2/s), c is the local moisture concentration (kg of H_2O/kg), T is the temperature (K), T_0 is the reference temperature (298 K), k is a dimensionless parameter, D_0 is a pre-exponential factor (m^2/s), and E_a is the activation energy of the diffusion process (K).

B.3 Experimental evidence of thickness influence on water mobility

Evidence that thickness has an influence on the diffusion coefficient was found when an experimental study was conducted to analyze the transformer's drying processes

both with non-impregnated cellulose (as in factory drying) and with impregnated cellulose (as in field dryings). The aim of the study was to determine the moisture diffusion coefficient of the following materials: impregnated Kraft-paper, non-impregnated kraft paper, impregnated pressboard and non-impregnated pressboard. In this work was observed that the estimates obtained by the models were not accurate enough and so the estimated drying times do not coincide with the experimental ones.

B.3.1 Experimental procedure

The experiments carried out on mineral oil impregnated and non-impregnated Kraft paper and pressboard insulations consisted in determining the evolution of the average moisture concentration (c_m) in time, the so called drying curve, of insulation samples of different thickness. Those drying curves were obtained during drying processes performed at different temperatures. Figure B.1 shows some experimental drying curves for non-impregnated insulations of Kraft paper.

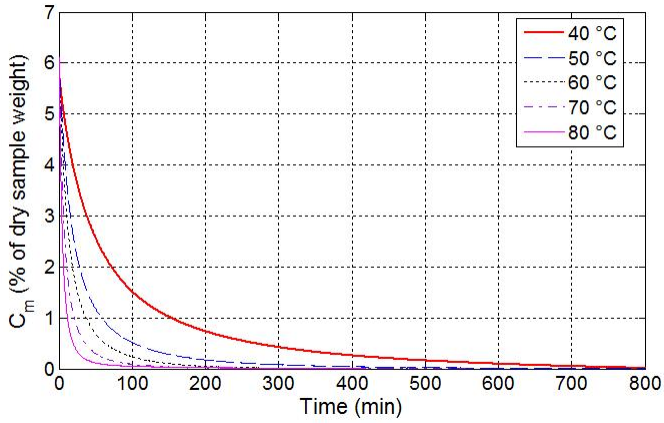

Figure B.1: Experimental drying curves for non-impregnated Kraft-paper insulations stacks 2 mm thick.

B.3.2 Experiments on non-impregnated samples

For non-impregnated insulation, the drying curves were obtained by means of a thermogravimetric analyzer (*TGA*), TA model Q500. Drying experiments in the *TGA* consisted in applying a determinate temperature to the humid samples while a nitrogen flux was forced to circulate around these. During the experiment the loss of mass of the sample is continuously registered and then the drying curve can be easily calculated.

To prepare moistened samples pressboard or paper samples were introduced in a climatic chamber. The climatic chamber settings and the time that the samples remained inside it were established to obtain a homogeneous moistening into the samples. The average moisture in Kraft paper samples, obtained after the aforementioned moistening process was around 7.5 % whereas in pressboard was about 8.5 %.

To find the diffusion coefficient dependence with temperature and thickness, isothermal drying experiments were carried out in the *TGA* at different temperatures and on samples of different thickness. Table B.1 summarizes the drying conditions used for non-impregnated insulation.

Table B.1: Drying conditions used to obtain the drying curves for non-impregnated insulation.

	Kraft paper	**Pressboard**
Thickness (mm)	2, 3, 4 and 5	1, 2 and 3
Temperature (ºC)	40, 50, 60, 70 and 80	40, 50, 60, 70, 80, 90, 100 and 120

Samples of non-impregnated insulation, were cut into circular pieces and placed into a pan of Polytetrafluoroethylene (PTFE) with a single opening at the top whose purpose is to force the moisture desorption in an unidirectional way (figure B.2). This was made with the aim to emulate what happens in a real transformer where the moisture desorption inside the solid insulation takes place mainly in transverse direction. In the case of paper, the desired thicknesses were obtained by stacking multiple layers of paper of 0.1 mm thick, whereas for pressboard a single layer manufactured with a certain thickness was used.

In the *TGA* experiments, the nitrogen flow allows quick moisture evaporation at the insulation surface, causing the diffusion to be the prevalent phenomenon of moisture reduction. As mentioned before *TGA* continuously records the sample loss of mass during the experiment. As the loss of mass is due to the moisture desorption, the recorded data can be used to determine the drying curve of the sample.

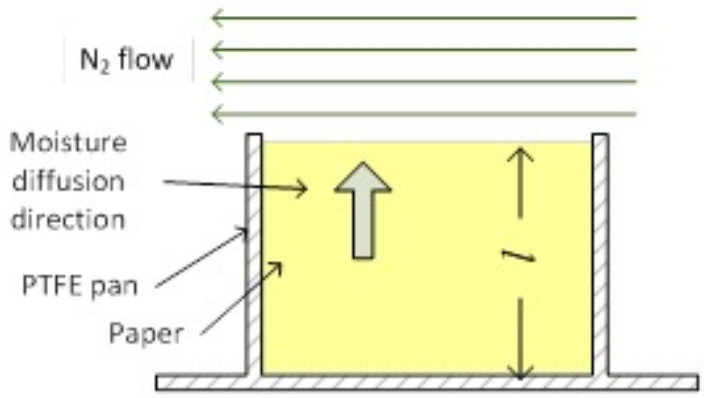

Figure B.2: Schema for non-impregnated Kraft paper insulation samples for drying experiments in the *TGA* oven.

B.3.3 Experiments on oil-impregnated samples

In the case of oil-impregnated insulation an experimental drying plant (figure B.3) was used to emulate the hot-oil drying method to dry transformers in field. For impregnated insulation, samples of Kraft paper with different thicknesses were prepared by winding paper layers 0.1 mm thick around an aluminium core. Same to the PTFE pan in *TGA* experiments, the aluminium core forces the moisture desorption to be unidirectional.

In the case of the pressboard, samples of different thickness were provided by the manufacturer. In figure B.4 some of the pressboard samples tested in the hot-oil drying plant can be seen. As can be appreciated the edges of the samples were sealed with epoxy resin to force the moisture desorption towards the side faces, that is, as a one-directional desorption.

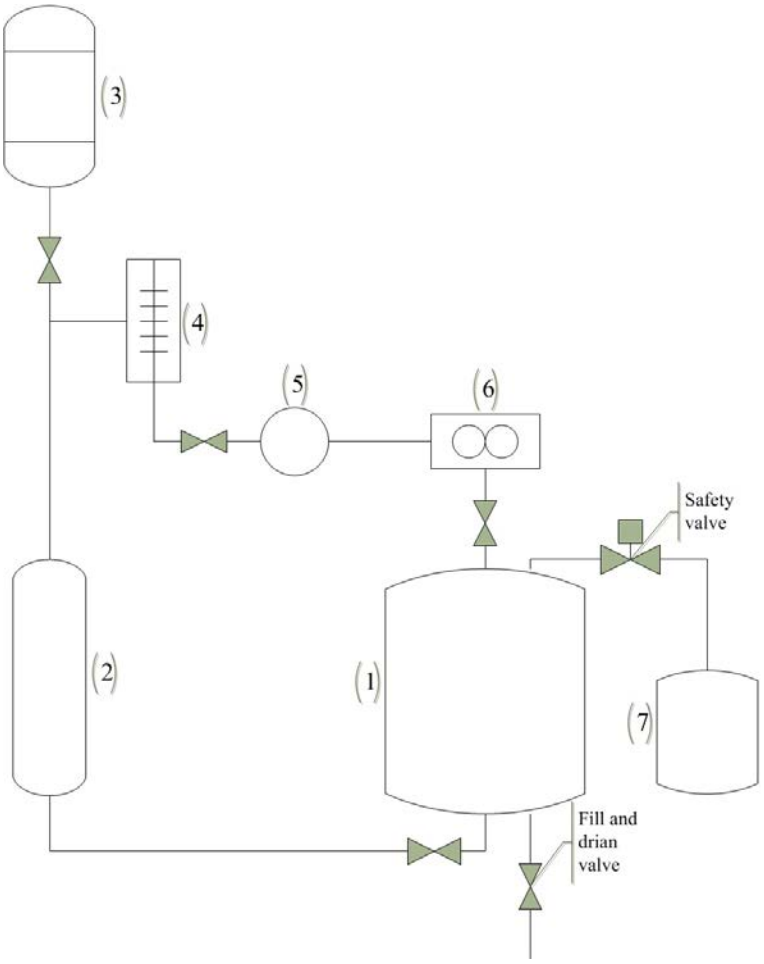

Figure B.3: Drying plant, general scheme. Sample container (1), oil filter (2), expansion vessel (3), heater (4), circulating pump (5), flowmeter (6) and security deposit (7).

(a) View 1 (b) View 2

Figure B.4: Pressboard samples.

The preparation of the samples for experiments in the hot-oil drying plant includes three steps: firstly the samples are pre-moistened in a climatic chamber. Then they are impregnated with mineral oil by direct immersion of the samples at room temperature. Finally the samples are re-moistened in the climatic chamber. The settings of the climatic chamber and the times that the samples remain into the oil and into the chamber are carefully established to obtain homogeneous moisture content in the samples.

After applying the above mentioned process, the samples of impregnated Kraft-paper reached an average moisture concentration around 8 % whereas in the press-board samples, the average moisture value was approximately 9 %. To find the dependence of the diffusion coefficient with temperature and thickness of the impregnated insulation, drying experiments were carried out at different temperatures and using insulation samples of different thickness. Table B.2 summarizes the drying conditions tested in the experiments on impregnated insulation.

Table B.2: Drying conditions used to obtain the drying curves for oil-impregnated insulation.

	Kraft paper	**Pressboard**
Thickness (mm)	1, 3 and 5	1, 2 and 3
Drying temperature (^{o}C)	60, 70 and 80	60, 70 and 80

During the drying experiments on impregnated insulation, the drying curves were determined by measuring the evolution of the average moisture concentration in the insulation samples, this was carried out by means of the Karl-Fischer titration method [46].

B.3.4 Determination of the diffusion coefficient

Once the drying curves were obtained, a drying diffusion model based on finite element method (FEM) was used to simulate each experiment [26]. In the simulation models, the cellulose insulation was characterized by the moisture diffusion coeffi-

cient. According to [36], diffusion coefficient was assumed to respond to a general expression (B.3), valid for most hygroscopic materials.

$$D_{(c,T)} = D_0 \cdot e^{k \cdot c} \tag{B.3}$$

In (B.3), D is dependent on the local moisture concentration. The dependence of the moisture diffusion coefficient on other variables as temperature can be included in the parameter D_0.

To determine the moisture diffusion coefficient of the cellulose insulation is necessary to find the parameters D_0 and k of equation (B.3). These parameters were found using an optimization process based on genetic algorithms. The optimization process finds the values of D_0 and k by fitting the simulated curves, obtained from the FEM drying model, to the experimental data. Figure B.5 shows the flow chart of the optimization process used for obtaining the moisture diffusion coefficient. In [26] a detailed description of this methodology can be found.

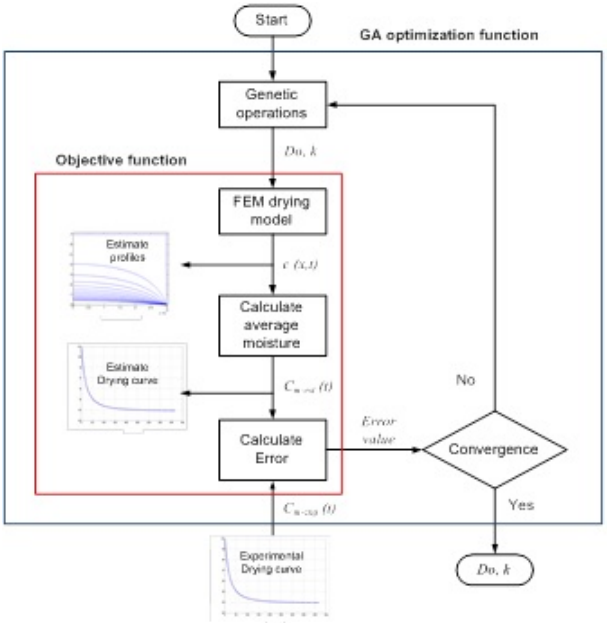

Figure B.5: Flow chart of the optimization process used to find the parameters of the diffusion coefficient.

After obtaining the values of the parameter D_0, for each experimental drying curve, the dependence of this parameter on different variables was studied and expressed as a mathematical equation. Figure B.6 shows the D_0 curves, for non-impregnated Kraft paper and pressboard insulation as a function of temperature and insulation thicknesses, obtained after applying the aforementioned optimization process.

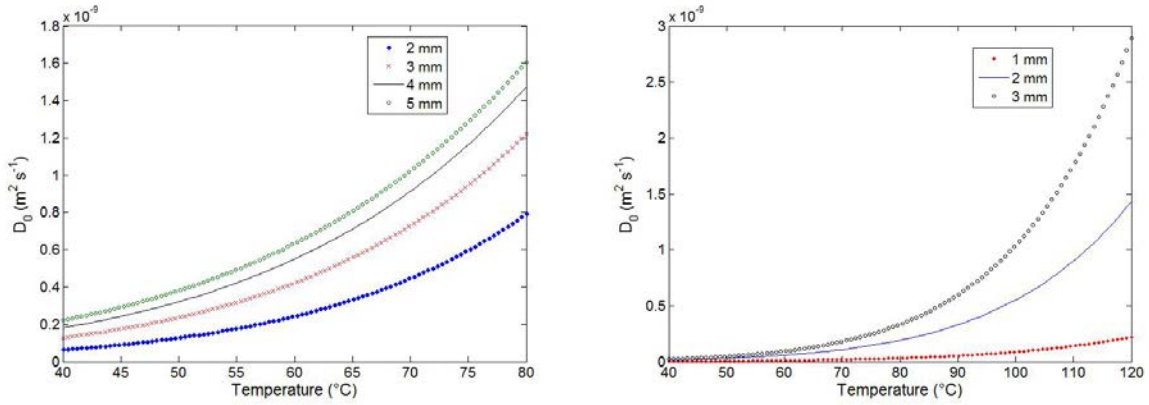

(a) Kraft paper (b) Pressboard

Figure B.6: D_0 as function of temperature and thickness for non-impregnated materials.

On the other hand, figure B.7 shows the D_0 curves, for impregnated Kraft paper and pressboard insulation as a function of temperature and insulation thicknesses, obtained after applying the aforementioned optimization process.

In these figures it can be seen how the value of D_0, increases with sample thickness at a given temperature. Consequently, the value of the moisture diffusion coefficient and the moisture mobility inside the insulations rises with thickness. The behaviour observed in pressboard and in Kraft paper is similar.

That dependence appears in all the different kinds of insulation tested in this work, following always the same tendency: i.e. higher mobility for greater thicknesses. The obtained values of D_0 may be fitted by regression and including the expressions found for D_0 into (B.3), equations (B.4) to (B.7) results.

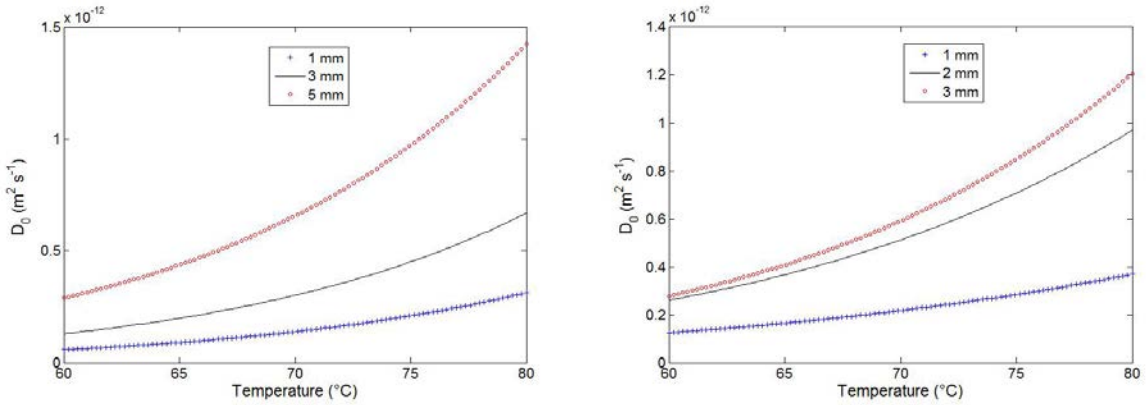

(a) Kraft paper (b) Pressboard

Figure B.7: D_0 as function of temperature and thickness for oil-impregnated materials.

$$D_{(NI_{paper})} = 3.18 \cdot l^{-3.67} \cdot e^{\left(0.32 \cdot c - \frac{8{,}241.6 \cdot l^{-0.25}}{T}\right)} \tag{B.4}$$

$$D_{(I_{paper})} = 0.5 \cdot e^{\left(0.5 \cdot c - \frac{10{,}057 - 133.7 \cdot l}{T}\right)} \tag{B.5}$$

$$D_{(NI_{pressboard})} = (2.37 \cdot 10^{-3} \cdot l^{4.96} + 5.24 \cdot 10^{-3}) \cdot e^{\left(0.43 \cdot c - \frac{27.43 \cdot l^{2.95} + 6{,}796}{T}\right)} \tag{B.6}$$

$$D_{(I_{pressboard})} = 2.89 \cdot 10^{-5} \cdot l^{6.79} \cdot e^{\left(0.2 \cdot c - \frac{6{,}419 \cdot l^{0.27}}{T}\right)} \tag{B.7}$$

where D is the diffusion coefficient (m^2/s), c is the local moisture concentration (kg of H_2O/kg), T is the temperature (K), l is the insulation thickness (mm). (NI subscript corresponds with non-impregnated insulations while the subscript I with insulations impregnated by mineral oil).

Equations (B.4) and (B.5) are the expressions of the moisture diffusion coefficient for non-impregnated and impregnated Kraft paper insulation respectively, while equations (B.6) and (B.7) correspond to the non-impregnated and impregnated pressboard insulation.

B.4 Discussion

Moisture diffusion dependence of cellulose insulation on geometric properties like thickness has not been reported in literature until now. No other author considered it neither in his experiments nor in the mathematical models used. This can be explained because in the general diffusion theory, the moisture diffusion coefficient is considered an intrinsic property of the material and therefore it is only affected by local conditions like temperature and moisture concentration.

However, several authors found experimental evidence in food materials, of the moisture diffusion dependence on this geometric property, as was mentioned before.

The first experiments performed in this work were done on non-impregnated Kraft-paper, and the samples of different thickness were prepared by changing the number of paper layers stacked together. When the dependence on thickness appeared it was assumed that it was a consequence of the different number of interfaces involved in the migration process. This initial hypothesis was discarded after repeating the experiments on pressboard samples. These insulations were composed of single layers of pressboard manufactured with different thicknesses, and a similar behavior to that observed in Kraft paper was found in this case.

Later experiments on pressboard samples, formed by multiple layers corroborated that the observed increase of the moisture diffusion coefficient with thickness was due to internal conditions of the material and not to the interfaces between the insulation layers.

Figure B.8 shows one of the multilayer pressboard samples and figure B.9 shows the drying curves of oil-impregnated pressboard samples of thickness 3 mm, composed by different number of layers. As can be seen, the evolution of the average moisture concentration is very similar, despite of the different number of layers of the

samples.

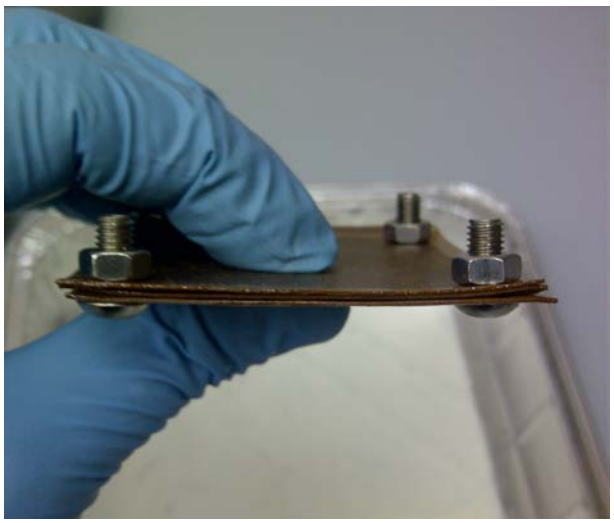

Figure B.8: Impregnated pressboard sample formed by multiple layers.

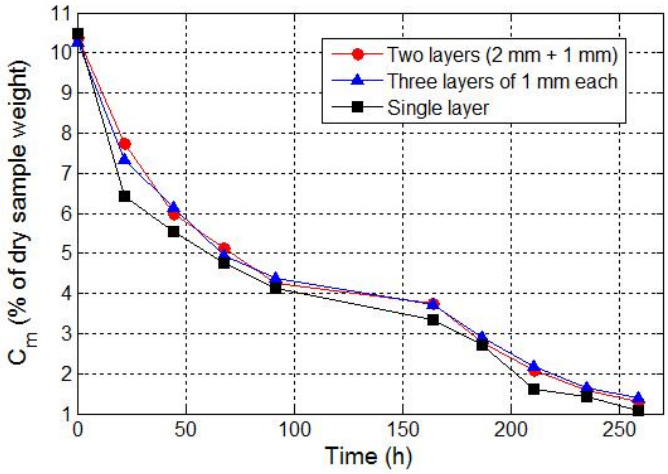

Figure B.9: Drying curves of oil-impregnated pressboard's insulations of 3 mm thick.

According to the basic theory, the diffusion coefficient cannot be a function of geometric properties, like length or thickness, as it is an intrinsic property of the material, and thus should depend just on its physical properties i.e., permeability, porosity, tortuosity and capillarity. Therefore, the increase in the moisture mobility with the thickness of the samples that is observed in the experiments can be due to several complex intrinsic and extrinsic factors which influence the transport of moisture inside the cellulosic insulation material.

The presence of the insulation thickness in the equation of the diffusion coefficient, can be explained by the fact that the assumed diffusion model does not fully represents all the transport phenomena involved in the moisture migration through the solid material (e.g. molecular diffusion, capillary motion, liquid diffusion through solid pores, vapour diffusion in air-filled pores, Knudsen flow, vaporisation-condensation sequence flow and others), and the consideration of the insulation thickness acts compensating the inaccuracies of the diffusion model.

The inclusion of the thickness in the diffusivity equation may be not so rigorous from the physical point of view, but it allows modelling the studied phenomena with much more accuracy. The previous argument can be corroborated when experiments are modeled taking into account the thickness insulation in the diffusion coefficient equation and comparing it with the simulations obtained when it is not taken into account.

Figure B.10 shows an example of the simulation in the case of a non-impregnated 2 mm sample dried at 60 ^{o}C. As can be seen, the estimations of moisture desorption obtained from the diffusion model that uses the moisture diffusion coefficients dependent on thickness are much more accurate than those obtained when the diffusion coefficients that do not include this dependence are considered.

An interesting analysis can be done by using the coefficients proposed by Du [30] to simulate the whole set of experiments performed on non-impregnated pressboard that are included in table B.1. Du did a very rigorous work to obtain a diffusion coefficient for non-impregnated pressboard and is considered one of the main references in this topic. She performed drying experiments over pressboard of a single thickness (1.5 mm) and proposed an empirical coefficient.

Figure B.11 shows the root mean square deviation (*RMSD*) obtained from (B.8), used to compare the experimental and simulated drying curves.

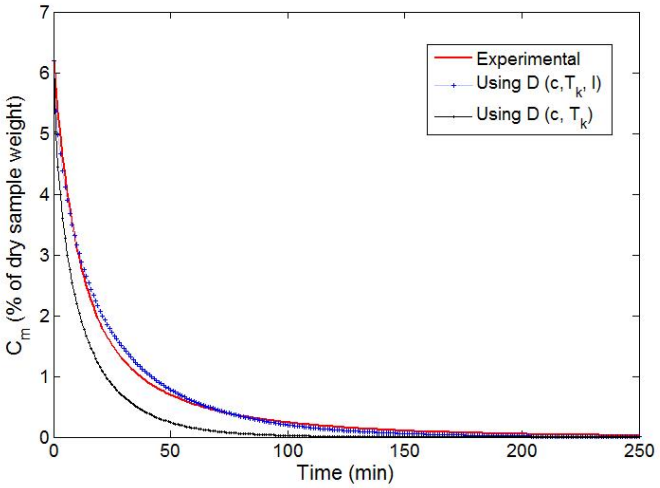

Figure B.10: Experimental and estimated drying curves of non-impregnated insulations of 2 mm thick paper, dried at 60 °C.

$$RMSD = \sqrt{\frac{1}{n}\sum_{i=1}^{n}\left[c_{m-est(t_i)} - c_{m-exp(t_i)}\right]^2} \tag{B.8}$$

where n is the number of experimental measurements, c_{m-exp} is the measured average moisture concentration, c_{m-est} is the estimated average moisture concentration and t_i is the instant of the drying experiment when the i-th measurement was performed.

Each point of this plot corresponds to the simulation of the drying curve of a pressboard piece of a certain thickness dried at a single temperature. As can be seen simulations have better agreement with experimental values in the case of 1 mm insulation pieces, as these were closer to the pieces used by Du in the determination of the moisture diffusion coefficient. The error sharply increases with thickness, especially at low temperatures.

Figure B.12 shows the drying curves of a 5 mm pressboard piece, which might be representative of a power transformer drying process performed at a temperature 60 ºC. The drying curve estimated using the diffusion coefficient proposed by Du is extremely optimistic, leading to the conclusion that the thick insulation could be dried

to a level of 2 % in just 40 h. This result would justify the programming of a short drying process that would not be effective to remove the water of the inner part of the thick insulation. The experimental results showed a much longer time required to dry the thick insulation, that could be properly estimated considering the dependency on thickness reported in this paper.

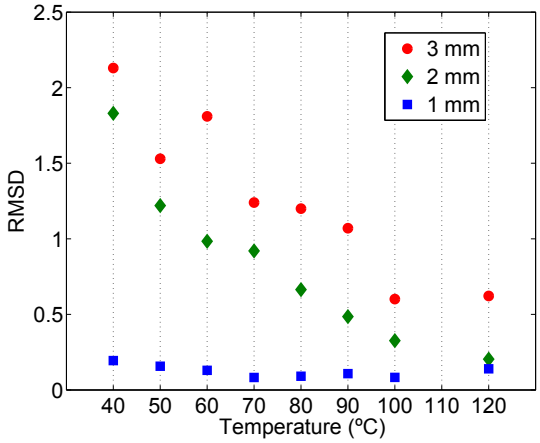

Figure B.11: *RMSD* values from drying curves of non-impregnated pressboard, using the moisture diffusion coefficient proposed by Du.

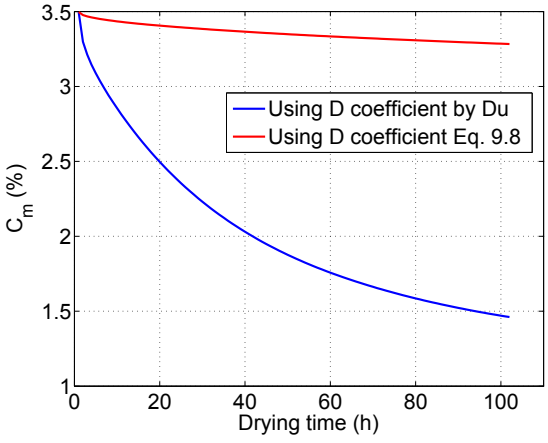

Figure B.12: Estimated drying curves of pressboard barrier of 5 mm thick, dried by the hot oil drying method with oil circulating at 60 °C and 10 ppm.

B.5 Conclusions

In this appendix it is presented how the mobility of the moisture in cellulose insulating materials, represented by the experimental moisture diffusion coefficient, increases with the thickness of the insulation. Although this behavior has not been considered in the previous works reported on transformer insulation, it has been shown in studies performed on several food materials.

The experiments reported in the paper allowed to show that this effect is due to intrinsic conditions of the material and also to some extrinsic factors that are not included in the diffusion model, and also allowed to discard that this behavior was due to the interlayer spaces or voids.

The probable cause of the reported result can be found in the fact that the moisture diffusion model is basically an approximation of the real transport phenomena and thus the inaccuracy of the model might be limited by introducing the thickness of the insulation in the equation of the diffusion coefficient used to characterize the material in the model.

Although the inclusion of the insulation thickness in the expression of the moisture diffusion coefficient may be not rigorous from the theoretical point of view, it can lead to more accurate estimations of the water migration process. This allows improving the simulation of moisture migration in cellulosic insulations for practical applications, as the optimization of field and factory drying processes of transformers and the development of moisture monitoring systems.

This work has also shown the importance of defining the range of validity of the proposed equations for the diffusion coefficient. As has been demonstrated in this work, the application of the classical expressions of the diffusion coefficient to simulate moisture dynamics, in conditions away from the ranges of validity of the coefficients

could lead to wrong results that could justify taking un-adequate decisions on the operation of the transformers.